Cellular electrophysiological mechanism of arrhythmias in athlete's heart

PhD Thesis

Péter Gazdag
MSc

Department of Pharmacology and Pharmacotherapy
University of Szeged

Szeged
Hungary

2021

Szeged

STUDIES RELATED TO THE THESIS

I. ***Péter Gazdag****, Kinga Oravecz, Károly Acsai, Vivien Demeter-Haludka, Balázs Ördög, Jozefina Szlovák, Zsófia Kohajda, Alexandra Polyák, Bálint András Barta, Attila Oláh, Tamás Radovits, Béla Merkely, Julius Gy. Papp, István Baczkó András, Varró, Norbert Nagy, János Prorok*

Increased Ca^{2+} content of the sarcoplasmic reticulum provides arrhythmogenic trigger source in swimming-induced rat athlete's heart model

Sci. Rep. 2020 Nov 11;10(1):19596. doi: 10.1038/s41598-020-76496-2.PMID: 33177643

II. *Péter Orvos, Zsófia Kohajda, Jozefina Szlovák,* ***Péter Gazdag****, Tamás Árpádffy-Lovas, Dániel Tóth, Amir Geramipour, László Tálosi, Norbert Jost, András Varró, László Virág*

Evaluation of possible proarrhythmic potency: Comparison of the effect of Dofetilide, Cisapride, Sotalol, Terfenadine, and Verapamil on hERG and native IKr currents and on cardiac action potential

Toxicol Sci. 2019 Apr 1;168(2):365-380. doi: 10.1093/toxsci/kfy299.PMID: 30561737

III. *Bence Pászti, János Prorok, Tibor Magyar, Tamás Árpádffy-Lovas, Balázs Györe, Leila Topal,* ***Péter Gazdag****, Jozefina Szlovák, Muhammad Naveed, Norbert Jost, Norbert Nagy, András Varró, László Virág, István Koncz*

Cardiac electrophysiological effects of ibuprofen in dog and rabbit ventricular preparations: possible implication to enhanced proarrhythmic risk

Can J Physiol Pharmacol. 2021 Jan;99(1):102-109. doi: 10.1139/cjpp-2020-0386. Epub 2020 Sep 16.PMID: 32937079

Other Studies

I. *Balázs Horváth, Tamás Hézső, Norbert Szentandrássy, Kornél Kistamás, Tamás Árpádffy-Lovas, Richárd Varga,* ***Péter Gazdag****, Roland Veress, Csaba Dienes, Dóra Baranyai, János Almássy, László Virág, Norbert Nagy, István Baczkó, János Magyar, Tamás Bányász, András Varró, Páter P Nánási*

Late sodium current in human, canine and guinea pig ventricular myocardium

J Mol Cell Cardiol. 2020 Feb;139:14-23. doi: 10.1016/j.yjmcc.2019.12.015. Epub 2020 Jan 17.PMID: 31958464

II. *Péter Orvos, Bence Pászti, Leila Topal,* ***Péter Gazdag****, János Prorok, Alexandra Polyák, Tivadar Kiss, Edit Tóth-Molnár, Boglárka Csupor-Löffler, Ákos Bajtel, András Varró, Judit Hohmann, László Virág, Dezső Csupor*

The electrophysiological effect of cannabidiol on hERG current and in guinea-pig and rabbit cardiac preparations

Sci Rep. 2020 Sep 30;10(1):16079. doi: 10.1038/s41598-020-73165-2.PMID: 32999428

III. *Tibor Magyar, Tamás Árpádffy-Lovas, Bence Pászti, Noémi Tóth, Jozefina Szlovák, Péter Gazdag, Zsófia Kohajda, András Gyökeres, Balázs Györe, Zsolt Gurabi, Norbert Jost, László Virág, Julius Gy Papp, Norbert Nagy, István Koncz*

Muscarinic agonists inhibit the ATP-dependent potassium current and suppress the ventricle-Purkinje action potential dispersion

Can J Physiol Pharmacol. 2021 Feb;99(2):247-253. doi: 10.1139/cjpp-2020-0408. Epub 2020 Nov 26.PMID: 33242286

IV. *Zsófia Kohajda, Noémi Tóth, Jozefina Szlovák, Axel Loewe, Gergő Bitay,* ***Péter Gazdag****, János Prorok, Norbert Jost, Jouko Levijoki, Piero Pollesello, Julius Gy Papp, András Varró, Norbert Nagy*

Novel Na^+/Ca^{2+} Exchanger Inhibitor ORM-10962 Supports Coupled Function of Funny-Current and Na^+/Ca^{2+} Exchanger in Pacemaking of Rabbit Sinus Node Tissue

Front Pharmacol. 2020 Jan 29;10:1632. doi: 10.3389/fphar.2019.01632. eCollection 2019.PMID: 32063850

ACRONYMS AND ABREVIATIONS

AP: Action potential

APD: Action potential duration

AWd: Anterior wall in diastole

AWs: Anterior wall in systole

AWT: Anterior wall thickness

CASQ: Calsequestrin

CaT: Ca^{2+} transient

CICR: Calcium induced calcium release

CPVT: Catecholaminerg polymorphic ventricular tachycardia

EC: Extracellular

ECC: Excitation-contraction coupling

EDD: End-diastolic diameter

ES: Extrasystole

ESD: End-systolic diameter

ERP: Effective refractory period

FS: Fractional shortening

GAPDH: Glyceraldehyde-3-phospate dehydrogenase

HCM: Hypertrophic cardiomyopathy

hERG: human ether-a-go-go-related gene

HR: Heart rate

ICaL: L-type calcium current

IgG: Immunoglobulin G

IK1: Inward rectifier potassium current

IKr: Rapid component of the delayed rectifier potassium current

IKs: Slow component of the delayed rectifier potassium current

Ito: Transient outward potassium current

LTCC: L-type calcium channel

LV: Left ventricular

LVAWTd: Left ventricular anterior wall thickness at diastole

LVAWTs: Left ventricular anterior wall thickness at systole

LVDP: Left ventricular developed pressure

LVEDD: Left ventricular end-diastolic diameter

LVEDP: Left ventricular end-diastolic pressure

LVESD: Left ventricular end-systolic diameter

LVESP: Left ventricular end-systolic pressure

LVP: Left ventricular pressure

LVPWTd: Left ventricular posterior wall thickness at diastole

LVPWTs: Left ventricular posterior wall thickness at systole

NCX: Sodium/calcium exchanger (Na^+/Ca^{2+}exchanger)

NSAID: NonSteroidal Anti-Inflammatory Drug

fwd NCX: forward sodium/calcium exchanger

rev NCX: reverse sodium/calcium exchanger

PLN: Phospholamban

PMCA: Sarcolemma Ca^{2+} ATPase

PKA: protein kinase A

pPKAC: Phospho-protein kinase A C

pPLN: Phospho-phospholamban

PWd: Posterior wall in diastole

PWs: Posterior wall in systole

PWT: Posterior wall thickness

qRT-PCR: Real Time Quantitative Reverse Transcription PCR

RyR: Ryanodine receptor

SCD: Sudden cardiac death

SERCA2a: Sarcoplasmic reticulum Ca^{2+}-ATPase

SL: Sarcolemma

SR: Sarcoplasmic reticulum

TL: Tibial length

TnC: Troponin C

Table of Contents

Abstract

Purpose: Sudden cardiac death is a very rare occurrence in top athletes, occurring 2-4 times more often than in the age-matched control population. The 3-6 % of the underlying cause of sudden cardiac death events remains unclear. It is known that considerable electrical remodeling exists in the athlete's heart as a consequence of the intensive physical training, additionally, several drugs that are in daily use among athletes may further facilitates arrhythmias. In the current research, the electrophysiological effects of long-term exercise training on Ca^{2+} homeostasis and repolarization, as well as the underlying alterations in ion channel expression, were examined in a rat athlete's heart model and in healthy dogs.

Methods: We used 12 weeks long swimming exercise-trained and control Wistar rats. The left ventricular morphological alterations in control (n=18) and trained (n=18) groups were observed by echocardiography. The ECG was recorded and left ventricular pressure was measured by Langendorff-apparatus, the ion currents were monitored by the whole cell configuration of the patch clamp technique. The Ca^{2+} transients were measured by fluorescent optical technique and cell contractions were detected by video-edge detector. Western immunoblot method was used to quantify the PKA, phospholamban (Pln) and the sarcoplasmic reticulum Ca^{2+}-ATPase (SERCA)2a. The expression of mRNA was calculated using the qRT-PCR process. Ionic currents were determined in isolated left ventricular cells using the whole cell configuration of the patch clamp technique in dog experiments.

Key results: The trained group showed higher incidence of extrasystoles and greatly lower resting heart rate. The trained group had significantly higher steady-state Ca^{2+} release, sarcoplasmic reticulum (SR) Ca^{2+} content, and cell shortening. The expression level of phosphorylated form of phospholamban (Pln) was increased. 250 μM ibuprofen, and terfenadine significantly reduced the rapid delayed rectifier (I_{Kr}) potassium current in canine ventricular myocytes.

Conclusion: The intensive physical training could be associated with elevated SR Ca^{2+} content and left ventricular performance *via* modification of the Pln. This remodeling, on the other hand, may be an essential part of the heart's physiological adaptation process in response to exercise, and it could make it more susceptible to spontaneous Ca^{2+} releases and extrasystoles. Furthermore, frequently used drugs such as ibuprofen attenuate the repolarization reserve providing arrhythmogenic substrate and could aggravate the arrhythmogenic propensity in the athlete's heart.

1. Introduction

Physical activity and competitive sport are two of the most effective strategies for improving fitness, and they are linked to positive improvements in the majority of cardiovascular disease risk factors (including blood lipids, blood pressure, insulin sensitivity, and weight) [1]. Moderate aerobic activity has reliably been linked to a lower risk of coronary heart disease (CHD) and death in a significant number of epidemiological studies. Even a small amount of exercise will greatly reduce the risk as compared to a sedentary lifestyle [1]. Compared with a sedentary lifestyle, even a small amount of exercise can significantly reduce the risk. Although the debate about potential in general, the link between vigorous endurance exercise and the increased risk of certain heart diseases (such as atrial fibrillation, ventricular fibrosis) is clearly health-promoting for most people. Exercise, on the other hand, may increase the risk of sudden death in a small number of people with cardiac conditions. Fortunately, sudden death among top athletes is very rare, approximately 1:50,000-1:100,000 per year [1, 2]. It commonly affects young, seemingly healthy athletes and has a significant emotional and social effect on the group. Hypertrophic cardiomyopathy, which causes high electrical instability in ventricular tissues, is one of the most common causes of SCD in top athletes [3]. Therefore, great efforts have been made to better understand the causes of sudden cardiac death (SCD) in athletes.

We assumed that the sudden cardiac death of top athletes may be the result of the concurrent existence of trigger mechanisms, such as delayed afterdepolarization and repolarization inhomogeneity, which represent an increased substrate for arrhythmia. Furthermore we hypothesized the different ordinary drugs could influence the potassium channels and aggravates the arrhythmia propensity.

Intracellular calcium homeostasis of myocardial cells

Transport processes of the $[Ca^{2+}]_i$ cycle

Ca homeostasis of myocardial cells is initiated during the plateau phase of the action potential provides balanced Ca cycle for beat-to-beat contraction of the myocardium (Figure 1). The dynamic change in calcium creates a relationship between changes of transsarcolemmal voltage and myocyte contraction, a process called *excitation-contraction coupling*.

As the initial step of the calcium cycle, calcium ions enter the cell from the extracellular space (Ca influx), causing further calcium release (Ca release) from the sarcoplasmic reticulum, creating a

calcium transient (CaT). After contraction, the amount of the released Ca is taken back to the SR (Ca reuptake) and the amount of Ca influx is extruded from the cell by Ca removal mechanisms (Ca efflux) [4-6].

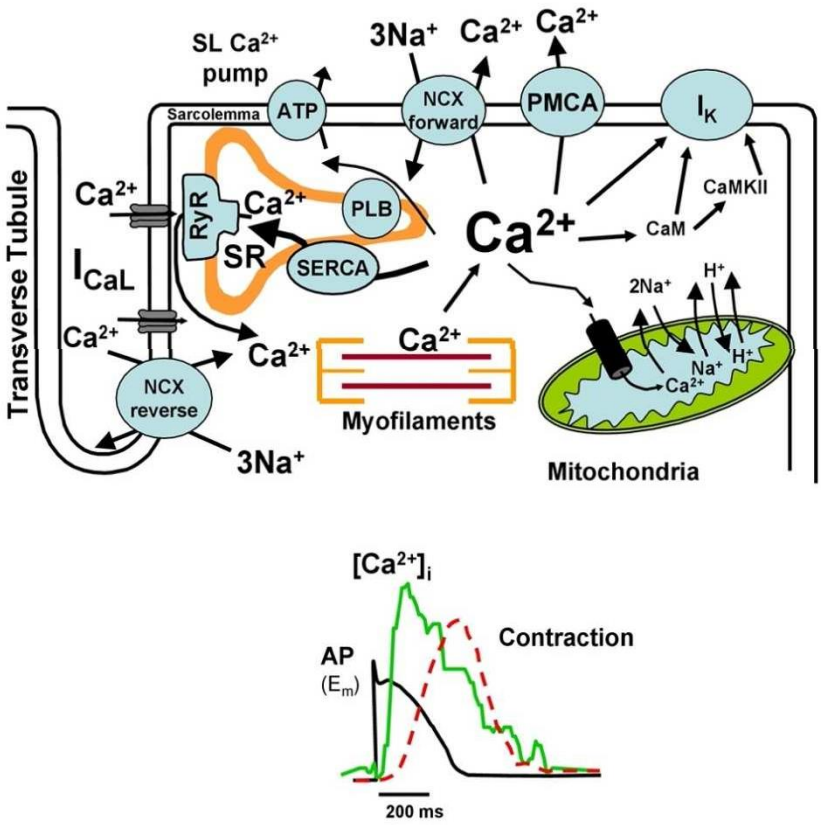

Figure 1. Major transport processes of the $[Ca^{2+}]_i$ cycle of ventricular myocardial cells. The most important Ca^{2+} movements ($[Ca^{2+}]_i$ cycle) parallel to the electrical activation of myocardial cells, the coupling of excitation-contraction, and the contraction-relaxation cycle (ECC) of the heart are summarized [4, 7].

Ca influx

The initial step of the calcium cycle is the Ca influx. Ca ions enter the cell from the extracellular space through various pathways during this process. Nevertheless, reverse NCX and Na channels may contribute to Ca influx [4], however, in mammalian myocardial cells, the vast majority of Ca enters through Ca channels (Figure 2) [8]. 2 types of Ca-channels are known in myocardial cells. T-type Ca channels show significant expression primarily in atrial cells and in nodal tissues (sinus node, AV node), while their role in ventricular cells is negligible. In contrast, L-type Ca channels

show significant expression in the sarcolemmal region in ventricular cells. As a result of depolarization, L-type Ca channels are activated, and between 0 and +10 mV, a significant Ca current can be measured through the channels (Ca current, I_{CaL}). A smaller proportion of Ca influx may result from the operation of the reverse mode of sodium calcium exchange, in which 3 sodium is pumped out of the cell into the extracellular space and at the same time 1 calcium is entered the cell, contributing to an increase in intracellular calcium levels. The contribution of the reverse mode to Ca influx is small, however, when the function of L-type Ca channels is impaired, the importance of reverse NCX may be increased, and may contribute in the initiation of Ca-release in some extent [4, 9].

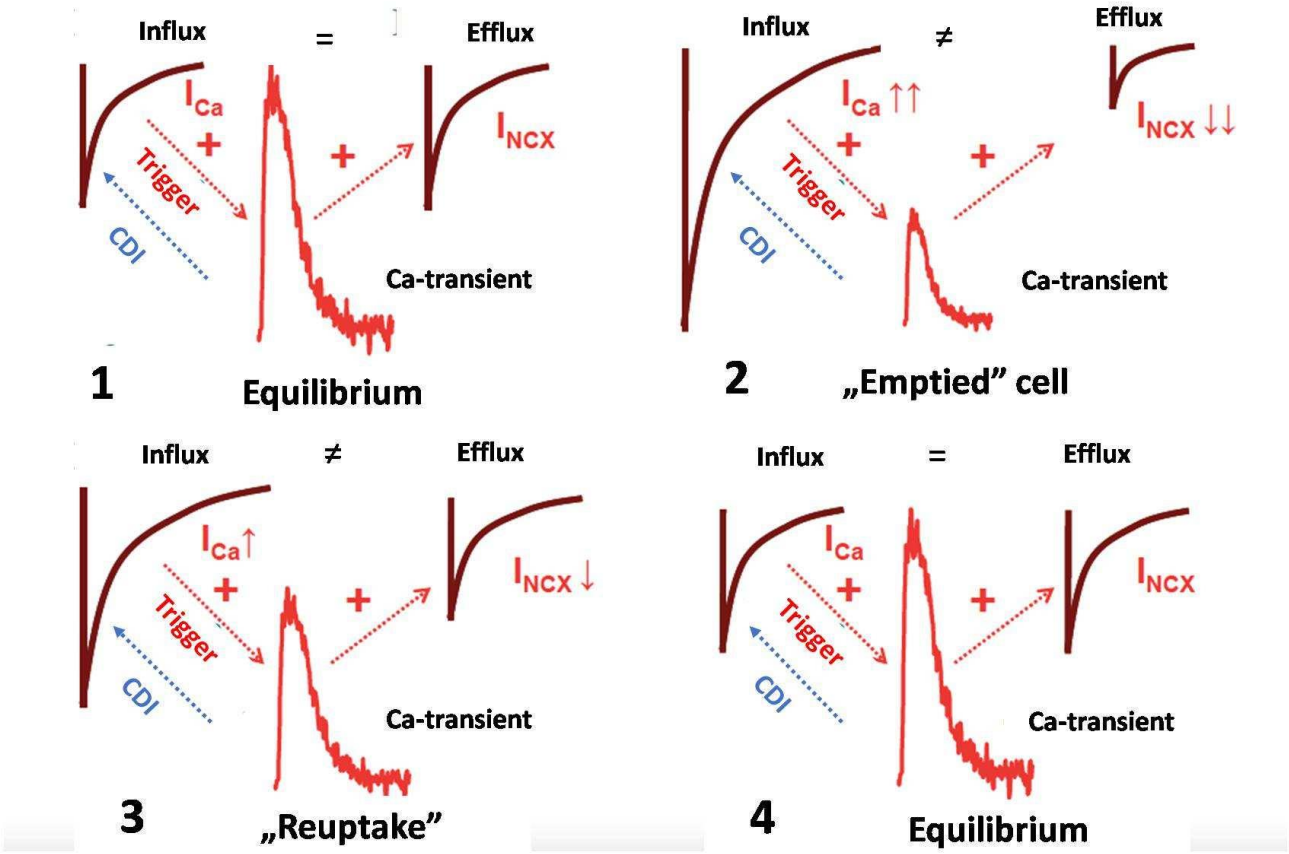

Figure 2. Closely coupled local autoregulation of Ca^{2+} influx (LTCC) and SR Ca^{2+} content. (1) Dynamic equilibrium when influx is equal to efflux. (2) Ca-handling disturbance (eg.: use caffeine for 'depletion'), when $Ca^{2+}i$ is reduced, the CDI is suppressed providing considerable larger influx than efflux. (3) The $Ca^{2+}i$ is increasing, the fluxes approximates equal value again (4) New equilibrium [10].

Ca release

The main function of SR is to store calcium, mainly by the Ca-binding protein calsequestrin. Trigger calcium during Ca influx binds to ryanodine receptors on the surface of the sarcoplasmic reticulum (SR). When the trigger Ca opens the RyR, the stored Ca is released from SR, via a process called calcium-induced-Ca-release (CICR). The released Ca binds to the myofilaments and ensures the contraction of the myocardium. The normal diastolic intracellular Ca concentration of 100 nM reaches 1 µM during the release. The extent of intracellular Ca releases can be monitored by various techniques, such as fluorescent optical method [4, 9, 11].

Ca reuptake and Ca efflux

Following the contraction of the myocardium, it is necessary to take back and remove the released Ca from the cell, to ensure diastolic Ca. Most of the systolic Ca (approximately 70% in mammalian cells) is taken back/stored in the SR by the ATP-dependent SR Ca pump (SERCA2a). Most of the remaining Ca is removed from the cell by the forward mode of NCX. It is known that the actual function of the NCX is influenced by the momentary membrane potential as well as the extra- and intracellular Na and Ca concentrations. The increased intracellular Ca level favours the forward mode, providing 1 net positive charge for the cell, and inward current. It is important to mention that in addition to forward NCX, the plasma membrane ATP-dependent Ca pump (PMCA) is also involved in Ca removal. The contribution of PMCA is suggested to be a fine-tuning of diastolic Ca levels [12].

Balance of intracellular Ca homeostasis is important for normal cardiac function. Under physiological conditions, Ca influx and Ca efflux must be equal, ensuring optimal intracellular Ca concentration during each cycle when neither Ca gain nor Ca loss does not happen. The Ca cycle of myocardial cells is regulated by intrinsic and extrinsic mechanisms. Among the intrinsic mechanisms, the role of autoregulation is crucial, and among the extrinsic factors, the regulation of the neurohormonal system ensures the appropriate adaptation to external environmental factors [11].

Principles of regulating Ca^{2+} movements - the conditions of equilibrium

Intra- and transcellular Ca^{2+} movements during the contraction-relaxation cycle of the heart are precisely regulated. The two most important components of homeostatic regulation are the "local

feed-back" control of Ca^{2+} fluxes, and the autonomic control.. Both mechanisms are based on the dynamic interaction of Ca^{2+} fluxes in SL and SR.

Local (submembrane) autoregulation of Ca^{2+} handling

In the case of steady-state cardiac function, the uptake of Ca^{2+} by cells during a single cardiac cycle must be equal to the amount of Ca-efflux, which means their average Ca^{2+} content does not change. The amount of Ca^{2+} (trigger) under the systole (I_{Ca}) is regulated by the magnitude of CaT by calcium-dependent inactivation (CDI) through a negative feedback mechanism. The number of activated LTC channels as well as the duration of their open state also affect Ca influx. The number of activated LTC channels is basically determined by transmembrane potential changes. In contrast, the open state duration of the channels is very sensitive to changes in the submembrane $[Ca^{2+}]$ ($[Ca^{2+}]_{sm}$). If, for some reason, the $Ca^{2+}{}_i$ level decreases, the Ca^{2+} content of the SR decreases due to the reduced reuptake (SERCA2 transport activity), thus the amplitude of CaT will be smaller - and more importantly - the $[Ca^{2+}]_{sm}$ will also decrease markedly. Due to the smaller CaT, the amount of Ca^{2+} removed by NCX decreases, however, the reducing $[Ca^{2+}]_{sm}$ inhibits LTCCs much less, which is manifested in a marked increase in their open state probability. As both processes lead to Ca^{2+} accumulation, the $Ca^{2+}{}_i$ content of the cells gradually increases until it reaches equilibrium again, where it stabilizes.

Autonomic regulation of Ca^{2+} handling

The extrinsic regulation of the Ca cycle is based on the function of the neurohormonal system. It promotes adaptation to different physiological and pathological conditions. This pathway acts primarily through cAMP and protein kinase A (PKA) signalling pathways following binding of individual metabolites to β-adrenergic receptors. Phosphorylation of Ca channels, RyR, SERCA2a, troponin, and phospholamban increase Ca influx and reuptake, leading to faster and improved contraction.

Cellular Mechanism for cardiac arrhythmias

The cellular mechanism of arrhythmias can be classified into 3 major types. *The abnormal automaticity* is considered as abnormal impulse generation due to changes in normal automatic mechanisms. *Abnormal automaticity* (formation of spontaneous action potentials) reflects to action potential generation at sites out of the nodal tissues. The underlying mechanism could be the

downregulation of the I_{K1} causing depolarization of the membrane potential that is able to reach the threshold potential of the Na-channels. Another possible mechanism of the abnormal automaticity is the up-regualtion of the so-called “funny” channels causing slow depolarizations and spontaneous action potentials. The triggered activity requires a previous action potential that will trigger extra depolarization, and if its magnitude is sufficiently large, a new action potential. Depending of the coupling time, early and delayed afterdepolarizations could develop [13].

Early afterdepolarization

The characteristic of early afterdepolarization (EAD) is depolarization that occurs before the termination of the previous action potential during phase 2 or phase 3 polarization. EAD is usually generated when the action potential is excessively long (for example, when I_{Kr} is damaged, or during extreme bradycardia). Due to the prolongation of the action potential, those L-type calcium channels that have recovered from inactivation can be reopened, and some calcium channels carry Ca^{2+} window currents, [14, 15] causing positive voltage oscillations during the plateau (phase 2 EAD) or terminal repolarization (phase 3 EAD). The Luo-Rudy study [14, 15] also proposed the second type of EADs, phase 3, which is caused by the spontaneous release of calcium during the repolarization process, and then converted to depolarization via NCX. The mechanism of this EAD is very similar to delayed afterdepolarization, but the timing is different (during AP and after AP). Both types of EADs are rate-dependent. The mechanism of EAD based on reactivating ionic currents mainly occurs in slow pacing, while the release-driven EAD occurs at fast pacing [16].

Delayed afterdepolarization

The delayed afterdepolarization (DAD) is characterized by depolarizing changes of the membrane potential after terminating the previous action potential [17-19] during diastole. DAD is usually attributed to calcium-sensitive depolarizing currents or CaMKII-dependent phosphorylation [20, 21] after the spontaneous Ca^{2+} release from SR during Ca^{2+} overload. This mechanism can be caused by chronic AF, ischemia, heart failure [21-23], catecholaminergic polymorphic ventricular tachycardia (CPVT) or drugs such as digitalis. The foremost important calcium-sensitive current involved in the formation of DAD is the forward NCX, but the role of calcium-sensitive chloride current has also been proposed [24]. Calcium-induced depolarization is mainly opposed by the I_{K1}, which contributes to maintain the resting membrane potential [25]. When the depolarization caused by the calcium-sensitive current is large enough to overcome I_{K1}, it will activate I_{Na}, thereby triggering the a new action potential. The automatism that occurs within the pulmonary veins and cardiomyocytes

represents important abnormal impulse formation. At present, it seems that their cellular mechanisms are complex, including the possibility of DAD and EAD generation also. Spontaneous calcium release is a random phenomenon, represented by calcium sparks [26, 27] and intracellular calcium waves [27-30], and multiple calcium release sites need to be synchronized to produce cell-wide calcium release [31].

2. Arrhyhtmogenesis in top atheletes

Many clinical and epidemiological studies provided evidence that moderate physical exercise markedly improves cardiovascular function, decrease mortality and prevents sudden cardiac death [3, 32, 33]. Athlete's heart has been described by complex structural, functional, and electrical cardiac remodeling induced by long-term exercise training [34]. It has been known for a long time that strong physical exercise in competitive athletes induces hemodynamic changes leading to morphological and functional remodeling of the heart (cardiac hypertrophy) [35, 36]. This adaptation includes increased left and right ventricular diameters, enhanced cardiac mass and left ventricular wall thickness accompanied by bradycardia, higher heart rate variability, and ion channel remodeling. These changes are classically characterized as the "athlete's heart". Cardiac enlargement in athletes has been reported since the late 1890s [37], and a number of other aspects of athlete's heart are intensively investigated in humans [34, 38] also in experimental animals [39]. Variety of animal models of exercise-induced cardiac hypertrophy is developed, and several sorts of endurance exercise training are recognized to effectively induce physiological cardiac hypertrophy in experimental animals, just like swim training. Swim training appears equally effective as treadmill running programs. Numerous studies concerning the cellular and molecular remodeling [40] as well as structural and morphological changes [34, 41, 42] are published in recent years; however, we still have limited data about the functional regards of exercise-induced cardiac hypertrophy. Several in vitro experimental studies from isolated rodent hearts [43, 44], papillary muscles [42, 45], and isolated cardiomyocytes [46-48] have demonstrated positive effect of exercise training on myocardial function [37].

Nevertheless, despite these physiologic adaptive mechanisms, a number of tragic sudden cardiac death (SCD) events involving young athletes has been reported recently. While SCD among athletes is rare it is still 2-4 times more frequent in athletes compared to their age-matched controls [49]. However, numerous pathological anomalies could be associated with sudden cardiac death in athletes such as hypertrophic cardiomyopathy, coronary artery abnormalities, or myocarditis, normal hearts were demonstrated in the 3-6 % of the SCD cases among top athletes, where the underlying cause of the SCD is unclear.

The proposed mechanism could be an adverse and arrhythmogenic consequence of the exercise-induced cardiac adaptation. In normal circumstances, conduction within the heart is fast (1 to 2 m/s), and therefore the duration of the action potential (AP) in myocardial cells is long (200–300 ms). Thus, these cells are unable to become stimulated early since they are during a refractory state (effective refractory period, ERP). Importantly, within normal settings, the difference between the action potential durations (APD) and consequently the ERPs of adjacent cells is

extremely small, thus, repolarization is homogenous. Fast conduction and homogenous repolarization (and refractory period) together prevent the circular reentry of excitation, and arrhythmia will not develop. On the other hand, when the APD between the adjacent cells becomes larger, it leads to increased spatial repolarization inhomogeneity (Figure 3). As a consequence, an extrasystole generated after a normal sinus beat can propagate within cells with shorter APD but its propagation, will be blocked after meeting with cells with an extended APD (Figure 3). Thus, this extra stimulus can travel back by using a complicated path toward the location of its origin and everywhere else where excitability is recovered may generate a chaotic tachycardia or fibrillation. Ventricular fibrillation does not revert to sinus rhythm spontaneously in humans and results in sudden cardiac death without intervention during a few minutes.

It is important to note that two independent factors are needed for the arrhythmia development. The inhomogeneity of repolarization after prolonged repolarization time ("substrate") is itself not enough for arrhythmia development. In order to induce an arrhythmia, an extrasystole within the vulnerable period is required ("trigger") which will travel to the reentry paths created by the inhomogeneous repolarization. The timing of this trigger is critical, since before the vulnerable period its conduction is blocked, and after the vulnerable period, it does not lead to tachycardia or fibrillation, only a harmless single extrasystole [2].

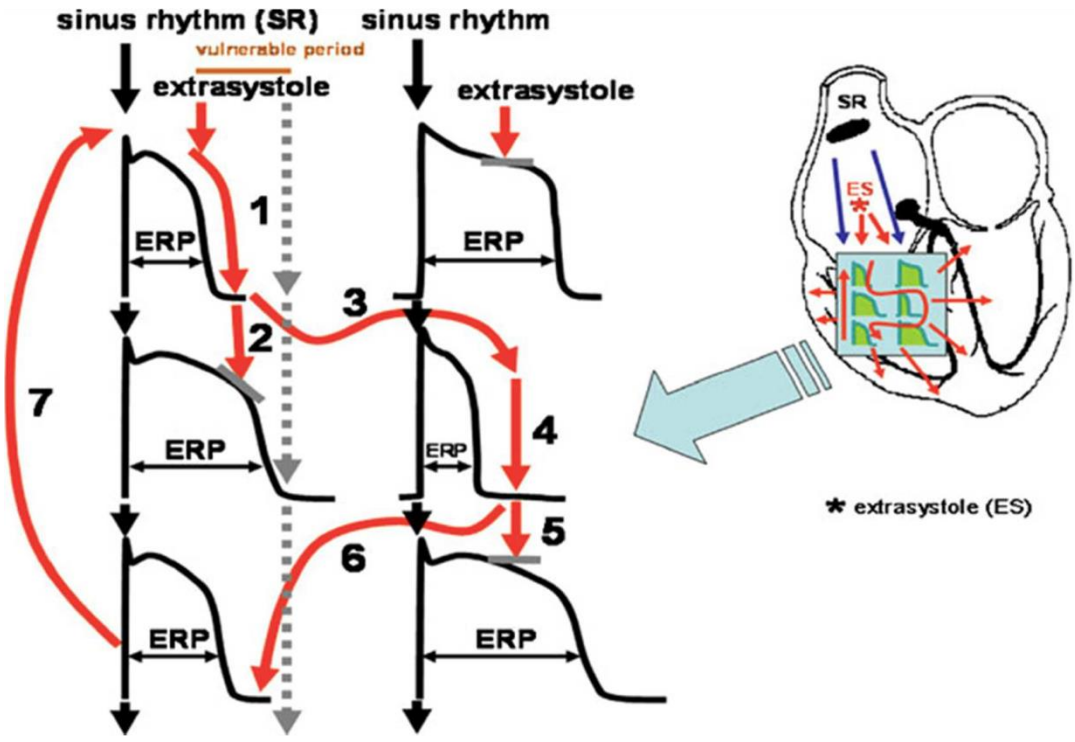

Figure 3. Schematic, simplified illustration of the mechanism of arrhythmia development [2]

2.1 Hypothetical mechanisms of sudden cardiac death in top athletes

The remodeling induced repolarization abnormalities due to potassium channel downregulation provide arrhythmogenic substrate and a parallel presence of altered Ca^{2+} handling proteins together with increased sympathetic tone cause arrhythmia triggers (Figure 4). Furthermore, several factors could also contribute such as hypertrophic cardiomyopathy, acquired-genetic diseases, several drugs, hypokalemia and hypomagnesemia, doping, steroids, food or dietary ingredients. It is important to note that the misfortune is also a crucial factor of the arrhythmia development, since in the presence of repolarization inhomogeneity, a critically timed extrasystole is needed to find the narrow period when the hearts are more vulnerable than under normal condition. In other cases, arrhythmia will not develop.

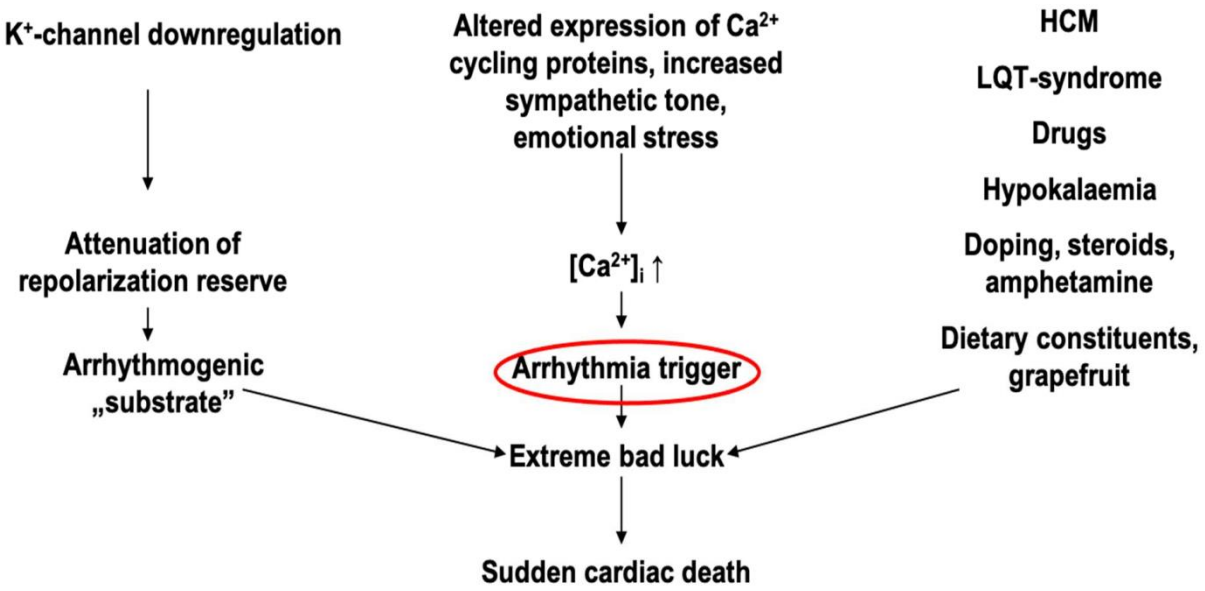

Figure 4. Hypothetical mechanism of sudden cardiac death in top athletes [2]

Additional factors

Cardiac diseases

Autopsies found that the most common cause of sudden cardiac death in young athletes was the hypertrophic cardiomyopathy (HCM) [50-52]. The disease may be a familial malformation [50, 53] and mutations during a number of sarcomeric genes identified that hypertrophic cardiomyopathy and the resulting cardiomegaly and interstitial fibrosis were even more pronounced in these patients. Hypertrophic cardiomyopathy is relatively common (1 in 500 is common population) and the

mortality rate in young adults is 1-6%. It is very difficult to differentiate hypertrophic cardiomyopathy from normal compensatory hypertrophy in the early stages of athletes. After 2-3 months of sports activity, leisure time is suspected, which can be identified by echocardiographic examinations, as this hypertrophy is irreversible. Those athletes who suffer from hypertrophic cardiomyopathy the effect of compensatory hypertrophy (athlete's heart) and abnormal hypertrophy may add up and increased repolarization which may result in significant arrhythmia substrate formation. In addition to HCM, other abnormalities may be associated with sudden cardiac death in top athletes [51, 52, 54], including congenital coronary artery disease, myocarditis, and Brugada syndrome, aortic stenosis, and arrhythmogenic right ventricular cardiomyopathy [55, 56].

Genetic defects

Fortunately, the incidence of genetic defects is relatively low. The estimated prevalence of different types of congenital long QT syndromes is usually 1: 5000 in the population. Studies of competitive athletes have shown a similar prevalence [57, 58]. About 10% of people with long QT syndrome die because of sudden cardiac death. The arrhythmogenic consequences of congenital long QT syndrome is increased in athletes since the repolarization reserve was slightly impaired based on cardiac hypertrophy. Therefore, mutations that might otherwise cause only mild abnormalities of repolarization can cause serious arrhythmias in these athletes. Another danger for athletes is catecholaminergic polymorphic ventricular tachycardia (CPVT) [55] . CPVT is a severe disorder associated with mutations in genes of RYR or CASQ2. Sports activities and workouts result in the release of calcium from the SR into the cytoplasm in the CPVT because of the increased sympathetic tone even during diastole. These events can provoke extrasystoles, that increase the trigger frequency that ultimately leads to increased arrhythmia susceptibility [2].

Drugs

We know that some drugs primarily reduce the rapid component of the delayed rectifier potassium current [59]; this leads to prolongation of repolarization, sometimes proarrhythmic side effects, and very rarely sudden cardiac death. Several commonly used medications, such as antihistamines for hay fever or antibiotics used against infections, have been found to have this type of side effect [60, 61]. Because these drugs are not on the doping list, athletes can also use them. However, in the case of elite athletes, as already mentioned, myocardial hypertrophy may weaken the repolarization reserve, thus amplifying the undesirable arrhythmogenic effects of drugs. It cannot be ruled out that the drugs, together with other factors, contribute to the occurrence of lethal arrhythmias in athletes with a somewhat weakened repolarization reserve. It would also be particularly important to

thoroughly investigate the potential marginal effects of NSAIDs on repolarization, as athletes use these agents very frequently and in high doses to treat their injuries, but relatively little is known about their effects on myocardial electrophysiological parameters. The frequency of extrasystoles (triggers) may also be increased by nasal sprays with sympathetic agonist effect associated with seasonal allergies [2].

Hypokalemia

During exercise, significant temporary loss of fluid can occur, which in the case of inadequate supplementation can result in hypokalemia or hypomagnesaemia. The repolarization disturbances can be caused by the effect of hypokalemia and hypomagnesaemia are well known, so this may be an even greater concern for athletes with hypertrophied hearts. If the extracellular potassium concentration will be reduced then a substantial AP prolongation due to decreased I_{Kr} and I_{K1} occurs in the late repolarization phase of the AP [2].

Doping

Doping is primarily a problem in top athletes and bodybuilders [62]. Because its use is an illegal activity, we have few reliable statistics or studies available. However, it is known that steroid-type doping agents cause hypertrophy of the muscles [63, 64]. A similar mechanism can be assumed for growth hormone. Thus, as discussed above, doping may additively contribute to the prolongation of repolarization and the increase of repolarization inhomogeneity, which may greatly increase the arrhythmia propensity from the substrate side. A different mechanism can be hypothesized for amphetamine-type sympathetic stimulants. These agents, similar to the increase in sympathetic tone, increase intracellular cAMP levels, leading to elevated number of extrasystoles, thus inducing lethal arrhythmias in individuals with inhomogeneous ventricular repolarization from the trigger side [2].

Foods

Athletes, especially competitive athletes, often use a special diet, special dietary supplements, vitamins, however their cardiac electrophysiology effects are not fully clarified. For example soy formulations, have been shown in animal experiments to exacerbate myocardial hypertrophy and exacerbate heart failure [65]. The effects were stronger in male animals than in females [66, 67]. Interesting data were also reported after consuming grapefruit. According to these studies, a significant detectable QT interval prolongation was observed even after consuming 1 liter of grapefruit, which was associated with the potassium channel (I_{Kr}) inhibitory effects of flavonoids found in large amounts in grapefruit [68]. It is also well known that grapefruit inhibits P450 and this can cause further unexpected problems. It should be emphasized, however, that little is known

about the direct cardiac electrophysiological effects of food additives, preservatives, and food dyes, so these examples are probably only the tip of the iceberg [2].

Bad luck

According to the mechanism shown in Figure 3, two basic conditions are required for the development of an arrhythmia. On one hand, there must be a degree of ventricular repolarization inhomogeneity, that defines the length of the vulnerable period. The greater ventricular repolarization inhomogeneity results in longer vulnerability period (substrate). On the other hand, the increased frequency of extrasystoles (triggers), has an increased probability to cause chaotic tachycardia or ventricular fibrillation when they fall into the vulnerable period. At the individual level, however, bad luck should be highlighted as a factor. When an extrasystole develops up to 1 ms later or earlier than the vulnerable period, no severe arrhythmia occurs. In other words, even in the presence of objective conditions (substrate + trigger), the random appearance of extrasystoles determines the development of fatal arrhythmias in a given individual. In statistical terms, however, the vulnerable period in top athletes is presumably longer compared to the healthy average population in association with greater repolarization inhomogeneity due to myocardial hypertrophy, and sympathetic tone also increased persistently at regular intervals due to frequent training. Thus, the risk of top athletes to suffer sudden cardiac death based on repolarization abnormalities are presumably higher than that of a healthy population [2].

3. Materials and methods

Ethical considerations

Animals

All experimental procedures were reviewed and submitted by Ethical Committee of Hungary for Animal Experimentation in accordance with the ‘‘Principles of Laboratory Animal Care’’ defined by the National Society for Medical Research (permission number: PEI/001/2374-4/2015) and the Guide for the Care and Use of Laboratory Animals, provided by the Institute of Laboratory Animal Resources and published by the National Institute of Health (NIH Publication No. 85-23, revised 1996.); and to the EU Directive 2010/63/EU guidelines. All animals received human care. 8-week-old Wistar male rats (Toxi-Coop, Dunakeszi, Hungary) (n = 36, m = 240-280 g) were housed in standard rat cages at a constant room temperature (22 ± 2 °C) with 12/12-h light/dark cycles. Animals (rats, rabbits, dogs) received standard laboratory diet and water ad libitum. The body weight of animals was controlled regularly (three times a week). We used 2-3 kg male New Zealand rabbits and 10-15 kg Beagle dogs of both sexes. Rabbits were terminated by rapid cervical dislocation, dogs and rats were anesthetized and sacrificed using high dose sodium pentabarbital.

Exercise training protocol

The rats were randomly divided into control (n = 18) and trained groups (n = 18) after the acclimatization. Trained group underwent a 12-week-long swimming training protocol to provoke physiological myocardial hypertrophy as described previously by Radovits et al. It was a 150 liter water container which was divided into 6 lanes with a surface area of 20x25 cm and a depth of 45 cm per lane and filled with tap water maintained at 30-32°C. The dimensions of lanes were selected to avoid reclining to the walls and floating of rats. Swimming training was performed 5 days/week. For the rats adaptation, the duration of swimming was raised by 15 minutes every second training day from a baseline of 15 minutes on the first day, until obtaining the maximal 200 min/day. Control rats were placed into the water for 5 minutes/day via 12 weeks to reduce the possible differences caused by the stress of water contact [37].

Echocardiography

At the completion of the swimming training program, LV morphological alterations in control (n =18) and trained (n = 18) rats were observed by echocardiography as described before [69], except

that rats were anesthetized with isoflurane (5% induction dose, 1–2% maintenance dose). Animals were placed on controlled heating pads, and therefore the core temperature was maintained at 37°C. After shaving the anterior chest, transthoracic echocardiography was performed within the supine position employing a 13 MHz linear transducer (12LRS,GE Healthcare, Horten, Norway), connected to an echocardiography system (Vivid i, GE Healthcare). Standard two-dimensional and M-mode long-and short axis (at mid-papillary level) images were acquired. Recordings were analyzed off-line employing a dedicated software (EchoPac, GE Healthcare). We counted heart rate (HR) on images recorded by M-mode. On two-dimensional recordings of the short-axis at the mid-papillary level, LV end-diastolic (LVEDD) and end-systolic diameter (LVESD) also as LV anterior (AWT) and posterior (PWT) wall thickness in diastole (index: d) and systole (index: s) were measured. End systole was defined because the time point of minimal LV dimensions, while end-diastole because the time point of maximal dimensions. All values were averaged over three consecutive cycles [69].

Fractional shortening (FS) was examined from the measurements of LV chamber diameters: FS =[(LVEDDLVESD)/LVEDD] Å~ 100. LV mass was consistent with the subsequent formula: LV mass = [(LVEDD + AWTd + PWTd)3 − LVEDD3] Å~ 1.04 Å~ 0.8 + 0.14. To calculate left ventricular mass index, we normalized the left ventricular mass values to the tibial length (TL) of the animal [69].

Morphometric assessment

Standard morphometric measurements were obtained including bodyweight and post-mortem heart weight, also as tibial length. All animals body weight were weighed before termination. After Langendorff isolated heart measurements, the dry heart weights were measured (n = 12/group). Tibias were prepared and length were measured after termination. For morphometric analysis, we were utilizing a conventional analytical balance and a ruler.

Isolated heart experiments

After the training protocol, 20-week-old male Wistar rats were used (12 control and 12 trained). ECG and left ventricular pressure (LVP) of isolated hearts were measured in Langendorff-perfused hearts as described before [70]. Animals were anaesthetized with Na-pentobarbital (300 mg/kg,i.p.), and were injected with heparin sodium (300 IU) into the hepatic portal vein. Hearts were rapidly excised, placed via the aorta on a Langendorff apparatus and retrogradely perfused with warm

(37°C) modified Krebs–Henseleit bicarbonate buffer (KHB) at a continuing pressure (80 mmHg). The KHB solution contained (in mmol/L):$NaHCO_3$25; KCl 4.3;NaCl 118.5; $MgSO_4$1.2; $KH_2PO_4$1.2; glucose 10; $CaCl_2$1.8, having a pH of 7.4 ± 0.05 when gassed with 95% O_2+ 5% CO_2.The LVP was measured by a water-filled latex balloon which was inserted into the left ventricular cavity and inflated to get an impact state end-diastolic pressure (LVEDP) of 4–8 mmHg [70]. A pump (Masterflex) provided continous exchange of the KHB and the constant column pressure. The electrical activity as electrocardiogram (ECG) detected by the three lead self-made electrodes and signal amplifier (Experimetria, Hungary). The LVP and the ECG were simultaneously recorded using the WinWCP software(V4.9.1. Whole Cell Electrophysiology Analysis Program, John Dempster, University of Strathclyde,UK). Ventricular extrasystoles were generated by hypokalemic (2.7 mM K^+) KHB solution.

Measurement of ionic currents

Rat ventricular cardiomyocytes were isolated enzymatically from the left ventricular as described in our previous study [71]. The L-type Ca^{2+}current, K^+ currents, Ca^{2+} transient measurements were also described earlier [72]. The estimation of sarcoplasmic reticulum Ca^{2+}content by caffeine method was applied as previously described [73].

Determination of phospho-PKA C, phospho-phospholamban and SERCA2 by western blot

The pan and phosphorylated forms of PKAC, phospholamban (PLN) and SERCA2 were measured in myocardial tissue samples taken from the left ventricle (n = 6/group). The fresh LV tissue samples were immediately frozen in liquid nitrogen and stored at -80°C. 30 µg (PKA C, pPKA C), 50 µg (PLN, pPLN) and 20 µg (SERCA2) total protein extracts were fixed using 10% (PKA C, pPKA C), 15% (PLN, pPLN) and 8% (SERCA2) sodium dodecyl sulphate-polyacrylamide gel electrophoresis and transferred onto polyvinylidene fluoride membranes. After blocking in 5% milk-TBS-T, the membranes were immunolabeled with the respective primary antibodies supported by the Calcium Ion Regulation Antibody Sampler Kit (Cell Signalling Technology; Danvers, MA,USA; overnight, at 4°C; dilutions: anti-PKA C, antipPKA C (-α, -β, and -γ when phosphorylated at Thr197):1:7000, anti-PLN, anti-pPLN (when phosphorylated at Ser16/Thr17): 1:2500, anti-SERCA2: 1:7000). We used a secondary antibody Horseradish peroxidase which conjugated goat anti-rabbit IgG (Southern Biotech, Birmingham, AL, USA; 1 h, RT; 1:8000). The membranes were developed with an ECL kit (Advansta; SanJose, CA, USA)and exposed to X-ray

film. The equivalent protein loading was verified by coomassie blue staining and normalized to total protein. The equivalent protein loading was verified by coomassie blue staining. Use Image J(FIJI; NIH, Bethesda, MD, USA) to evaluate the integrated optical density values(sum of every band corrected to the background).

Gene expression analysis by qRT-PCR

All mRNA analyses were applied as described previously [74]. Fresh left ventricular tissue samples (n =6/group) were excised and snap-frozen in liquid nitrogen and stored at -80°C.We homogenized the myocardial samples in a lysis buffer (RLT buffer; Qiagen, Hilden, Germany), total RNA was separated from the tissue using the RNeasy Fibrous Tissue Mini Kit (Qiagen) consistent with the manufacturer's instructions and quantified by measuring optical density at 260 nm.1 µg total RNA was used for reverse transcription [QuantiTect Reverse Transcription Kit (Qiagen)]. Quantitative real-time PCR was performed with the StepOnePlus Real-Time PCR System (Applied Biosystems, Foster City, CA, USA) in triplicates of every sample, in the total volume of 10 µl in each well containing cDNA, TaqMan Universal PCR MasterMix and a TaqMan Gene Expression Assay for the subsequent genes: alpha-1 subunit of a voltage-dependent calcium channel (Cacna1c, assay ID: Rn00709287_m1), alpha-2 and delta subunits of the voltage-dependent Ca^{2+} channel complex (Cacna2d1, Rn01442580_m1), beta-2 subunit of the voltage-dependent Ca^{2+} channel complex (CACNB2, Rn00587789_m1), ryanodine receptor 2 (Ryr2, Rn01470303_m1), calsequestrin 2 (CASQ2, Rn00567508_m1), Na^{+}/Ca^{2+}exchanger (NCX) SLC8A1, Rn04338914_m1), sarco/endoplasmic reticulum Ca^{2+}-ATPase (SERCA2) (Atp2a2, Rn00568762_m1) and phospholamban (PLN, Rn01434045_m1) purchased from Applied Biosystems. Data were normalized to glyceraldehyde-3-phosphate dehydrogenase (GAPDH; assayID: Rn01775763_g1). We calculated the expression levels using by the CT comparative method (2-ΔCT). All results were expressed as values normalized to the average values of the control group.

Statistical analysis

All data were analyzed as mean ± SEM. We used unpaired Student's t-test to compare post-mortem, morphological, hemodynamic parameters and ionic currents of control and trained animals. Asterisks indicate significant differences ($p<0.05$).

4. Results

Echocardiographic results

The echocardiographic results are shown in Table 1. Compared with the control group, the resting heart rate (HR) of the trained group was significantly lower. Echocardiography also showed significant myocardial hypertrophy, and the thickness of the anterior and posterior walls of the left ventricle (LV) during systole and diastole and the LV mass index also increased. Left ventricular end-diastole was unchanged and end-systolic size reduction resulted in a considerably higher fractional shortening in trained rats, suggesting increased systolic performance (Figure 5).

	Control (n=18)	**Trained (n=18)**	**p**
HR, beat/s	371±6	314±8	<0.05
LVAWTd, mm	2.07±0.04	2.31±0.05	<0.05
LVAWTs, mm	3.16±0.07	3.67±0.09	<0.05
LVPWTd, mm	1.98±0.06	2.24±0.06	< 0.05
LVPWTs, mm	2.82±0.09	3.23±0.09	< 0.05
LVEDD, mm	7.66±0.10	7.53±0.13	0.415
LVESD, mm	4.62±0.10	4.17±0.18	< 0.05
FS, %	38.9±1.4	45.4±1.8	< 0.05
LV mass, g	1.19±0.04	1.41±0.05	< 0.05
LV mass index, g/kg	2.38±0.07	3.21±0.10	<0.05

	Control (n=12)	**Trained (n=12)**	**p**
Tibia lenght, mm	45.6±0.8	45.1±0.7	0.62
Body weight, g	501.12±12.2	428.85±5.86	<0.05
Heart weight, g	1.91±0.08	2.18±0.08	<0.05
Heart weight index, g/kg	3.83±0.10	5.1±0.20	<0.05
Ventricles weight, g	1.41±0.06	1.63±0.05	<0.05
Ventricles index, g/kg	2.48±0.10	3.81±0.12	<0.05

Table 1. Echocardiographic and morphometric data

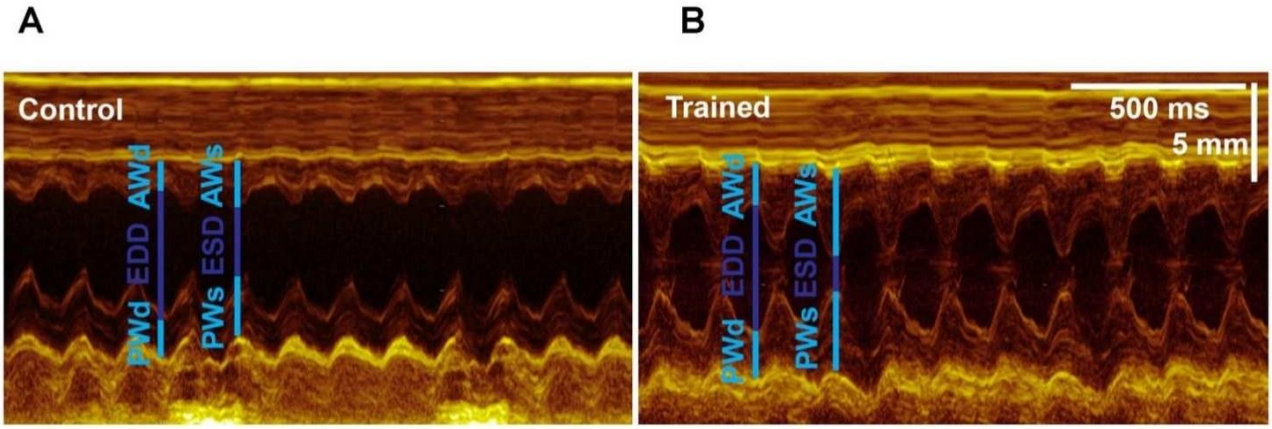

Figure 5. Representative left ventricular (LV) M-mode recordings from a control and a trained animal. Exercise training is related to an increase in wall thickness and a significant decrease in the end-systolic diameter of the left ventricle.

Morphometric results and Langendorff-perfused experiments

Table 1 shows the morphological data of training-induced cardiac hypertrophy measured at the end of the training program. The unchanged length of tibia confirmed that the control animals and the trained animals were at the same age. The body weight of sedentary rats was significantly larger, and the physical dimensions of the heart including total weight, body mass index, and ventricles weight and index of the trained rats were significantly increased.

Table 2 illustrates the obtained results in the ex-vivo Langendorff experiment. Compared with the control group, the ECG recordings showed that the long-term R-R variability of the training group increased significantly, while the R-R interval between the two groups remained unchanged. Similarly, there are no differences in QT intervals, while long-term QT variability was decreased in trained rats. Consistent with ECG data, it was found that the left ventricular end-systolic pressure became greater in the trained group (Figure 6a, b). Arrhythmia analysis showed that the extra ventricular beats increased significantly in the trained group (21±4 vs 75±21 extra beats, $n = 12$, $p < 0.05$). There were no significant differences between the two groups in bigeminy (6±2 vs 10±2 extra beats, n=12) or salvos (2±1 vs 3±1 unison, n=12; Figure 7).

	Control (n=12)	Trained (n=12)	p
RR, ms	210.8±5.76	214.17±5.36	0.670
RRSTV, ms	0.77±0.13	1.25±0.36	0.21
RRLTV, ms	0.65±0.06	1.57±0.51	<0.05
QT, ms	87.24±7.46	85.43±4.41	0.839
QTSTV, ms	0.310±0.03	0.258±0.06	0.44
QTLTV, ms	0.506±0.03	0.363±0.05	<0.05
LVESP, mmHg	108.24±6.49	133.56±6.53	< 0.05
LVEDP, mmHg	4.69±0.93	4.58±0.44	0.924
LVDP	103.55±6.35	128.98±6.19	< 0.05

Table 2. Echocardiographic and left ventricular pressure parameters measured from isolated, Langendorff -perfused rat hearts

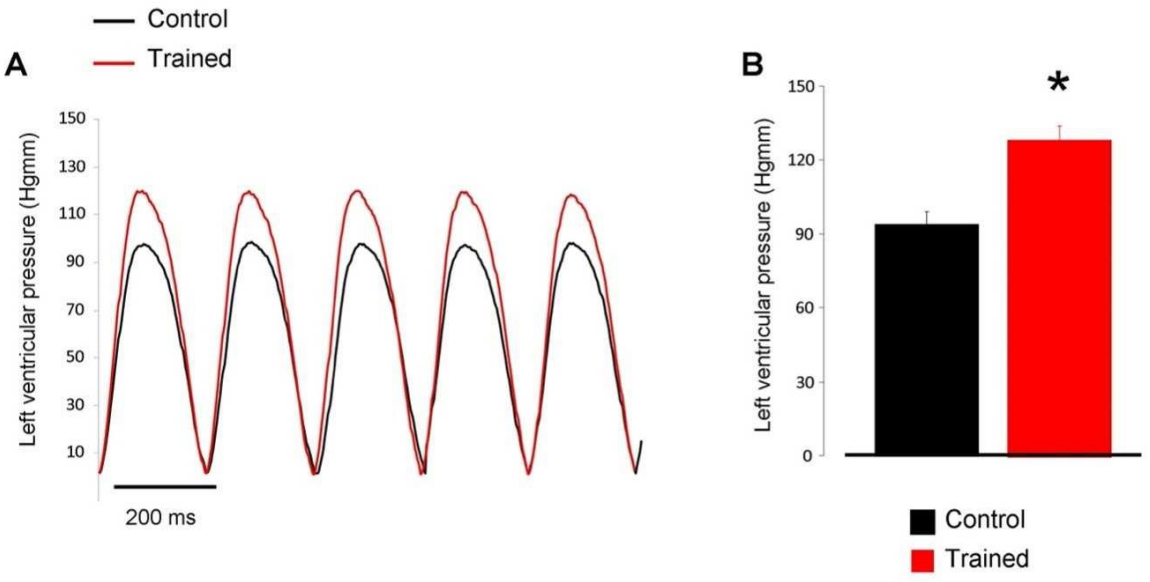

Figure 6. Panel (A) shows representative left ventricular developed pressure curves in control (black trace) and in trained rats (red trace) during Langendorff-perfused measurement. As shown by the bar graph in panel (B), the left ventricular pressure in the trained group (red bar) was significantly higher.

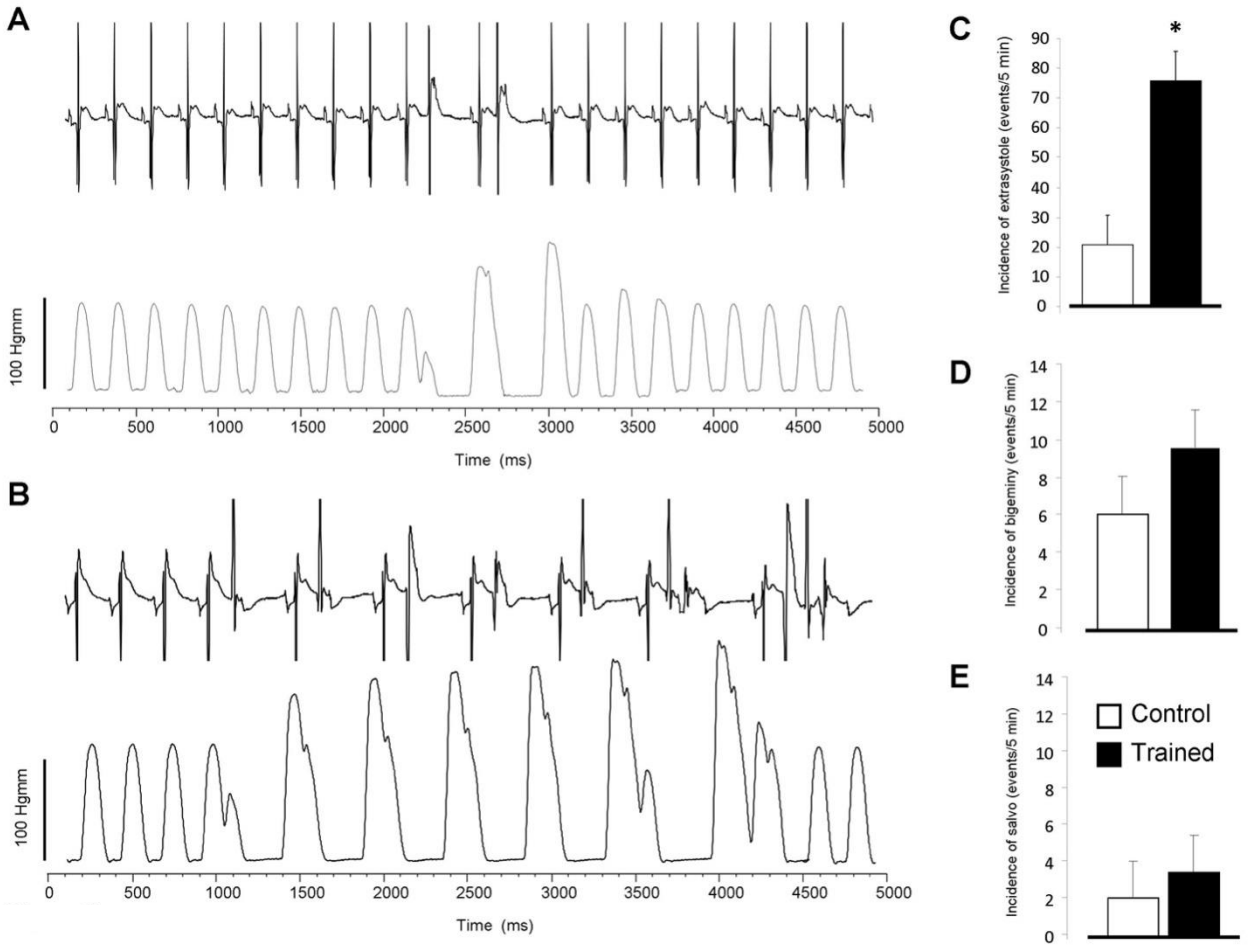

Figure 7. During Langendorff-perfusion, the incidence of arrhythmia between the training group and the control group was measured by the parallel registration of the ECG and the left ventricular pressure. Representative electrocardiogram and pressure curve of the control group show few ectopic events (panel A). In the trained group (panel B), the number of extrasystoles were significantly increased. Panels (C–E) compare the extrasystole, bigeminy and salvo incidences of the control group and the trained group, respectively.

Figure 8 illustrates further analysis of the characteristics of premature beats. In all experiments, a 5-minutes-long section was evaluated. The data analysis involved only single extra beats that were clearly separated, and bigeminy and salvo were excluded. Figure 8, panel A represents the distribution of a single extra heartbeat/steady-state heartbeat amplitude ratio in the function of the corresponding coupling interval. The coupling interval was determined as the time between the initiation of the extra beat and the initiation of the upstroke of the previous steady-state beat. Compared with the control group, the coupling interval were significantly shorter in the trained group (red dots in panel A and red bars in panel B; 143.7±1.86 ms vs 166.5±4.12 ms; panel b; $p < 0.05$, $n = 135$ and 63 respectively, both from 12 animals). The amplitude ratios of premature beats/steady-state beats were compared at 3 discrete coupling intervals, where we could collect a

sufficient amount of data (130, 141, and 149 ms). Since the control group produced only a small number of additional beats during these time intervals, we extended the analysis of the control group to 10 minutes. As shown in panel C, the ratio of amplitudes was slightly larger in trained animals at 141 ms (0.64±0.04 vs. 0.51±0.03, $p < 0.05$, n = 18 and 12, from 12 respectively, both from 12 animals,) and 149 ms (0.76±0.03vs 0.58±0.04, $p < 0.05$, n = 12 and 13 respectively both from 12 animals), compared with control.

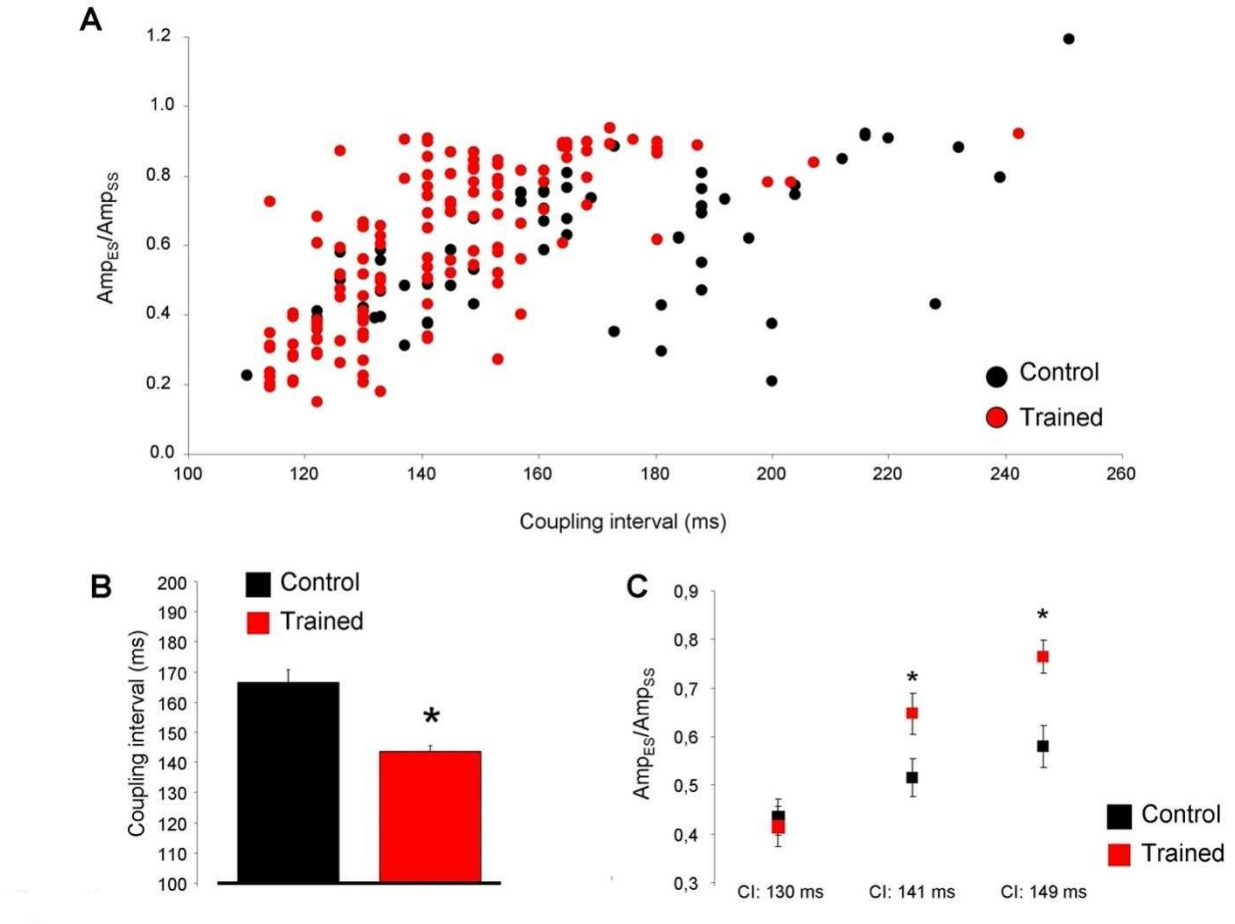

Figure 8. Analysis of the premature beats of Langendorff-perfused heart (A, B) indicates that the trained group had a shorter coupling interval and a larger amplitude of extra beats (C) compared with the control group.

Spontaneous Ca^{2+} release measurement

Spontaneous Ca^{2+} release was measured in single cardiomyocytes field-stimulated at 4 Hz for 15 s. Although we observed spontaneous Ca^{2+} release events in both groups, the amount of spontaneous

events within the trained group increased significantly (11.7 ± 3.9 events /15 s and 2.7 ± 1.2 events /15 s, n = 10/5 and 10/5respectively, p <0.05), (Figure 9).

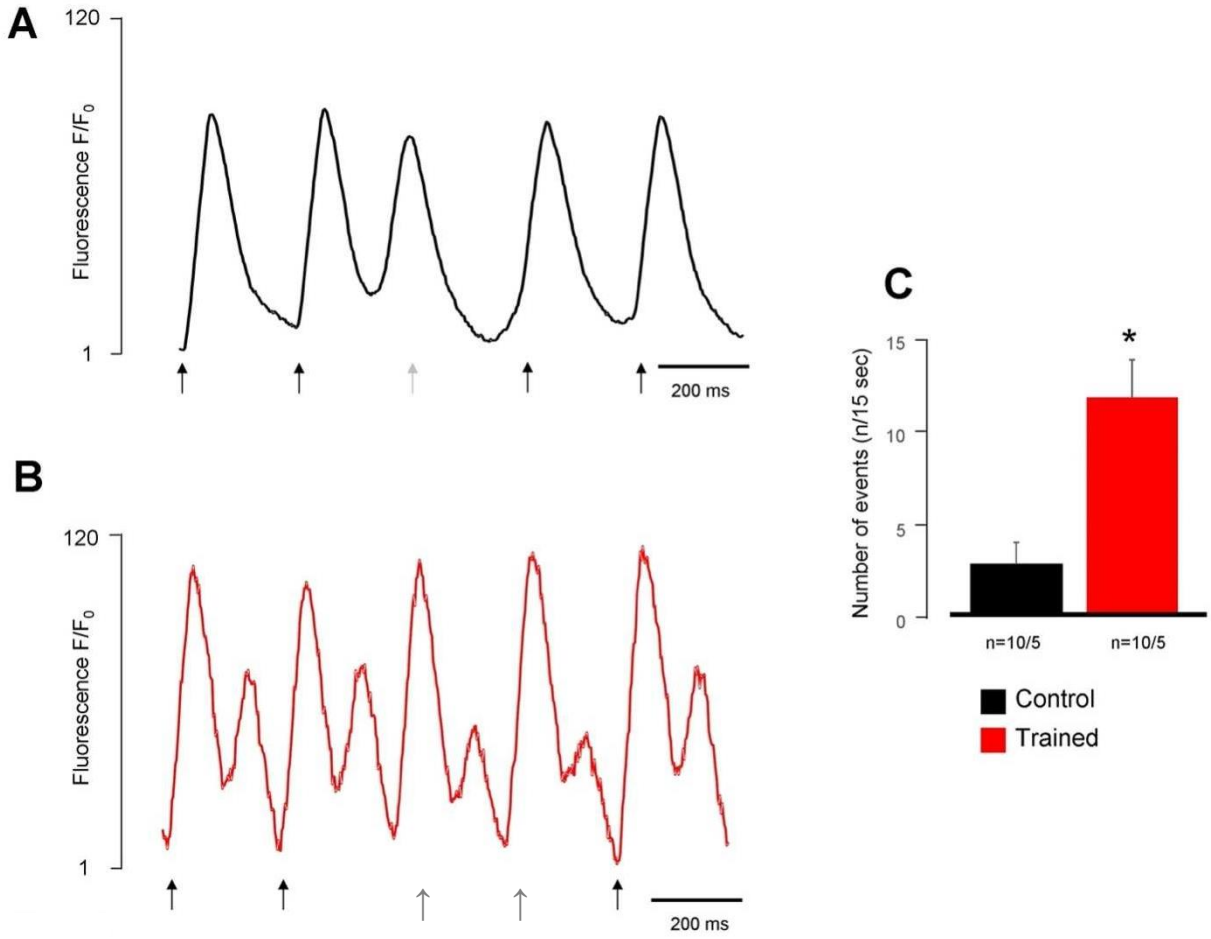

Figure 9. Comparison of spontaneous Ca $^{2+}$ release in control (A) and trained (B) rats at a stimulation frequency of 4 Hz. Black arrows mark the electrical stimulation, and gray arrows indicate the spontaneous event. We found that compared with the control group, the spontaneous Ca^{2+} release was larger in the trained group.

Measurements of Ca^{2+} transient, SR Ca^{2+} content and $I_{Ca,L}$

Figure 10A demonstrates the voltage-current relationship of L-type Ca^{2+} current ($I_{Ca,L}$) within the presence of buffered intracellular solution. 50 ms long depolarization pulse with a holding potential from -80 mV to -40 mV were applied to inactivate the sodium current, and then voltage steps to 30 mV were applied to induce a Ca^{2+} current. Superimposed traces and bar graphs (at 10 mV) show that the $I_{Ca,L}$ density was not different between groups (n = 5/4 and n = 5/4). Rapid application of 10 mM caffeine (Figure 10B) with a holding potential of -80 mV was used to estimate the SR Ca^{2+}

content. Before caffeine is applied, 10 consecutive pulses from -80 to 0 mV were used to reach a steady-state SR Ca^{2+} level. We analyzed the integral of caffeine-induced NCX current as an indicator of SR Ca^{2+} content and we found that SR Ca^{2+} content was significantly increased in the trained group compared to the control group (-1.84±0.4 (pA * s)/ pF vs-1.25±0.5 (pA * s)/ pF n=8/5 and 8/4, respectively, $p < 0.05$) (Figure 10B). Ca^{2+} transients were measured at a pacing frequency of 4 Hz to approximate the physiological heart rate of rats (Figure 10C). We found that the Ca^{2+} transient amplitudes obtained from the trained group were increased (trained: 114.1±8 AU vs. control: 91.1±10 AU, n = 10/5 and 10/5, respectively, $p < 0.05$, Figure 10D). The half-decay time of the Ca^{2+} transients, measured at 50% of the transient decay, was faster (118.7 ± 4 ms and 140.8 ± 5 ms, n = 10, $p < 0.05$, Figure 10e) in the trained group.

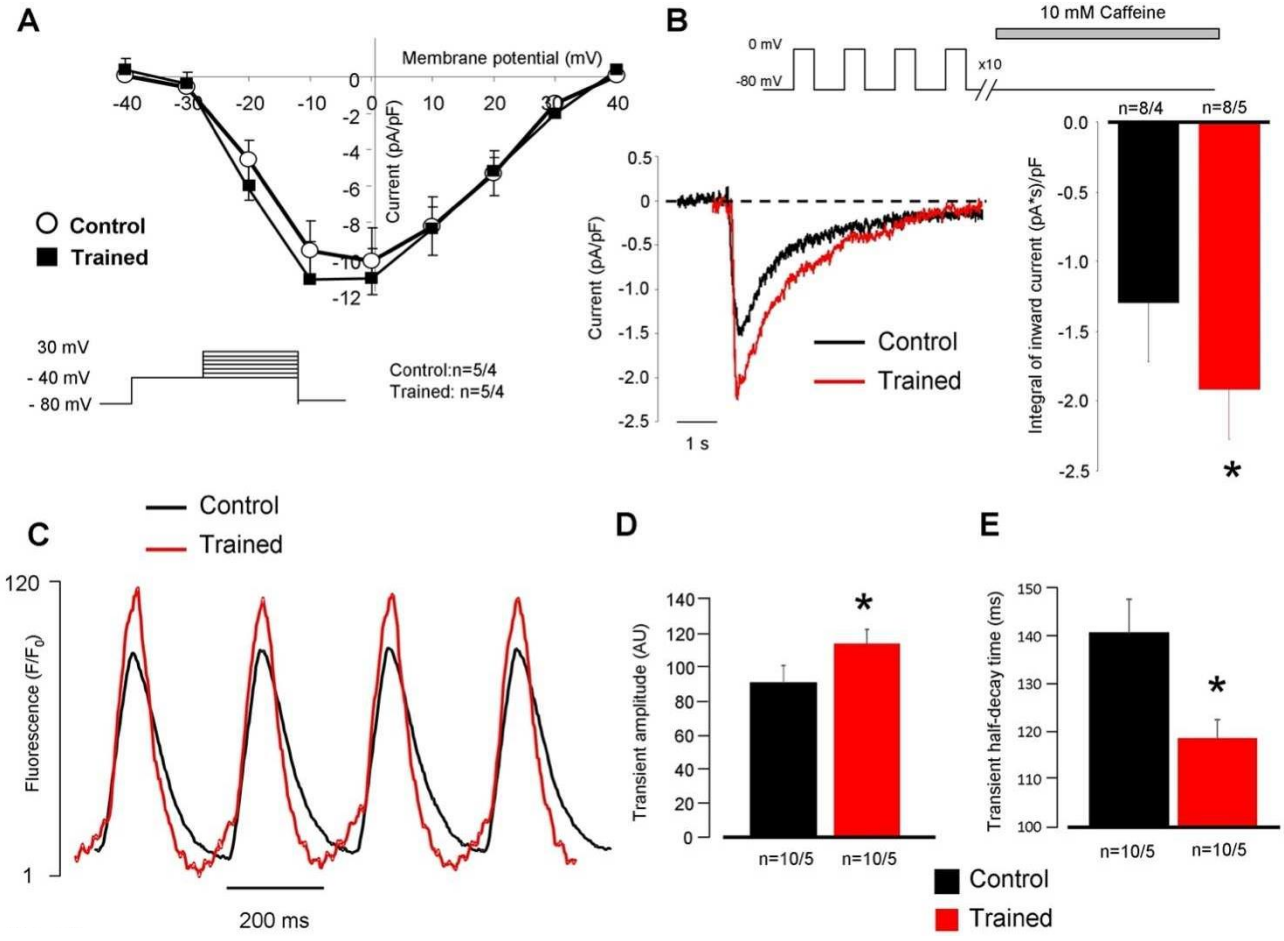

Figure 10. Investigation of Ca^{2+} handling on isolated cells. Panel (A) shows the current-voltage relationship of L-type Ca^{2+} current between the control and the trained group. Panel B illustrates the larger inward current due to the application of 10 mM caffeine. Panel C, D reports larger Ca^{2+} transient amplitude in the trained rats (red trace) compared to the control (black trace). Panel E indicates faster transient relaxation kinetics within the case of trained animals.

Ion channel gene expression level

The expression levels of genes involved in Ca^{2+} handling were analyzed by qRT-PCR. We found that the relative mRNA expression of ryanodine receptor 2 and calsequestrin were significantly higher in the trained group compared to the control. There were no differences in the mRNA levels of NCX, SERCA2, LTCC genes and PLN (Figure 11).

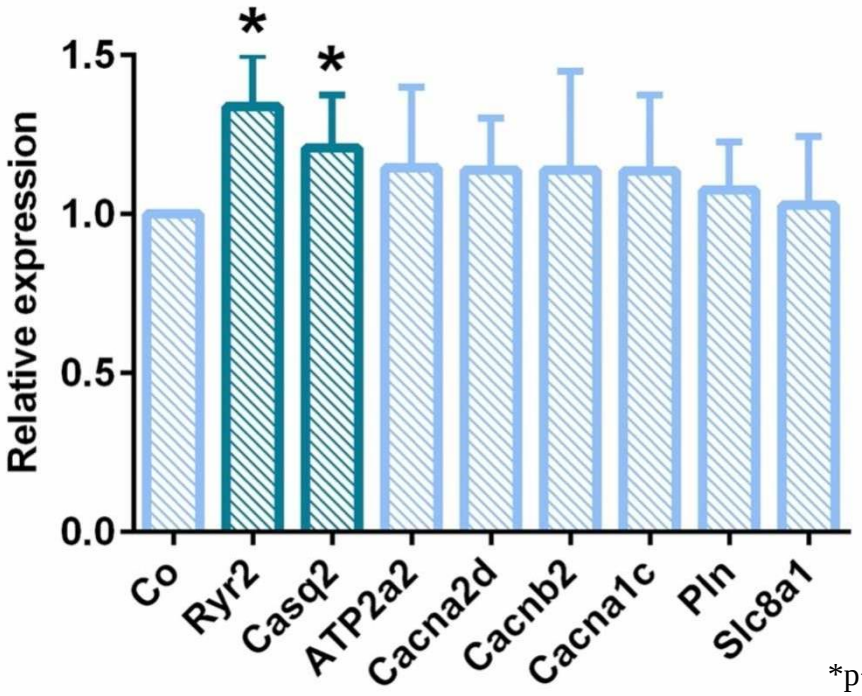

Figure 11. Myocardial gene expression analysis.

Phosphorylation of PKA C, PLN and SERCA2 protein expression

The pan and phosphorylated forms of key proteins involved in regulation of Ca^{2+} homeostasis, including PKA C, PLN and SERCA2 protein expression, were compared by using left ventricular biopsies from training and control rats. In the trained animals the phosphorylation of phospholamban oligomers was significantly increased. There were no significant differences in PKA C phosphorylation and SERCA expression between the two groups (Figure 12).

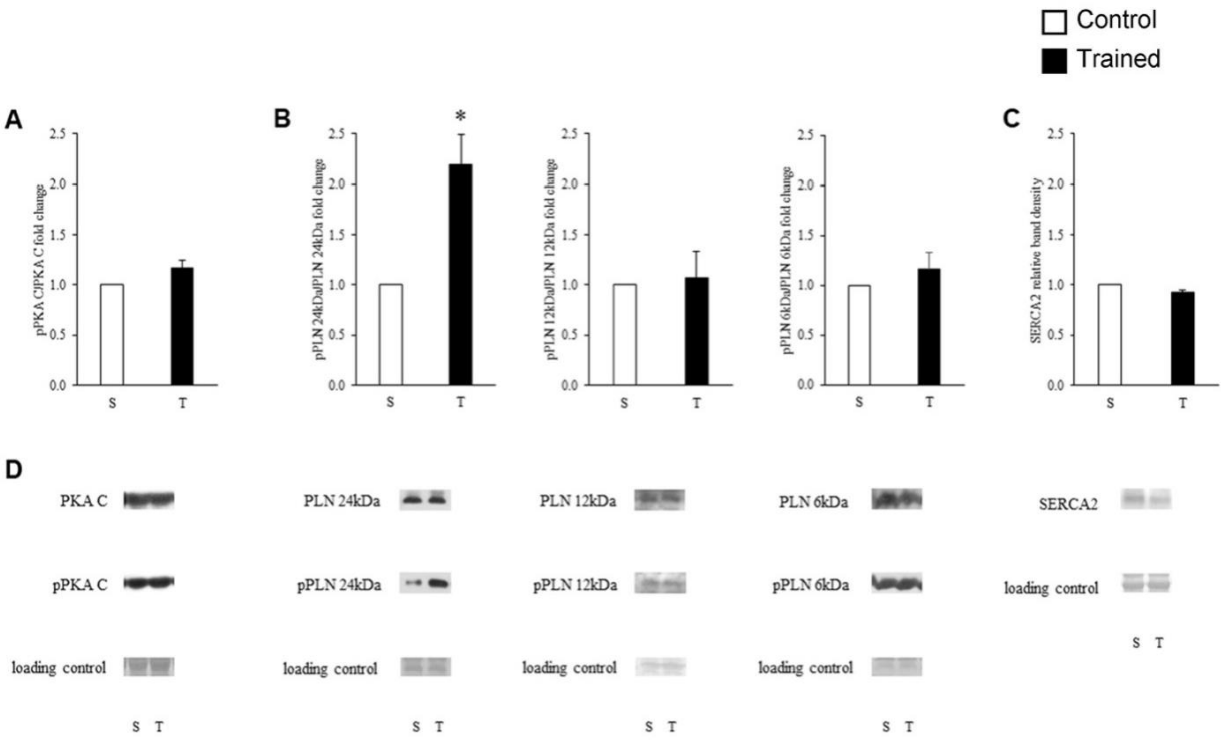

Figure 12. The effect of training on SERCA phosphorylation pathway. Expression of pan and phosphorylated PKA C (a), PLN (b) and SERCA2 (c) proteins.

Repolarizing potassium currents: I_{to} and I_{K1}

In the presence of 10 mM EGTA and I_{CaL} inhibition, the possible remodeling-induced I_{to} and I_{K1} density changes were examined. From a holding potential of -80 mV, (Figure 13A, C) voltage steps were used up to 60 mV by 300 ms-long to measure Ito. As shown in the original current trace (Figure 13A) and the current-voltage relationship (Figure 13C), the currents were identical between groups. $I_{K1}$was measured by using a 300 ms-long depolarizing pulses between -140 and -30 mV from a holding potential of -80 mV. Similarly to the I_{to}, there was no difference in I_{K1} between the control group and the trained group (Figure 13B, D). Compared with control cells, the average cell size of the cardiomyocytes of the trained animals (estimated from the whole cell capacitance obtained from our patch clamp experiment) was increased significantly (281±12 pF vs 232±15 pF, n = 20, $p < 0.05$) (Figure 10A and 13).

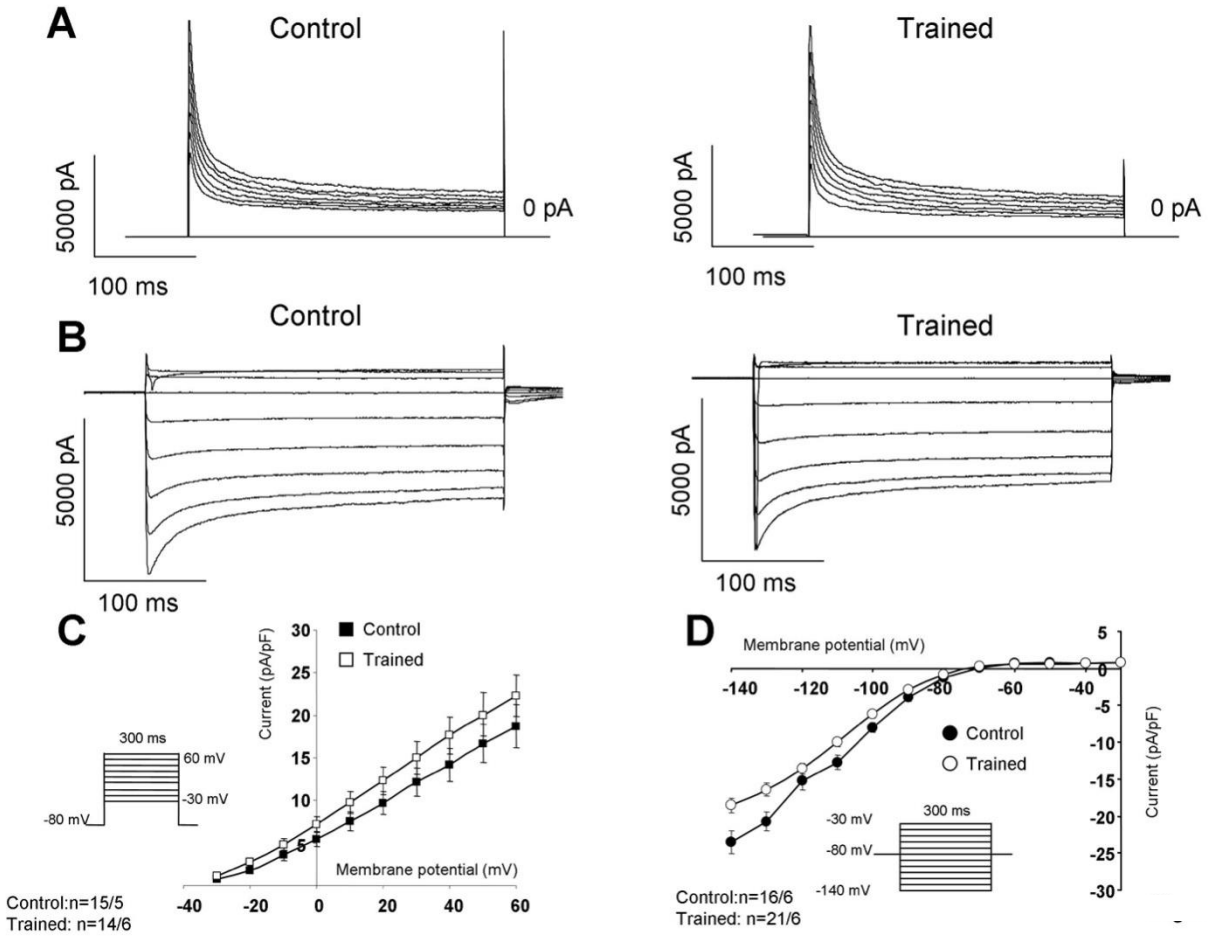

Figure 13. Investigation of the main repolarizing potassium currents on isolated cells. As shown in the representative current traces (Panel A,B) and current-voltage diagrams (Panel C), the currents between the control group and the training group were found identical.

The effect of ibuprofen on the rapid delayed rectifier (I_{Kr}) potassium current in rats and dogs

It was mentioned in the Introduction section that different drugs could have marked effect on the repolarization kinetics. It was previously demonstrated that a non-steroidal anti-inflammatory (NSAID) compound, diclofenac, inhibited the I_{Kr}, and lengthened the action potential duration when the repolarization reserve was attenuated [75]. Since NSAID (such as ibuprofen), and other compounds with extracardiac indication are often used by top athletes, it is feasible that they increase the arrhythmogenic propensity during a training-induced electrical remodeling. Since our rat model has markedly different repolarization process than the human, furthermore it did not show difference between control and trained groups, it is unsuitable for the analysis of drug-induced

repolarization changes. Therefore, our further experiments were performed on normal dogs that have comparable repolarization process to the human.

At first, the NSAID compound ibuprofen was investigated in 250 µM (51.5µg/ml) concentration in canine ventricular myocytes by using the whole-cell configuration of the patch clamp technique. The applied concentration of solvent DMSO did not affect the amplitude or kinetics of the measured transmembrane ion current (Figure 14). However, in canine ventricular myocytes, 250 µM ibuprofen significantly reduced the rapid delayed rectifier (I_{Kr}, Figure 14C) potassium current [76].

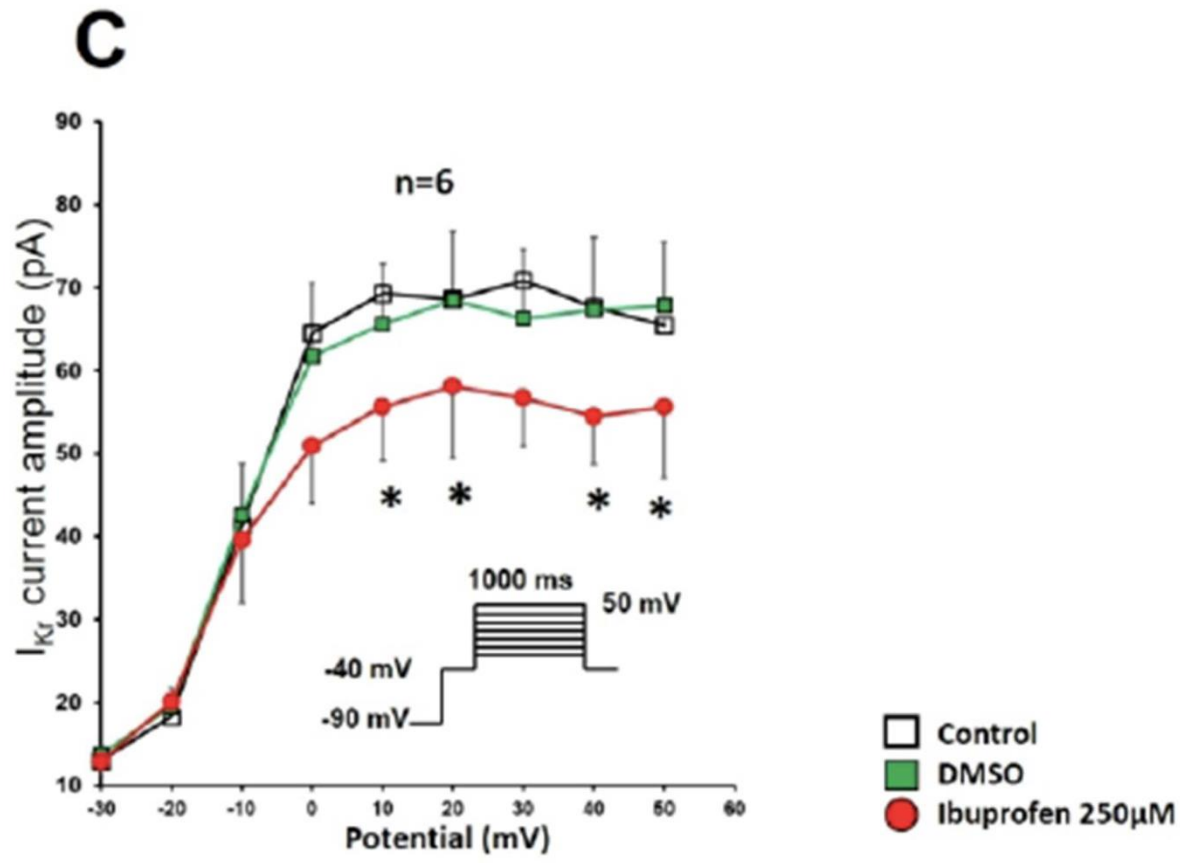

Figure 14. shows the effects of the solvent DMSO at 1% and ibuprofen at 250 µM on the rapid delayed rectifier potassium currents (I_{Kr}) respectively in canine ventricular myocytes; the insets show the applied voltage protocols. Values are means ± SEM, asterisks indicate $p<0.05$, ANOVA for repeated measurements followed by Bonferroni's post-hoc test.

Effects of cisapride and terfenadine on IKr current in rabbits

In the next experimental set, the antihistamine terfenadine, and the gastroprokinetic agent cisapride was also analyzed on the I_{Kr} current, by using rabbit ventricular myocytes and whole-cell patch clamp technique at 37°C. We found that both cisapride and terfenadine significantly reduces the I_{Kr}. (Figure 15) [77].

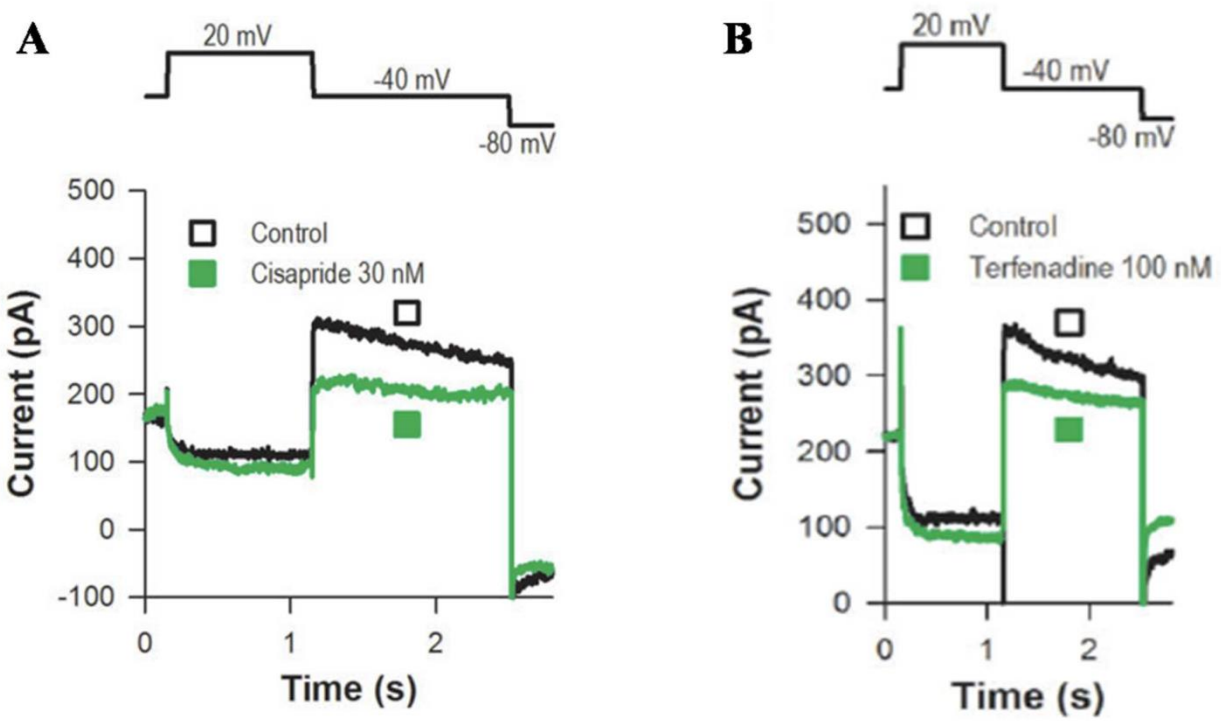

Figure 15. Representative I_{Kr} current traces obtained from rabbit left ventricular muscle cell treated with 30 nM cisapride (A) and 100 nM terfenadine (B). The currents were measured using the voltage protocols shown at the top of panels (A–B).

5. Discussion

In this work, we investigated the structural and electrical remodeling induced by intensive exercise training in rats, as well as the effects of certain drugs on the main repolarizing current (I_{Kr}). The most important findings of the study are: (i) ventricular hypertrophy and increased cardiac output in swimming trained rats are coupled with the enhancement of arrhythmogenic triggering activities; (ii) these arrhythmogenic events suggest delayed afterdepolarizations through increased SR Ca^{2+} content as an underlying mechanism. (iii) the improved SR Ca^{2+} content is maintained by increased expression of the phosphorylated form of phospholamban, and increased level of calsequestrin [3]; (iv) several drugs, potentially used by top athletes may contribute to the increased arrhythmogenic propensity.

Our results show that the physiological adaptation of Ca^{2+} homeostasis beyond providing increased cardiac output demand during exercise provides a potential source of harmful arrhythmias. In our study, compared to control rats, the key repolarization parameters and the repolarization inhomogeneity [2] were not significantly different in trained group, which indicated that there was no change in the arrhythmia substrate in the rat model. However, the increased triggering activity observed within the rat model of athlete's heart may help to explain the development of life-threatening arrhythmias among top athletes.

Increased vagal tone may be the basis of sinus bradycardia

Sinus bradycardia may be a hallmark feature of the athlete's heart [78, 79], and was supported by several animal training models [80-82]. Sinus bradycardia is often explained by the consequence of increased vagal tone [83], however, D'Souza et al [81] demonstrated a reduction in pacemaker (funny) current (I_f) after the training period of running-trained rats. In our experiments, sinus bradycardia was found under setting of in-vivo echocardiographic measurements (Table 1), but we did not observe sinus bradycardia in Langendorff-perfused isolated hearts (Table 2) where the heart is denervated, i.e. the sinus-frequency is exclusively regulated by the sinus-node automaticity. Therefore, our results indicate increased vagal tone as underlying mechanism of sinus bradycardia in the swimming-trained rat model. The obvious discrepancy between our study and D'Souza [81] may be due to the differences in training methods (between swimming and treadmill running).

Exercise training is coupled with improved cardiac output and enhanced arrhythmia propensity

Intensive physical training requires increased cardiac output to satisfy the enhanced metabolic demand of the body [3]. This could be attributed to remodeling of several components of Ca^{2+} homeostasis [84-86]. In line with this, the results of our in vivo and in vitro studies clearly showed that the left ventricular pressure increased in the training group (Figure 6), which was closely related to the higher incidence of ventricular spontaneous beats during Langendorff-perfusion (Figure 7). ECG analysis identified the ventricular origin of the extra beats measured in isolated hearts, suggesting delayed afterdepolarizations mediated by Ca^{2+}-overload as the underlying mechanism. In this case, due to the larger SR Ca^{2+} content, the premature beats are dominated by the facilitated forward NCX activity [72, 87, 88]. In trained animals, the shorter coupling intervals of premature beats may endorse this hypothesis, as the higher SR Ca^{2+} content due to enhanced Ca^{2+} sequestration may lead to earlier spontaneous events (Figure 8) [3]. As a consequence, in field-stimulated Ca^{2+} transient measurements in isolated cells, a significantly greater spontaneous Ca^{2+} release activity was found in the trained group, which may lead to Ca^{2+}-driven extra depolarization mediated by NCX (Figure 9).

The complex remodeling of SR proteins caused by physical training may lead to higher Ca^{2+} content

Experiments with rapid application of caffeine showed that the Ca^{2+} content of SR in trained animals was significantly higher (Figure 10b). The actual content of the SR depends on the dynamic balance between the uptake (through SR Ca-ATPase, SERCA) and the release through the ryanodine receptors. Phospholamban (PLN) is a regulatory protein of SERCA, which binds to SERCA in its unphosphorylated form reducing its activity. PLN exists in the form of monomers and pentamers. While it is suggested that the monomeric form inhibits SERCA [89], the role of the pentamers is still unclear [3]. This model is based on the observation, that monomers are better inhibitors of PLN [90, 91], but it was also found that there was a dynamic balance between monomer and pentameric forms. In addition, the phosphorylation of SERCA or the increased cytosolic Ca^{2+} level augmented the proportion of the pentamer pool at the expense of the monomer pool [92]. Overall, several independent reports claim that SERCA may interact with the oligomeric forms of PLN, and the presence of oligomers seems to provide a functional advantage for the SERCA-PLN interaction [93-97]. Based on these findings, our results indicate that the increase of PLN pentameric form is correlated with improved SERCA kinetics, providing faster decay of Ca^{2+}

transients, bigger Ca^{2+} content, and possible Ca^{2+} overload of the sarcoplasmic reticulum (Figure 10b-e) that may be the trigger source of arrhythmias via the spontaneous Ca^{2+} release. In addition, we found that the expression level of calsequestrin an ubiquitous luminal Ca^{2+} binding protein [98] (Figure 11) was increased. It has been suggested that CASQ binds to ryanodine receptors through triadin or junctin, and when free [Ca^{2+}] is low in SR, the possibility of ryanodine receptors being opened is reduced. When SR [Ca^{2+}] increases, CASQ dissociates from the ryanodine receptor increasing its open probability [99]. Studies have shown that CASQ can directly determine the magnitude and duration of the Ca^{2+} release. The release of Ca^{2+} from SR [100] provides a local source of Ca^{2+} that can be released and plays an important role in ryanodine receptor gating. It was further proved that CASQ modulated ryanodine receptor function through the interaction of two other intraluminal proteins, triadin and junctin [101-103]. Our results show that the increased SR Ca^{2+} content can be maintained by increased expression level of CASQ, thereby providing the molecular basis for improved cardiac output via enhancing the storage capacity and the amount of releasable $Ca^{2+}$from the SR.

Identical repolarizing currents between the trained and control animals

The crucial repolarizing currents, like I_{to} and I_{K1}, exerted no difference between cardiomyocytes isolated form trained and control groups (Figure 13). In our rat model, exercise-induced electrophysiological remodeling is limited to Ca^{2+} homeostasis and arrhythmias were promoted by increased triggering activity due to larger SR Ca^{2+} content [3]. However, it is important to note that the remodeling of potassium channels might occur in large mammals and may severely alter the transmural dispersion of potassium currents, providing an increased arrhythmogenic substrate. Considering that several potassium channels show Ca^{2+} dependence in some extent [104], the indirect influence of Ca^{2+} homeostasis alterations during repolarization may also play an important role, which may explain the increased long-term ECG QT variability in the trained rats (Table 2) [3].

Drug-induced repolarization attenuation

It is known that competitive athletes often take several types of medications principally non-steroidal anti-inflammatory drugs (NSAID) to relieve pain caused by injuries. It is important to note that NSAID drugs could influence the repolarization [75] therefore may represent an additional risk factor for the arrhythmogenesis of the athlete's heart. In our study [76] we demonstrated that in canine ventricular myocytes ibuprofen, an often used NSAID drug, significantly inhibits the I_{Kr}

(Figure 14) that may cause attenuated repolarization reserve. Similarly, two further drugs, the antihistamine terfenadine and the gastroprokinetic drug cisapride also suppressed the I_{Kr} in rabbit ventricular muscle cells. Since it was reported earlier that intensive physical training induces repolarization inhomogeneity it is feasible that ordinary drugs - having no effect on healthy heart - may aggravate repolarization dispersion and arrhythmogenic substrate.

6. Conclusion

Our results obtained from swimming trained rats lead us to the conclusion that sudden cardiac death related to training-induced remodeling could be based on the unfavorable results of Ca^{2+} homeostasis adaptation. The increased Ca^{2+} content of SR provides larger available Ca^{2+} when it is released, which is an adaptive response of Ca-cycling to meet the improved cardiac output demand during exercise. However, the increased Ca^{2+} load of the SR in the trained hearts may also serve as a potential arrhythmia trigger source, leading to spontaneous Ca^{2+} release events. During training, the spontaneous Ca^{2+} releases might be facilitated by increased sympathetic tone or electrolyte disturbances, causing extra Ca^{2+} load [3].

Our results obtained from dogs and rabbits indicate that different ordinary drugs could influence the potassium channels, aggravating repolarization inhomogeneity and providing/worsening arrhythmogenic substrate.

Taken together our results, the improved arrhythmogenic susceptibility of the athlete's heart could be attributed to the electrical remodeling of the heart but other factors that are closely coupled to the lifestyle of the competitive athletes – such as excessive drug use - could further aggravate the arrhythmia propensity.

7. Limitations

(i) Our rat model did not show changes of the repolarization process, so the transmural dispersion and therefore changes in arrhythmic substrates cannot be observed. This observation may derive from the species-dependent characteristics of repolarization. Since the repolarization of the action potential in rats depends on I_{to} and I_{K1}, I_{Kur} (Kv1.5), the action potential prolonging effect of a possible I_{Kr} and I_{Ks} downregulation cannot be detected and should be studied in other species such as rabbit, guinea-pig or dog. (Ii) In addition, compared to larger species (including human), the removal of Ca^{2+} from the intracellular space in rats depends on SERCA activity.

8. References

[1] Wasfy MM, Hutter AM, Weiner RB. Sudden Cardiac Death in Athletes. Methodist DeBakey cardiovascular journal. 2016;12:76-80.

[2] Varro A, Baczko I. Possible mechanisms of sudden cardiac death in top athletes: a basic cardiac electrophysiological point of view. Pflugers Archiv : European journal of physiology. 2010;460:31-40.

[3] Gazdag P, Oravecz K, Acsai K, Demeter-Haludka V, Ordog B, Szlovak J, et al. Increased Ca(2+) content of the sarcoplasmic reticulum provides arrhythmogenic trigger source in swimming-induced rat athlete's heart model. Scientific reports. 2020;10:19596.

[4] Bers DM. Cardiac excitation-contraction coupling. Nature. 2002;415:198-205.

[5] Wier WG, Balke CW. Ca(2+) release mechanisms, Ca(2+) sparks, and local control of excitation-contraction coupling in normal heart muscle. Circulation research. 1999;85:770-6.

[6] Eisner DA, Choi HS, Diaz ME, O'Neill SC, Trafford AW. Integrative analysis of calcium cycling in cardiac muscle. Circulation research. 2000;87:1087-94.

[7] Eisner DA, Caldwell JL, Kistamas K, Trafford AW. Calcium and Excitation-Contraction Coupling in the Heart. Circulation research. 2017;121:181-95.

[8] Wasserstrom JA, Vites AM. The role of Na(+)-Ca2+ exchange in activation of excitation-contraction coupling in rat ventricular myocytes. The Journal of physiology. 1996;493 (Pt 2):529-42.

[9] Bers DM, Merrill DB. The role of Ca influx in cardiac muscle excitation-contraction coupling. Assessment by extracellular Ca microelectrodes. Advances in myocardiology. 1985;6:49-57.

[10] Dibb KM, Eisner DA, Trafford AW. Regulation of systolic [Ca2+]i and cellular Ca2+ flux balance in rat ventricular myocytes by SR Ca2+, L-type Ca2+ current and diastolic [Ca2+]i. The Journal of physiology. 2007;585:579-92.

[11] Varro A, Tomek J, Nagy N, Virag L, Passini E, Rodriguez B, et al. Cardiac Transmembrane Ion Channels and Action Potentials: Cellular Physiology and Arrhythmogenic Behavior. Physiological reviews. 2020.

[12] Puglisi JL, Bassani RA, Bassani JW, Amin JN, Bers DM. Temperature and relative contributions of Ca transport systems in cardiac myocyte relaxation. The American journal of physiology. 1996;270:H1772-8.

[13] Hoffman BF, Rosen MR. Cellular mechanisms for cardiac arrhythmias. Circulation research. 1981;49:1-15.

[14] Luo CH, Rudy Y. A dynamic model of the cardiac ventricular action potential. II. Afterdepolarizations, triggered activity, and potentiation. Circulation research. 1994;74:1097-113.

[15] Luo CH, Rudy Y. A dynamic model of the cardiac ventricular action potential. I. Simulations of ionic currents and concentration changes. Circulation research. 1994;74:1071-96.

[16] Vandersickel N, de Boer TP, Vos MA, Panfilov AV. Perpetuation of torsade de pointes in heterogeneous hearts: competing foci or re-entry? The Journal ofphysiology. 2016;594:6865-78.

[17] Ferrier GR. Digitalis arrhythmias: role of oscillatoryafterpotentials. Progress in cardiovascular diseases. 1977;19:459-74.

[18] Ferrier GR, Moe GK. Effect of calcium on acetylstrophanthidin-induced transient depolarizations in canine Purkinje tissue. Circulation research. 1973;33:508-15.

[19] Verkerk AO, Veldkamp MW, Bouman LN, van Ginneken AC. Calcium-activated Cl(-) current contributes to delayed afterdepolarizations in single Purkinje and ventricular myocytes. Circulation. 2000;101:2639-44.

[20] Uchinoumi H, Yang Y, Oda T, Li N, Alsina KM, Puglisi JL, et al. CaMKII-dependent phosphorylation of RyR2 promotes targetable pathological RyR2 conformational shift. Journal of molecular and cellular cardiology. 2016;98:62-72.

[21] van Oort RJ, McCauley MD, Dixit SS, Pereira L, Yang Y, Respress JL, et al. Ryanodine receptor phosphorylation by calcium/calmodulin-dependent protein kinase II promotes life-threatening ventricular arrhythmias in mice with heart failure. Circulation. 2010;122:2669-79.

[22] Luo M, Anderson ME. Mechanisms of altered Ca(2)(+) handling in heart failure. Circulation research. 2013;113:690-708.

[23] Voigt N, Li N, Wang Q, Wang W, Trafford AW, Abu-Taha I, et al. Enhanced sarcoplasmic reticulum Ca2+ leak and increased Na+-Ca2+ exchanger function underlie delayed afterdepolarizations in patients with chronic atrial fibrillation. Circulation. 2012;125:2059-70.

[24] Gomis-Tena J, Saiz J. Role of Ca2+-dependent Cl- current on delayed afterdepolarizations. A simulation study. Annals of biomedical engineering. 2008;36:752-61.

[25] Liu MB, Ko CY, Song Z, Garfinkel A, Weiss JN, Qu Z. A Dynamical Threshold for Cardiac Delayed Afterdepolarization-Mediated Triggered Activity. Biophysical journal. 2016;111:2523-33.

[26] Chang SH, Chen YC, Chiang SJ, Higa S, Cheng CC, Chen YJ, et al. Increased Ca(2+) sparks and sarcoplasmic reticulum Ca(2+) stores potentially determine the spontaneous activity of pulmonary vein cardiomyocytes. Life sciences. 2008;83:284-92.

[27] Cheng H, Lederer WJ. Calcium sparks. Physiological reviews. 2008;88:1491-545.

[28] Belevych AE, Ho HT, Bonilla IM, Terentyeva R, Schober KE, Terentyev D, et al. The role of spatial organization of Ca(2+) release sites in the generation of arrhythmogenic diastolic Ca(2+) release in myocytes from failing hearts. Basic research in cardiology. 2017;112:44.

[29] Cheng H, Lederer MR, Lederer WJ, Cannell MB. Calcium sparks and [Ca2+]i waves in cardiac myocytes. The American journal of physiology. 1996;270:C148-59.

[30] Niggli E, Lederer WJ. Voltage-independent calcium release in heart muscle. Science. 1990;250:565-8.

[31] Nivala M, de Lange E, Rovetti R, Qu Z. Computational modeling and numerical methods for spatiotemporal calcium cycling in ventricular myocytes. Frontiers in physiology. 2012;3:114.

[32] Marshall KD, Muller BN, Krenz M, Hanft LM, McDonald KS, Dellsperger KC, et al. Heart failure with preserved ejection fraction: chronic low-intensity interval exercise training preserves myocardial O2 balance and diastolic function. Journal of applied physiology. 2013;114:131-47.

[33] O'Keefe JH, Patil HR, Lavie CJ, Magalski A, Vogel RA, McCullough PA. Potential adverse cardiovascular effects from excessive endurance exercise. Mayo Clinic proceedings. 2012;87:587-95.

[34] Prior DL, La Gerche A. The athlete's heart. Heart. 2012;98:947-55.

[35] Olah A, Kovacs A, Lux A, Tokodi M, Braun S, Lakatos BK, et al. Characterization of the dynamic changes in left ventricular morphology and function induced by exercise training and detraining. International journal of cardiology. 2019;277:178-85.

[36] Olah A, Matyas C, Kellermayer D, Ruppert M, Barta BA, Sayour AA, et al. Sex Differences in Morphological and Functional Aspects of Exercise-Induced Cardiac Hypertrophy in a Rat Model. Frontiers in physiology. 2019;10:889.

[37] Radovits T, Olah A, Lux A, Nemeth BT, Hidi L, Birtalan E, et al. Rat model of exercise-induced cardiac hypertrophy: hemodynamic characterization using left ventricular pressure-volume analysis. American journal of physiology Heart and circulatory physiology. 2013;305:H124-34.

[38] Maron BJ, Pelliccia A. The heart of trained athletes: cardiac remodeling and the risks of sports, including sudden death. Circulation. 2006;114:1633-44.

[39] Wang Y, Wisloff U, Kemi OJ. Animal models in the study of exercise-induced cardiac hypertrophy. Physiological research. 2010;59:633-44.

[40] Ellison GM, Waring CD, Vicinanza C, Torella D. Physiological cardiac remodelling in response to endurance exercise training: cellular and molecular mechanisms. Heart. 2012;98:5-10.

[41] Kemi OJ, Haram PM, Hoydal MA, Wisloff U, Ellingsen O. Exercise training and losartan improve endothelial function in heart failure rats by different mechanisms. Scandinavian cardiovascular journal : SCJ. 2013;47:160-7.

[42] Pelliccia A, Maron MS, Maron BJ. Assessment of left ventricular hypertrophy in a trained athlete: differential diagnosis of physiologic athlete's heart from pathologic hypertrophy. Progress in cardiovascular diseases. 2012;54:387-96.

[43] Fuller EO, Nutter DO. Endurance training in the rat. II. Performance of isolated and intact heart. Journal of applied physiology: respiratory, environmental and exercise physiology. 1981;51:941-7.

[44] Libonati JR. Cardiac remodeling and function following exercise and angiotensin II receptor antagonism. European journal of applied physiology. 2012;112:3149-54.

[45] Mole PA. Increased contractile potential of papillary muscles from exercise-trained rat hearts. The American journal of physiology. 1978;234:H421-5.

[46] Kemi OJ, Haram PM, Loennechen JP, Osnes JB, Skomedal T, Wisloff U, et al. Moderate vs. high exercise intensity: differential effects on aerobic fitness, cardiomyocyte contractility, and endothelial function. Cardiovascular research. 2005;67:161-72.

[47] Kemi OJ, Haram PM, Wisloff U, Ellingsen O. Aerobic fitness is associated with cardiomyocyte contractile capacity and endothelial function in exercise training and detraining. Circulation. 2004;109:2897-904.

[48] Wisloff U, Loennechen JP, Falck G, Beisvag V, Currie S, Smith G, et al. Increased contractility and calcium sensitivity in cardiac myocytes isolated from endurance trained rats. Cardiovascular research. 2001;50:495-508.

[49] Corrado D, Michieli P, Basso C, Schiavon M, Thiene G. How to screen athletes for cardiovascular diseases. Cardiology clinics. 2007;25:391-7, v-vi.

[50] Basavarajaiah S, Wilson M, Whyte G, Shah A, McKenna W, Sharma S. Prevalence of hypertrophic cardiomyopathy in highly trained athletes: relevance to pre-participation screening. Journal of the American College of Cardiology. 2008;51:1033-9.

[51] Maron BJ. Hypertrophic cardiomyopathy and other causes of sudden cardiac death in young competitive athletes, with considerations for preparticipation screening and criteria for disqualification. Cardiology clinics. 2007;25:399-414, vi.

[52] Pigozzi F, Rizzo M. Sudden death in competitive athletes. Clinics in sports medicine. 2008;27:153-81, ix.

[53] Bos JM, Towbin JA, Ackerman MJ. Diagnostic, prognostic, and therapeutic implications of genetic testing for hypertrophic cardiomyopathy. Journal of the American College of Cardiology. 2009;54:201-11.

[54] Basso C, Corrado D, Thiene G. Arrhythmogenic right ventricular cardiomyopathy in athletes: diagnosis, management, and recommendations for sport activity. Cardiology clinics. 2007;25:415-22, vi.

[55] Ng B, Maginot KR. Sudden cardiac death in young athletes: trying to find the needle in the haystack. WMJ : official publication of the State Medical Society of Wisconsin. 2007;106:335-42.

[56] Thiene G, Corrado D, Basso C. Arrhythmogenic right ventricular cardiomyopathy/dysplasia. Orphanet journal of rare diseases. 2007;2:45.

[57] Basavarajaiah S, Wilson M, Whyte G, Shah A, Behr E, Sharma S. Prevalence and significance of an isolated long QT interval in elite athletes. European heart journal. 2007;28:2944-9.

[58] Kapetanopoulos A, Kluger J, Maron BJ, Thompson PD. The congenital long QT syndrome and implications for young athletes. Medicine and science in sports and exercise. 2006;38:816-25.

[59] Frolov RV, Berim IG, Singh S. Inhibition of delayed rectifier potassium channels and induction of arrhythmia: a novel effect of celecoxib and the mechanism underlying it. The Journal of biological chemistry. 2008;283:1518-24.

[60] Anderson ME, Mazur A, Yang T, Roden DM. Potassium current antagonist properties and proarrhythmic consequences of quinolone antibiotics. The Journal of pharmacology and experimental therapeutics. 2001;296:806-10.

[61] Berul CI, Morad M. Regulation of potassium channels by nonsedating antihistamines. Circulation. 1995;91:2220-5.

[62] De Rose EH. Doping in athletes--an update. Clinics in sports medicine. 2008;27:107-30, viii-ix.

[63] Payne JR, Kotwinski PJ, Montgomery HE. Cardiac effects of anabolic steroids. Heart. 2004;90:473-5.

[64] Pereira-Junior PP, Chaves EA, Costa ESRH, Masuda MO, de Carvalho AC, Nascimento JH. Cardiac autonomic dysfunction in rats chronically treated with anabolic steroid. European journal of applied physiology. 2006;96:487-94.

[65] Stauffer BL, Konhilas JP, Luczak ED, Leinwand LA. Soy diet worsens heart disease inmice. The Journal of clinical investigation. 2006;116:209-16.

[66] Csaky I, Fekete S. Soybean: feed quality and safety. Part 1: biologically active components. A review. Acta veterinaria Hungarica. 2004;52:299-313.

[67] Xin HB, Senbonmatsu T, Cheng DS, Wang YX, Copello JA, Ji GJ, et al. Oestrogen protects FKBP12.6 null mice from cardiac hypertrophy. Nature. 2002;416:334-8.

[68] Zitron E, Scholz E, Owen RW, Luck S, Kiesecker C, Thomas D, et al. QTc prolongation by grapefruit juice and its potential pharmacological basis: HERG channel blockade by flavonoids. Circulation. 2005;111:835-8.

[69] Olah A, Kellermayer D, Matyas C, Nemeth BT, Lux A, Szabo L, et al. Complete Reversion of Cardiac Functional Adaptation Induced by Exercise Training. Medicine and science in sports and exercise. 2017;49:420-9.

[70] Szepesi J, Acsai K, Sebok Z, Prorok J, Pollesello P, Levijoki J, et al. Comparison of the efficiency of Na+/Ca2+ exchanger or Na+/H+ exchanger inhibition and their combination in reducing coronary reperfusion-induced arrhythmias. Journal of physiology and pharmacology : an official journal of the Polish Physiological Society. 2015;66:215-26.

[71] Nagy N, Szuts V, Horvath Z, Seprenyi G, Farkas AS, Acsai K, et al. Does small-conductance calcium-activated potassium channel contribute to cardiac repolarization? Journalof molecular and cellular cardiology. 2009;47:656-63.

[72] Kohajda Z, Farkas-Morvay N, Jost N, Nagy N, Geramipour A, Horvath A, et al. The Effect of a Novel Highly Selective Inhibitor of the Sodium/Calcium Exchanger (NCX) on Cardiac Arrhythmias in In Vitro and In Vivo Experiments. PloS one. 2016;11:e0166041.

[73] Oravecz K, Kormos A, Gruber A, Marton Z, Kohajda Z, Mirzaei L, et al. Inotropic effect of NCX inhibition depends on the relative activity of the reverse NCX assessed by a novel inhibitor ORM-10962 on canine ventricular myocytes. European journal ofpharmacology. 2018;818:278-86.

[74] Olah A, Nemeth BT, Matyas C, Hidi L, Lux A, Ruppert M, et al. Physiological and pathological left ventricular hypertrophy of comparable degree is associated with characteristic differences of in vivo hemodynamics. American journal of physiology Heart and circulatory physiology. 2016;310:H587-97.

[75] Kristof A, Husti Z, Koncz I, Kohajda Z, Szel T, Juhasz V, et al. Diclofenac prolongs repolarization in ventricular muscle with impaired repolarization reserve. PloS one. 2012;7:e53255.

[76] Paszti B, Prorok J, Magyar T, Arpadffy-Lovas T, Gyore B, Topal L, et al. Cardiac electrophysiological effects of ibuprofen in dog and rabbit ventricular preparations: possible implication to enhanced proarrhythmic risk. Canadian journal of physiology and pharmacology. 2021;99:102-9.

[77] Orvos P, Kohajda Z, Szlovak J, Gazdag P, Arpadffy-Lovas T, Toth D, et al. Evaluation of Possible Proarrhythmic Potency: Comparison of the Effect of Dofetilide, Cisapride, Sotalol, Terfenadine, and Verapamil on hERG and Native IKr Currents and on Cardiac Action Potential. Toxicological sciences : an official journal of the Society of Toxicology. 2019;168:365-80.

[78] al-Ani M, Munir SM, White M, Townend J, Coote JH. Changes in R-R variability before and after endurance training measured by power spectral analysis and by the effect of isometric muscle contraction. European journal of applied physiology and occupational physiology. 1996;74:397-403.

[79] Benito B, Gay-Jordi G, Serrano-Mollar A, Guasch E, Shi Y, Tardif JC, et al. Cardiac arrhythmogenic remodeling in a rat model of long-term intensive exercise training. Circulation. 2011;123:13-22.

[80] Chapman JH. Profound sinus bradycardia in the athletic heart syndrome. The Journal of sports medicine and physical fitness. 1982;22:45-8.

[81] D'Souza A, Bucchi A, Johnsen AB, Logantha SJ, Monfredi O, Yanni J, et al. Exercise training reduces resting heart rate via downregulation of the funny channel HCN4. Nature communications. 2014;5:3775.

[82] Northcote RJ, Canning GP, Ballantyne D. Electrocardiographic findings in male veteran endurance athletes. British heart journal. 1989;61:155-60.

[83] Jensen-Urstad K, Saltin B, Ericson M, Storck N, Jensen-Urstad M. Pronounced resting bradycardia in male elite runners is associated with high heart rate variability. Scandinavian journal of medicine & science in sports. 1997;7:274-8.

[84] Chen Y, Zhang H, Zhang Y, Lu N, Zhang L, Shi L. Exercise intensity-dependent reverse and adverse remodeling of voltage-gated Ca(2+) channels in mesenteric arteries from spontaneously hypertensive rats. Hypertension research : official journal of the Japanese Society of Hypertension. 2015;38:656-65.

[85] da Costa Rebelo RM, Schreckenberg R, Schluter KD. Adverse cardiac remodelling in spontaneously hypertensive rats: acceleration by high aerobic exercise intensity. The Journal of physiology. 2012;590:5389-400.

[86] de Waard MC, van der Velden J, Boontje NM, Dekkers DH, van Haperen R, Kuster DW, et al. Detrimental effect of combined exercise training and eNOS overexpression on cardiac function after myocardial infarction. American journal of physiology Heart and circulatory physiology. 2009;296:H1513-23.

[87] Diaz ME, Graham HK, O'Neill S C, Trafford AW, Eisner DA. The control of sarcoplasmic reticulum Ca content in cardiac muscle. Cell calcium. 2005;38:391-6.

[88] Nagy N, Kormos A, Kohajda Z, Szebeni A, Szepesi J, Pollesello P, et al. Selective Na(+) /Ca(2+) exchanger inhibition prevents Ca(2+) overload-induced triggered arrhythmias. British journal of pharmacology. 2014;171:5665-81.

[89] Stokes DL. Keeping calcium in its place: Ca(2+)-ATPase and phospholamban. Current opinion in structural biology. 1997;7:550-6.

[90] Autry JM, Jones LR. Functional Co-expression of the canine cardiac Ca2+ pump and phospholamban in Spodoptera frugiperda (Sf21) cells reveals new insights on ATPase regulation. The Journal of biological chemistry. 1997;272:15872-80.

[91] Kimura Y, Kurzydlowski K, Tada M, MacLennan DH. Phospholamban inhibitory function is activated by depolymerization. The Journal of biological chemistry. 1997;272:15061-4.

[92] Cornea RL, Jones LR, Autry JM, Thomas DD. Mutation and phosphorylation change the oligomeric structure of phospholamban in lipid bilayers. Biochemistry. 1997;36:2960-7.

[93] Colyer J. Control of the calcium pump of cardiac sarcoplasmic reticulum. A specific role for the pentameric structure of phospholamban? Cardiovascular research. 1993;27:1766-71.

[94] Fujii J, Maruyama K, Tada M, MacLennan DH. Expression and site-specific mutagenesis of phospholamban. Studies of residues involved in phosphorylation and pentamer formation. The Journal of biological chemistry. 1989;264:12950-5.

[95] Oxenoid K, Chou JJ. The structure of phospholamban pentamer reveals a channel-like architecture in membranes. Proceedings of the National Academy of Sciences of the United States of America. 2005;102:10870-5.

[96] Reddy LG, Jones LR, Thomas DD. Depolymerization of phospholamban in the presence of calcium pump: a fluorescence energy transfer study. Biochemistry. 1999;38:3954-62.

[97] Stokes DL, Pomfret AJ, Rice WJ, Glaves JP, Young HS. Interactions between Ca2+-ATPase and the pentameric form of phospholamban in two-dimensional co-crystals. Biophysical journal. 2006;90:4213-23.

[98] Gyorke S, Stevens SC, Terentyev D. Cardiac calsequestrin: quest inside the SR. The Journal of physiology. 2009;587:3091-4.

[99] Gyorke I, Hester N, Jones LR, Gyorke S. The role of calsequestrin, triadin, and junctin in conferring cardiac ryanodine receptor responsiveness to luminal calcium. Biophysical journal. 2004;86:2121-8.

[100] Terentyev D, Kubalova Z, Valle G, Nori A, Vedamoorthyrao S, Terentyeva R, et al. Modulation of SR Ca release by luminal Ca and calsequestrin in cardiac myocytes: effects of CASQ2 mutations linked to sudden cardiac death. Biophysical journal. 2008;95:2037-48.

[101] Gyorke S, Gyorke I, Lukyanenko V, Terentyev D, Viatchenko-Karpinski S, Wiesner TF. Regulation of sarcoplasmic reticulum calcium release by luminal calcium in cardiac muscle. Frontiers in bioscience : a journal and virtual library. 2002;7:d1454-63.

[102] Gyorke S, Terentyev D. Modulation of ryanodine receptor by luminal calcium and accessory proteins in health and cardiac disease. Cardiovascular research. 2008;77:245-55.

[103] Terentyev D, Viatchenko-Karpinski S, Valdivia HH, Escobar AL, Gyorke S. Luminal Ca2+ controls termination and refractory behavior of Ca2+-induced Ca2+ release in cardiac myocytes. Circulation research. 2002;91:414-20.

[104] Nagy N, Marton Z, Kiss L, Varro A, Nanasi PP, Toth A. Role of Ca(2)+-sensitive K+ currents in controlling ventricular repolarization: possible implications for future antiarrhytmic drug therapy. Current medicinal chemistry. 2011;18:3622-39.

9. Acknowledgement

I am especially thankful to my supervisor Norbert Nagy, PhD, for introducing me to the cellular fluorescent techniques, and for providing me the opportunity to work in the optical laboratory.

I am very grateful to Professor András Varró, MD, DSc, and Professor Julius Gy Papp, MD, DSc for their permanent support and personal guidance, advices, criticism, and suggestion at the Department of Pharmacology and Pharmacotherapy. Their personal guidance and the helpful discussion were exceptionally useful during my work and allowed me to develop the critical thinking needed in the scientific field.

I would like to thank you my colleagues, Jozefina Szlovák MSc, Noémi Tóth MD, Zsófia Kohajda PhD, Alexandra Polyák MD, László Virág PhD, Norbert Jost PhD, Vivien Demeter-Haludka PhD, Károly Acsai PhD, Leila Topal PharmD, Bence Pászti MD, Tibor Magyar MD, and Tamás Árpádffy-Lovas MD for their continous support ynd help in my work.

I am also very thankful to János Prorok PhD, my very first supervisor, who introduced me into Langendorff-perfusion system and animal experiments, as well as to Ms. Zsuzsanna Molnár, Ms. Erika Bakó and Gábor Girst for their excellent technical assistance.

Finally, I wish to thank and dedicate this thesis to my whole family and to my friends for their love, help and encouragement.

scientific reports

Check for updates

OPEN

Increased Ca^{2+} content of the sarcoplasmic reticulum provides arrhythmogenic trigger source in swimming-induced rat athlete's heart model

Péter Gazdag[1], Kinga Oravecz[1], Károly Acsai[1], Vivien Demeter-Haludka[1], Balázs Ördög[1], Jozefina Szlovák[1], Zsófia Kohajda[2], Alexandra Polyák[3], Bálint András Barta[4], Attila Oláh[4], Tamás Radovits[4], Béla Merkely[4], Julius Gy. Papp[1,2], István Baczkó[1,5], András Varró[1,2,5]✉, Norbert Nagy[1,2,6] & János Prorok[1,2,6]

Sudden cardiac death among top athletes is very rare, however, it is 2–4 times more frequent than in the age-matched control population. In the present study, the electrophysiological consequences of long-term exercise training were investigated on Ca^{2+} homeostasis and ventricular repolarization, together with the underlying alterations of ion channel expression, in a rat athlete's heart model. 12-week swimming exercise-trained and control Wistar rats were used. Electrophysiological data were obtained by using ECG, patch clamp and fluorescent optical measurements. Protein and mRNA levels were determined by the Western immunoblot and qRT-PCR techniques. Animals in the trained group exhibited significantly lower resting heart rate, higher incidence of extrasystoles and spontaneous Ca^{2+} release events. The Ca^{2+} content of the sarcoplasmic reticulum (SR) and the Ca^{2+} transient amplitude were significantly larger in the trained group. Intensive physical training is associated with elevated SR Ca^{2+} content, which could be an important part of physiological cardiac adaptation mechanism to training. However, it may also sensitize the heart for the development of spontaneous Ca^{2+} release and extrasystoles. Training-associated remodeling may promote elevated incidence of life threatening arrhythmias in top athletes.

Abbreviations

AWd	Anterior wall in diastole
AWs	Anterior wall in systole
AWT	Anterior wall thickness
CASQ	Calsequestrin
EDD	END-diastolic diameter
ESD	End-systolic diameter
FS	Fractional shortening
GAPDH	Glyceraldehyde-3-phospate dehydrogenase
HR	Heart rate
I_{CaL}	L-type calcium current
IgG	Immunoglobulin G
I_{K1}	Inward rectifier potassium current

[1]Department of Pharmacology and Pharmacotherapy, Faculty of Medicine, University of Szeged, Dóm tér 12, P.O. Box 427, Szeged 6720, Hungary. [2]MTA-SZTE Research Group of Cardiovascular Pharmacology, Hungarian Academy of Sciences, Szeged, Hungary. [3]2nd Department of Internal Medicine and Cardiology Centre, Faculty of Medicine, University of Szeged, Szeged, Hungary. [4]Experimental Research Laboratory, Heart and Vascular Center, Semmelweis University, Budapest, Hungary. [5]Department of Pharmacology and Pharmacotherapy, Interdisciplinary Excellence Centre, University of Szeged, Szeged, Hungary. [6]These authors jointly supervised this work: Norbert Nagy and János Prorok. ✉email: varro.andras@med.u-szeged.hu

I_{Kr}	Rapid component of the delayed rectifier potassium current
I_{Ks}	Slow component of the delayed rectifier potassium current
I_{to}	Transient outward potassium current
LTCC	L-type calcium channel
LV	Left ventricular
LVAWTd	Left ventricular anterior wall thickness at diastole
LVAWTs	Left ventricular anterior wall thickness at systole
LVDP	Left ventricular developed pressure
LVEDD	Left ventricular end-diastolic diameter
LVEDP	Left ventricular end-diastolic pressure
LVESD	Left ventricular end-systolic diameter
LVESP	Left ventricular end-systolic pressure
LVP	Left ventricular pressure
LVPWTd	Left ventricular posterior wall thickness at diastole
LVPWTs	Left ventricular posterior wall thickness at systole
NCX	Sodium/calcium exchanger (Na^+/Ca^{2+} exchanger)
PLN	Phospholamban
pPKAC	Phospho-protein kinase A C
pPLN	Phospho-phospholamban
PWd	Posterior wall in diastole
PWs	Posterior wall in systole
PWT	Posterior wall thickness
Ryr	Ryanodine receptor
SERCA2a	Sarcoplasmic reticulum Ca^{2+}-ATPase
TL	Tibial length

Many clinical and epidemiological studies provided evidence that moderate physical exercise markedly improves cardiovascular function, decreases mortality and prevents sudden cardiac death[1–3]. In contrast, highly increased physical exercise performed regularly by competitive top athletes causes structural remodeling of the left ventricle, including cardiac hypertrophy (structural remodeling)[4,5], alterations in the ion channel densities, possibly causing electrical instability (electrical remodeling), bradycardia[6] and arrhythmias. These alterations accompanied with a preserved ejection fraction have been classically termed as physiology of the "athlete's heart"[7]. Although sudden cardiac death in top athletes is very rare[8], it is 2–4 times more frequent than in the age-matched control population[9] and is mostly attributed to ventricular fibrillation. Therefore, long-term high intensity endurance exercise may produce increased arrhythmia sensitivity associated with sudden cardiac death[2,10]. One of the major suspected cause of sudden cardiac death in top athletes is hypertrophic cardiomyopathy which generates high electrical instability in ventricular tissues[11].

Several studies investigated the electrophysiological consequences of intensive exercise training and provided evidence that training can distort the normal transmural repolarization heterogeneity primarily by inducing changes in I_{to} density and ameliorating Ca^{2+} handling abnormalities[12]. Furthermore, repolarization attenuation was also reported[13,14]. In spite of these data, the electrophysiological consequences of cardiac adaptation during intensive exercise training are still controversial. We hypothesized that sudden cardiac death in top athletes could be the consequence of the parallel existence of a trigger mechanism, such as delayed afterdepolarizations, and repolarization inhomogeneity, representing an enhanced arrhythmogenic substrate[15].

Our aim was therefore to investigate, in a rat athlete's heart model, the role of selected components of exercise-induced cardiac adaptation in the increased arrhythmia propensity.

Materials and methods

Animals. All experimental procedures were reviewed and approved by Ethical Committee of Hungary for Animal Experimentation in accordance with the "Principles of Laboratory Animal Care" defined by the National Society for Medical Research (permission number: PEI/001/2374-4/2015) and the Guide for the Care and Use of Laboratory Animals, provided by the Institute of Laboratory Animal Resources and published by the National Institute of Health (NIH Publication No. 85-23, revised 1996.); and to the EU Directive 2010/63/EU guidelines. All animals received human care.

8-week-old Wistar male rats (Toxi-Coop, Dunakeszi, Hungary) (n = 36, m = 240-280 g) were housed in standard rat cages at a constant room temperature (22 ± 2 °C) with 12/12-h light/dark cycles. Rats received standard laboratory diet and water ad libitum. The body weight of animals was controlled regularly (three times a week).

Exercise training protocol. Following acclimatization the rats were randomly divided into control (n = 18) and trained groups (n = 18). Animals of the trained group underwent a 12-week-long swimming training protocol to induce physiological myocardial hypertrophy as described previously[16]. In brief, swimming training was performed 5 days/week in a divided container filled with tap water (45 cm deep) maintained at 30–32 °C. For adaptation, the duration of swimming was increased by 15 min every second training day from a baseline of 15 min on the first day, until obtaining the maximal 200 min/day. During this 12-week-long period, control animals were accommodated to water 5 min/day, 5 days/week to reduce the possible differences caused by the stress of water contact.

Echocardiography. At the completion of the swimming training program, LV morphological alterations in control (n = 18) and trained (n = 18) rats were observed by echocardiography as described before[17], except that rats were anesthetized with isoflurane (5% induction dose, 1–2% maintenance dose). Animals were placed on controlled heating pads, and the core temperature was maintained at 37 °C. After shaving the anterior chest, transthoracic echocardiography was performed in the supine position using a 13 MHz linear transducer (12L-RS, GE Healthcare, Horten, Norway), connected to an echocardiography system (Vivid i, GE Healthcare). Standard two-dimensional and M-mode long- and short axis (at mid-papillary level) images were acquired. Recordings were analyzed off-line using a dedicated software (EchoPac, GE Healthcare). We calculated heart rate (HR) on images recorded by M-mode. On two-dimensional recordings of the short-axis at the mid-papillary level, LV anterior (AWT) and posterior (PWT) wall thickness in diastole (index: d) and systole (index: s) as well as LV end-diastolic (LVEDD) and end-systolic diameter (LVESD) were measured. End-systole was defined as the time point of minimal LV dimensions, while end-diastole as the time point of maximal dimensions. All values were averaged over three consecutive cycles[17].

Fractional shortening (FS) was determined from the measurements of LV chamber diameters: FS = [(LVEDD-LVESD)/LVEDD] × 100. LV mass was calculated according to the following formula: LVmass = [(LVEDD + AWTd + PWTd)^3 – LVEDD^3] × 1.04 × 0.8 + 0.14. To calculate LV mass index, we normalized the LV mass values to the tibial length (TL) of the animal[17].

Morphometric assessment. Standard morphometric measurements were obtained including body weight and post-mortem heart weight, as well as tibial length. All animals were weighed before termination. At the end of Langendorff isolated heart measurements, the dry heart weights were measured (n = 12/group). Routinely prepared tibia length was measured after termination. For morphometric analysis, were using a conventional analytical balance and a ruler.

Isolated heart experiments. After 12-week-long swimming training 20-week-old male Wistar rats were used (12 control and 12 trained). ECG and left ventricular pressure of isolated hearts were measured in Langendorff-perfused hearts as described before[18]. Animals were anaesthetized with Na-pentobarbital (300 mg/kg, i.p.), and were injected with heparin sodium (300 IU) into the portal vein. Hearts were rapidly excised, mounted via the aorta on a Langendorff apparatus and retrogradely perfused with warm (37 °C) modified Krebs–Henseleit bicarbonate buffer (KHB) at a constant pressure (80 Hgmm). The KHB solution contained (in mmol/L): $NaHCO_3$ 25; KCl 4.3; NaCl 118.5; $MgSO_4$ 1.2; KH_2PO_4 1.2; glucose 10; $CaCl_2$ 1.8, having a pH of 7.4 ± 0.05 when gassed with 95% O_2 + 5% CO_2. The left ventricular pressure (LVP) was measured by a water-filled latex balloon which was inserted into the left ventricular cavity and inflated to obtain a control state end-diastolic pressure (LVEDP) of 4–8 mmHg[18]. The constant column pressure was provided by a pump (Masterflex) continuously changing the KHB.

The electrical activity as electrocardiogram (ECG) detected by the three lead self-made electrodes and signal amplifier (Experimetria, Hungary). The LVP and the ECG were simultaneously recorded using the WinWCP software (V4.9.1. Whole Cell Electrophysiology Analysis Program, John Dempster, University of Strathclyde, UK). Ventricular extrasystoles were induced by hypokalemic (2.7 mM K^+) KHB solution.

Measurement of ionic currents. Rat ventricular cardiomyocytes were isolated as described in our previous study[19]. The L-type Ca^{2+} current, K^+ currents, Ca^{2+} transient measurements were also described earlier[20]. The estimation of sarcoplasmic reticulum Ca^{2+} content by caffeine method was applied as previously described[21].

Determination of phospho-PKA C, phospho-phospholamban and SERCA2 by western blot. The pan and phosphorylated forms of PKA C, phospholamban (PLN) and SERCA2 were measured in myocardial tissue samples taken from the left ventricle (n = 6/group). Fresh tissue samples were immediately frozen in liquid nitrogen and stored at -80 °C. 30 µg (PKA C, pPKA C), 50 µg (PLN, pPLN) and 20 µg (SERCA2) total protein extracts were resolved using 10% (PKA C, pPKA C), 15% (PLN, pPLN) and 8% (SERCA2) sodium dodecyl sulphate–polyacrylamide gel electrophoresis and transferred onto polyvinylidene fluoride membranes. After blocking in 5% milk-TBS-T, the membranes were immunolabeled with the respective primary antibodies provided by the Calcium Ion Regulation Antibody Sampler Kit (Cell Signalling Technology; Danvers, MA, USA; overnight, at 4 °C; dilutions: anti-PKA C, anti-pPKA C (-α, -β, and -γ when phosphorylated at Thr197): 1:7000, anti-PLN, anti-pPLN (when phosphorylated at Ser16/Thr17): 1:2500, anti-SERCA2: 1:7000). Horseradish peroxidase-conjugated goat anti-rabbit IgG (Southern Biotech, Birmingham, AL, USA; 1 h, RT; 1:8000) was used as a secondary antibody. The membranes were developed with an ECL kit (Advansta; San Jose, CA, USA) and exposed to X-ray film. Equal protein loading was verified by coomassie blue staining, and normalized to total protein. Equal protein loading was verified by coomassie blue staining. Integrated optical density values (sum of each band corrected to the background) was assessed using Image J (FIJI; NIH, Bethesda, MD, USA).

Gene expression analysis by qRT-PCR. All mRNA analyses were carried out as described previously[22]. Fresh left ventricular tissue samples (n = 6/group) were excised and snap-frozen in liquid nitrogen and stored at − 80 °C. Myocardial samples were homogenized in a lysis buffer (RLT buffer; Qiagen, Hilden, Germany), total RNA was isolated from the tissue using the RNeasy Fibrous Tissue Mini Kit (Qiagen) according to the manufacturer's instructions and quantified by measuring optical density at 260 nm. 1 µg total RNA was used for reverse transcription [QuantiTect Reverse Transcription Kit (Qiagen)]. Quantitative real-time PCR was performed with the StepOnePlus Real-Time PCR System (Applied Biosystems, Foster City, CA, USA) in triplicates of each sample, in the total volume of 10 µl in each well containing cDNA, TaqMan Universal PCR MasterMix and a TaqMan

	Control (n = 18)	Trained (n = 18)	*p*
HR (beat/s)	371 ± 6	314 ± 8	< 0.05
LVAWTd (mm)	2.07 ± 0.04	2.31 ± 0.05	< 0.05
LVAWTs (mm)	3.16 ± 0.07	3.67 ± 0.09	< 0.05
LVPWTd (mm)	1.98 ± 0.06	2.24 ± 0.06	< 0.05
LVPWTs (mm)	2.82 ± 0.09	3.23 ± 0.09	< 0.05
LVEDD (mm)	7.66 ± 0.10	7.53 ± 0.13	0.415
LVESD (mm)	4.62 ± 0.10	4.17 ± 0.18	< 0.05
FS (%)	38.9 ± 1.4	45.4 ± 1.8	< 0.05
LV mass (g)	1.19 ± 0.04	1.41 ± 0.05	< 0.05
LV mass index (g/kg)	2.38 ± 0.07	3.21 ± 0.10	< 0.05
	Control (n = 12)	**Trained (n = 12)**	***p***
Tibial length (mm)	45.6 ± 0.8	45.1 ± 0.7	0.62
Body weight (g)	501.12 ± 12.2	428.85 ± 5.86	< 0.05
Heart weight (g)	1.91 ± 0.08	2.18 ± 0.08	< 0.05
Heart weight index (g/kg)	3.83 ± 0.10	5.1 ± 0.20	< 0.05
Ventricular weight (g)	1.41 ± 0.06	1.63 ± 0.05	< 0.05
Ventricular weight index (g/kg)	2.48 ± 0.10	3.81 ± 0.12	< 0.05

Table 1. Echocardiographic and morphometric data.

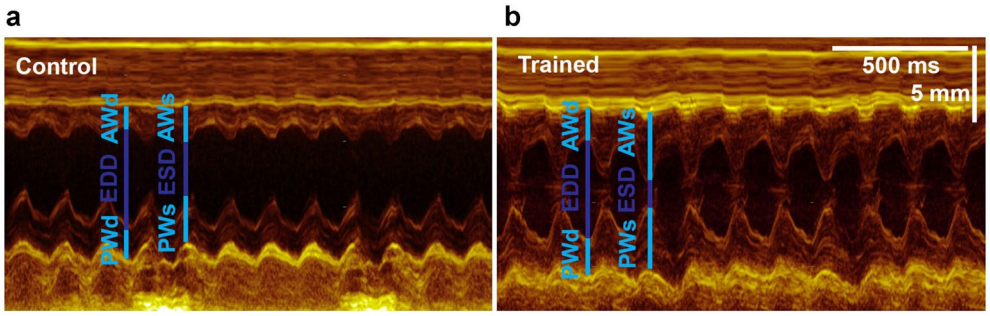

Figure 1. Representative left ventricular (LV) M-mode recordings from one control and one trained animal. Exercise training was associated with increased wall thickness values and markedly decreased LV end-systolic diameter.

Gene Expression Assay for the following genes: alpha-1 subunit of a voltage-dependent calcium channel (Cacna1c, assay ID: Rn00709287_m1), alpha-2 and delta subunits of the voltage-dependent calcium channel complex (Cacna2d1, Rn01442580_m1), beta-2 subunit of the voltage-dependent calcium channel complex (CACNB2, Rn00587789_m1), ryanodine receptor 2 (Ryr2, Rn01470303_m1), calsequestrin 2 (CASQ2, Rn00567508_m1), Na^+/Ca^{2+}exchanger (NCX) SLC8A1, Rn04338914_m1), sarco/endoplasmic reticulum Ca^{2+}-ATPase (SERCA2) (Atp2a2, Rn00568762_m1) and phospholamban (PLN, Rn01434045_m1) purchased from Applied Biosystems. Data were normalized to glyceraldehyde-3-phosphate dehydrogenase (GAPDH; assay ID: Rn01775763_g1) and expression levels were calculated using the CT comparative method ($2^{-\Delta CT}$). All results are expressed as values normalized to the average values of the control group.

Statistical analysis. All data are presented as mean ± SEM. To compare post-mortem, morphological, hemodynamic parameters and ionic currents of control and trained animals, unpaired Student's t-test was used. $p \leq 0.05$ was considered to be statistically significant.

Results

Echocardiographic results. The echocardiographic results are shown in Table 1. The resting heart rate (HR) was significantly decreased in the trained rats, compared to control animals. Echocardiography also revealed significant myocardial hypertrophy, with increased left ventricular (LV) anterior and posterior wall thickness both in systole and diastole, as well as LV mass index. Unchanged LV end-diastolic and decreased end-systolic dimensions resulted in a considerably higher fractional shortening in trained rats, suggesting increased systolic performance (Fig. 1).

	Control (n = 12)	Trained (n = 12)	*p*
RR (ms)	210.8 ± 5.76	214.17 ± 5.36	0.670
RRSTV (ms)	0.77 ± 0.13	1.25 ± 0.36	0.21
RRLTV (ms)	0.65 ± 0.06	1.57 ± 0.51	< 0.05
QT (ms)	87.24 ± 7.46	85.43 ± 4.41	0.839
QTSTV (ms)	0.310 ± 0.03	0.258 ± 0.06	0.44
QTLTV (ms)	0.506 ± 0.03	0.363 ± 0.05	< 0.05
LVESP (mmHg)	108.24 ± 6.49	133.56 ± 6.53	< 0.05
LVEDP (mmHg)	4.69 ± 0.93	4.58 ± 0.44	0.924
LVDP (mmHg)	103.55 ± 6.35	128.98 ± 6.19	< 0.05

Table 2. ECG and left ventricular pressure parameters measured from isolated, Langendorff perfused rat hearts.

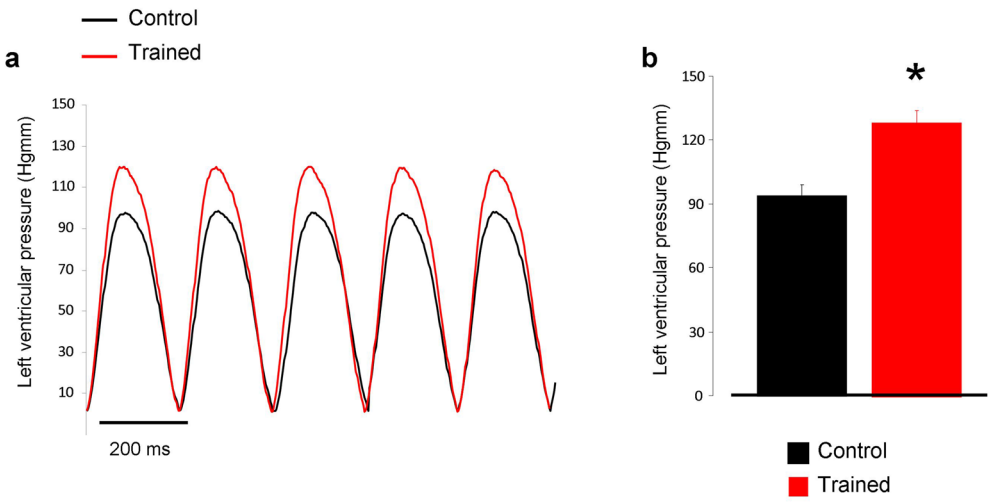

Figure 2. Panel (**a**) demonstrates representative left ventricular developed pressure curves in control (black trace) and in exercised rats (red trace) during Langendorff-perfused measurements. As bar graphs in panel (**b**) illustrate the left ventricular pressure was significantly higher in the case of trained group (red column).

Morphometric results and Langendorff-perfused experiments. The morphometric data of training induced cardiac hypertrophy, measured at the end of the training program, are shown in Table 1. The unchanged lengths of tibia verified the identical age between control and trained animals. The sedentary rats had significantly larger body weight, whereas physical dimensions of the heart including total weight, weight index, ventricles weight and index were significantly increased in the trained rats.

The obtained results of *ex-vivo* Langendorff experiments are shown in Table 2. ECG recordings showed significantly increased long-term R-R variability in the trained group compared to control hearts, while R-R intervals remained unchanged between the two groups. Similarly, QT intervals were not different, while the long-term QT variability was decreased in trained rats. In line with the echocardiographic data, the LV end-systolic pressure was found to be larger in trained animals (Fig. 2a,b). The arrhythmia analysis revealed that the trained group exerted significantly more ventricular extra beats (21 ± 4 vs 75 ± 21 extra beats, n = 12, $p < 0.05$). There were no significant difference between groups regarding bigeminy (6 ± 2 vs 10 ± 2 extra beats, n = 12) or salvos (2 ± 1 vs 3 ± 1 salvos, n = 12) (Fig. 3).

The characteristics of premature beats were further analyzed and the results are demonstrated in Fig. 4. The extra beats were analyzed for a 5-min-long section in all experiments. Only the clearly separated single extra beats were involved in the data analysis, bigeminy and salvo were excluded. Panel a represents the distribution of single extra beats/steady-state beats amplitude ratio in the function of the corresponding coupling interval. The coupling intervals were determined as the time between the initiation of the extra beat and the initiation of the upstroke of the previous steady-state beat. The trained animals (red dots in panel a, and red column in panel b) exerted significantly shorter coupling intervals compared to control (143.7 ± 1.86 ms vs 166.5 ± 4.12 ms; panel b; $p < 0.05$, n = 135 and 63 respectively, both from 12 animals). The amplitude ratio of premature beats/steady-state beats was compared at 3 discrete coupling intervals, where we could gather sufficient number of data (130, 141 and 149 ms). Since the control group exerted only a few numbers of extra beats at these intervals, we extended the analysis of control group to 10 min. As illustrated in panel c, the ratio of amplitudes were slightly larger in trained animals in 141 ms (0.64 ± 0.04 vs 0.51 ± 0.03, $p < 0.05$, n = 18 and 12 respectively, both from 12 animals) and 149 ms (0.76 ± 0.03 vs 0.58 ± 0.04, $p < 0.05$, n = 12 and 13 respectively both from 12 animals) compared to control.

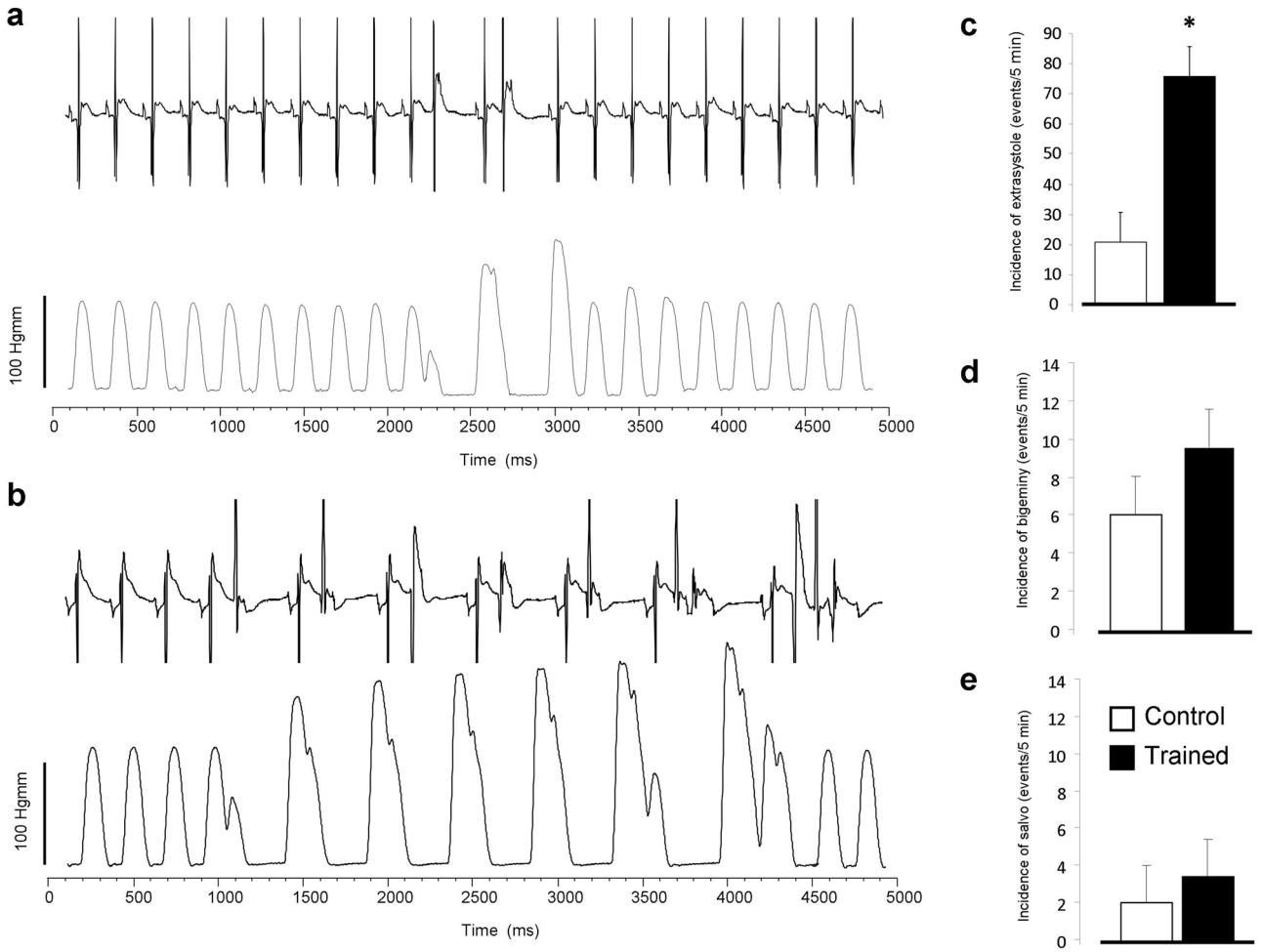

Figure 3. Arrhythmia incidence between trained and control groups measured by parallel registration of ECG and left ventricular pressure during Langendorff-perfusion. A representative section of ECG and pressure from control group indicate few extrasystoles in panel (**a**). In the trained group (panel **b**) the number of extrasystoles significantly increased. Panels (**c**–**e**) compares the extrasystole, bigeminy and salvo incidence between control and trained group, respectively.

Measurement of spontaneous Ca^{2+} releases. Spontaneous Ca^{2+} release was measured, in single cardiomyocytes field-stimulated at 4 Hz for 15 s. Although we observed spontaneous Ca^{2+} release episodes in both groups, the number of spontaneous events was significantly larger in the trained group (11.7 ± 3.9 events/15 s vs 2.7 ± 1.2 events/15 s, n = 10/5 and 10/5 respectively, $p < 0.05$, Fig. 5).

The $I_{Ca,L}$, SR Ca^{2+} content and Ca^{2+} transient measurements. Figure 6a shows the voltage-current relationship of the L-type Ca^{2+} current ($I_{Ca,L}$) in the presence of buffered intracellular solution. 50 ms-long depolarization pulses from a holding potential of − 80 mV to − 40 mV were applied to inactivate the sodium current, followed by voltage steps to 30 mV to elicit Ca^{2+} current. As the superimposed plot and the bar graph (at + 10 mV) show, $I_{Ca,L}$ density was not different in the trained group at all membrane potentials compared to control (n = 5/4 and n = 5/4). Rapid application of 10 mM caffeine (Fig. 6b) at a holding potential of − 80 mV was used to estimate the SR Ca^{2+} content. The caffeine flush was preceded by 10 consecutive conditioning pulses from -80 to 0 mV to reach a steady-state SR Ca^{2+} level. We analyzed the integral of caffeine-induced NCX currents as an indicator of the SR Ca^{2+} content and found that SR Ca^{2+} content was significantly increased in the trained group compared to controls (− 1.84 ± 0.4 (pA*s)/pF vs − 1.25 ± 0.5 (pA*s)/pF n = 8/5 and 8/4, respectively, $p < 0.05$; Fig. 6b). Ca^{2+} transients were measured at 4 Hz pacing frequency to approximate the physiological heart rate of rats (Fig. 6c). We found that the magnitudes of Ca^{2+} transients obtained from the trained group were increased compared to control animals (trained: 114.1 ± 8 AU vs control: 91.1 ± 10 AU, n = 10/5 and 10/5, respectively, $p < 0.05$, Fig. 6d). The half-decay time of the Ca^{2+} transients, measured at 50% of transient decay, was faster in the case of the trained group (118.7 ± 4 ms vs 140.8 ± 5 ms, n = 10, $p < 0.05$, Fig. 6e).

Repolarizing potassium currents, I_{to} and I_{K1}. The potential remodeling induced changes in the densities of the I_{to} and I_{K1} were examined in the presence of 10 mM EGTA and I_{CaL} inhibition. I_{to} (Fig. 7a,c) was

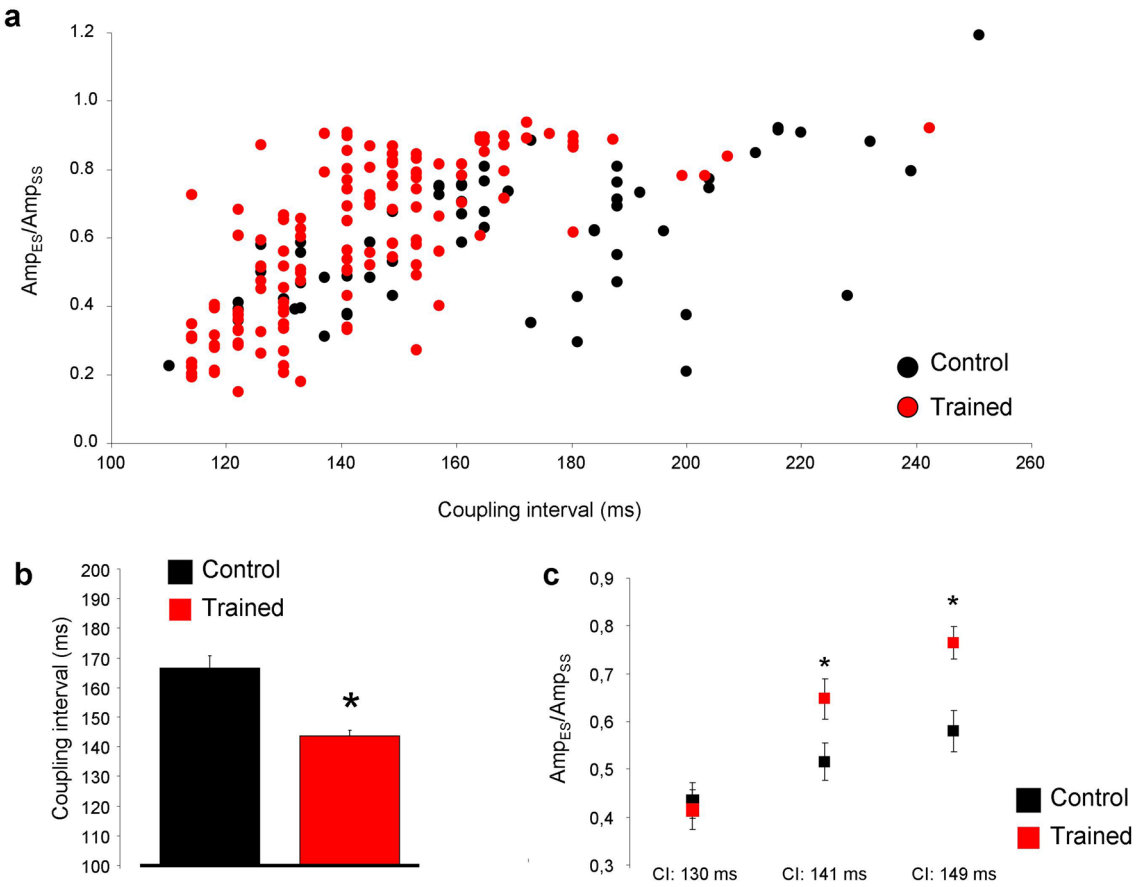

Figure 4. Analysis of premature beats of Langendorff-perfused hearts. (**a**,**b**) show that trained group has shorter coupling interval and larger amplitude of extra beats (**c**) compared to control.

elicited by 300 ms-long voltage steps to 60 mV from a holding potential of -80 mV. As original current traces (Fig. 7a), as well as current–voltage diagram (Fig. 7c) show, the currents were almost identical between groups. I_{K1} was measured by using 300 ms-long depolarizing pulses between – 140 and – 30 mV from a holding potential of -80 mV. Similarly to I_{to}, I_{K1} did not differ between the control and trained groups (Fig. 7b,d).

Average cell size, as estimated by the whole cell capacitance obtained from our patch clamp experiments was increased significantly, in cardiomyocytes from trained animals compared to control cells (281 ± 12 pF vs 232 ± 15 pF, n = 20, $p < 0.05$) (Figs. 6a and 7).

Ion channel gene expression levels. The expression levels of genes involved in Ca^{2+} handling were examined by qRT-PCR. We found that the relative mRNA expression of ryanodine receptor 2 and calsequestrin were significantly higher in the trained group compared to control. The mRNA levels of NCX, SERCA2, LTCC genes and PLN were not different (Fig. 8).

Phosphorylation of PKA C, PLN and SERCA2 protein expression. The pan and phosphorylated forms of key proteins involved in the regulation of Ca^{2+} homeostasis, including PKA C, PLN and SERCA2 protein expression were compared in biopsies from the left ventricles of trained and control rats. Training markedly increased phosphorylation of phospholamban oligomers. There were no significant differences between the groups regarding PKA C phosphorylation, and SERCA expression (Fig. 9).

Discussion

In this work, we studied the consequences of structural and electrical remodeling induced by intensive exercise training in rats. The most important findings of the study are: (i) ventricular hypertrophy and increased cardiac output in trained rats is associated with enhanced arrhythmogenic trigger activity; (ii) these arrhythmogenic events are predominantly of ventricular origin, suggesting delayed afterdepolarizations via increased SR Ca^{2+} content as an underlying mechanism; (iii) the enhanced SR Ca^{2+} content is maintained by increased expression of the phosphorylated form of phospholamban, and increased level of calsequestrin.

Our results suggest that the physiological adaptation of Ca^{2+} homeostasis underlying the increased cardiac output demand during exercise, provides a potentially harmful arrhythmia source. In our study, neither key repolarization parameters nor the repolarization inhomogeneity[15] differ significantly in trained compared to control

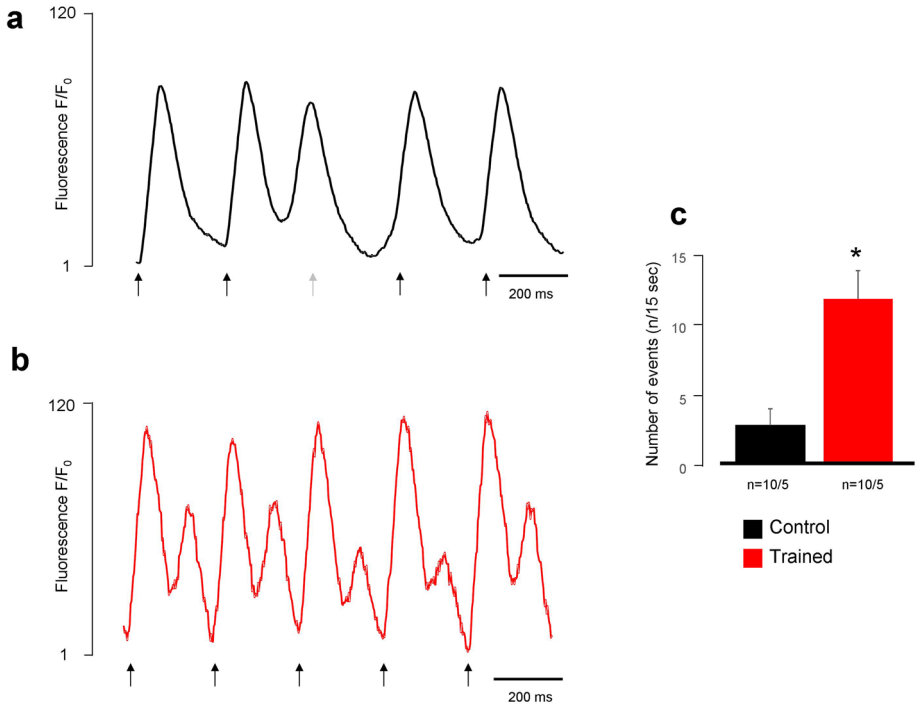

Figure 5. Comparison of spontaneous Ca^{2+} releases under 4 Hz stimulation frequency between control (**a**) and trained (**b**) rats. The black arrows indicate the electric stimuli, the grey arrow marks an ineffective stimulus. We found larger number of spontaneous Ca^{2+} releases in the trained group, compared to control (**c**).

rats, which suggests no change in the arrhythmia substrate in the rat model. However, the increased triggering activity observed in the rat model of the athlete's heart may be coupled with increased transmural dispersion of repolarization in humans (e.g.: as a possible consequence of certain medications and/or dietary supplements, steroid doping agents, or congenital genetic disorders) and therefore can be accounted for the development of life threatening arrhythmias in top athletes. It should be noted that, in contrast to other mammals including human, neither the rapid nor the slow (I_{Ks}) delayed rectifier potassium currents (I_{Kr} and I_{Ks}, respectively) operate in the rat. Therefore, these currents could not be studied in our model, warranting further studies using other species (e.g. rabbits, dogs) to investigate possible changes in repolarization potentially enhancing the arrhythmia substrate during endurance training.

Increased vagal tone may underlie sinus bradycardia. Sinus bradycardia is a hallmark characteristic of the athlete's heart[3,23] as it was the case in several animal training models[6,24,25]. Sinus bradycardia is generally considered as the consequence of increased vagal tone[26], however, D'Souza et al[6] demonstrated the down-regulation of the pacemaker (funny) current (I_f) after the training period of running-trained rats. In our experiments, sinus bradycardia was found in the setting of *in-vivo* echocardiographic measurements (Table 1), but not in Langendorff-perfused isolated hearts (Table 2). The apparent discrepancy between our study and that of D'Souza[6] is may be due to the fundamental differences between the training regime (swimming vs treadmill running). Nevertheless, our present results demonstrate a key role of increased vagal tone leading to sinus bradycardia in the swimming-trained rat model.

Exercise training is associated with improved cardiac output and arrhythmia propensity. Intensive exercise requires increased cardiac output to satisfy the enhanced metabolic demand of the body. This could be associated with remodeling of several components of Ca^{2+} homeostasis[27–29]. In line with this, our in vivo and in vitro results unequivocally show increased LV pressure in the trained group (Fig. 2) which was tightly associated with larger incidence of ventricular spontaneous beats during Langendorff perfusion (Fig. 3). ECG analysis revealed the ventricular origin of the extra beats in isolated hearts, suggesting delayed afterdepolarizations mediated by Ca^{2+}-overload, as the underlying mechanism. In this case, the premature beats are governed by facilitated forward NCX activity as a result of larger SR Ca^{2+} content[20,30,31]. The shorter coupling intervals of the premature beats in trained animals may support this hypothesis, since a higher SR Ca^{2+} content due to improved Ca^{2+} sequestration may lead to earlier spontaneous events (Fig. 4). Accordingly, in field-stimulated Ca^{2+} transient measurements in isolated cells, a markedly larger spontaneous Ca^{2+} release activity was found in the trained group that could cause Ca^{2+}-driven extra depolarizations mediated by the NCX (Fig. 5).

Training induced complex remodeling of SR proteins could be responsible to larger Ca^{2+} content. Experiments with rapid application of caffeine revealed significantly larger Ca^{2+} content of the SR

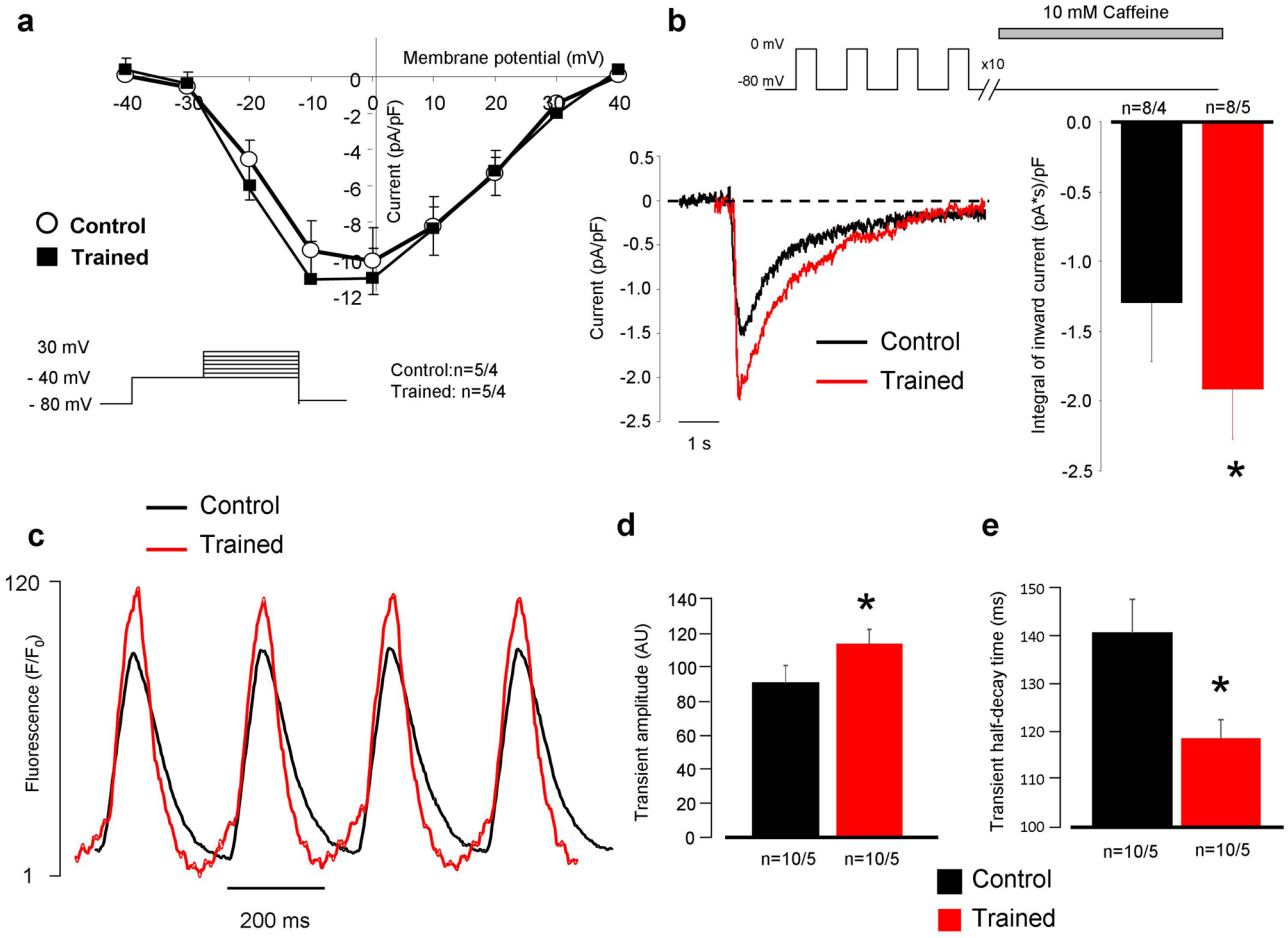

Figure 6. Assessment of Ca^{2+} handling on isolated cells. Panel (**a**) shows identical current–voltage relationship of L-type Ca^{2+} current between groups. Panel (**b**) illustrates significantly larger inward current as a response of 10 mM caffeine application. Panel (**c**,**d**) reports larger Ca^{2+} transient amplitude in the case of trained rats (red trace) compared to control (black trace). Panel (**e**) indicates faster transient relaxation kinetics in the case of trained animals.

in trained animals (Fig. 6b). The actual content of the SR is determined by the dynamic balance between the uptake (via SR Ca-ATPase, SERCA) and release through the ryanodine receptors. Phospholamban (PLN), the regulatory protein of SERCA binds to SERCA in its unphosphorylated form reducing its activity. PLN exists in monomeric and pentameric forms. While it is suggested that the monomeric form inhibits SERCA[32], the role of pentamers is still unclear. This model is derived from the observation that monomers are better inhibitors of PLN[33,34], however, it was also found that a dynamic equilibrium exists between monomeric and pentameric forms. Furthermore, phosphorylation of SERCA or increased cytosolic Ca^{2+} level increased the proportion of the pentameric pool at the expense of monomeric pool[35]. Taken together, several independent reports claim that SERCA may interact with oligomeric forms of PLN, and the existence of oligomers appears to offer a functional advantage for the SERCA-PLN interaction[36–40]. In line with these findings, our results suggest that the increase of PLN pentameric form is associated with improved SERCA kinetics, providing faster decay of the Ca^{2+} transient, and larger Ca^{2+} content and possible Ca^{2+} overload of the sarcoplasmic reticulum (Fig. 6b–e) that may serve as an arrhythmogenic trigger source by spontaneous Ca^{2+} release. Furthermore, we found enhanced expression level of calsequestrin, an ubiquitous luminal Ca^{2+} binding protein[41] (Fig. 8). It has been proposed that CASQ binds to ryanodine receptor via triadin or junctin, and when free $[Ca^{2+}]$ is low in the SR, ryanodine receptor open probability is reduced. When SR $[Ca^{2+}]$ increases, CASQ dissociates from the ryanodine receptor increasing its open probability[42]. It has been shown that CASQ intimately determines the magnitude and duration of the Ca^{2+} release from the SR[43] providing a local source of the releasable Ca^{2+} and it has an important role in ryanodine receptor gating. It was further demonstrated that CASQ modulated ryanodine receptor function via the interaction of two further intraluminal proteins, triadin and junctin[44–46]. Our results indicate that the increased SR Ca^{2+} content is maintained by the increased expression level of CASQ, providing the molecular basis for the improved cardiac output via enhancing the storage capacity and the amount of releasable Ca^{2+} from the SR.

Identical repolarizing currents between trained and control groups. Crucial repolarizing currents, such as I_{to} and I_{K1}, did not differ in cardiomyocytes isolated form trained and control animals (Fig. 7). In

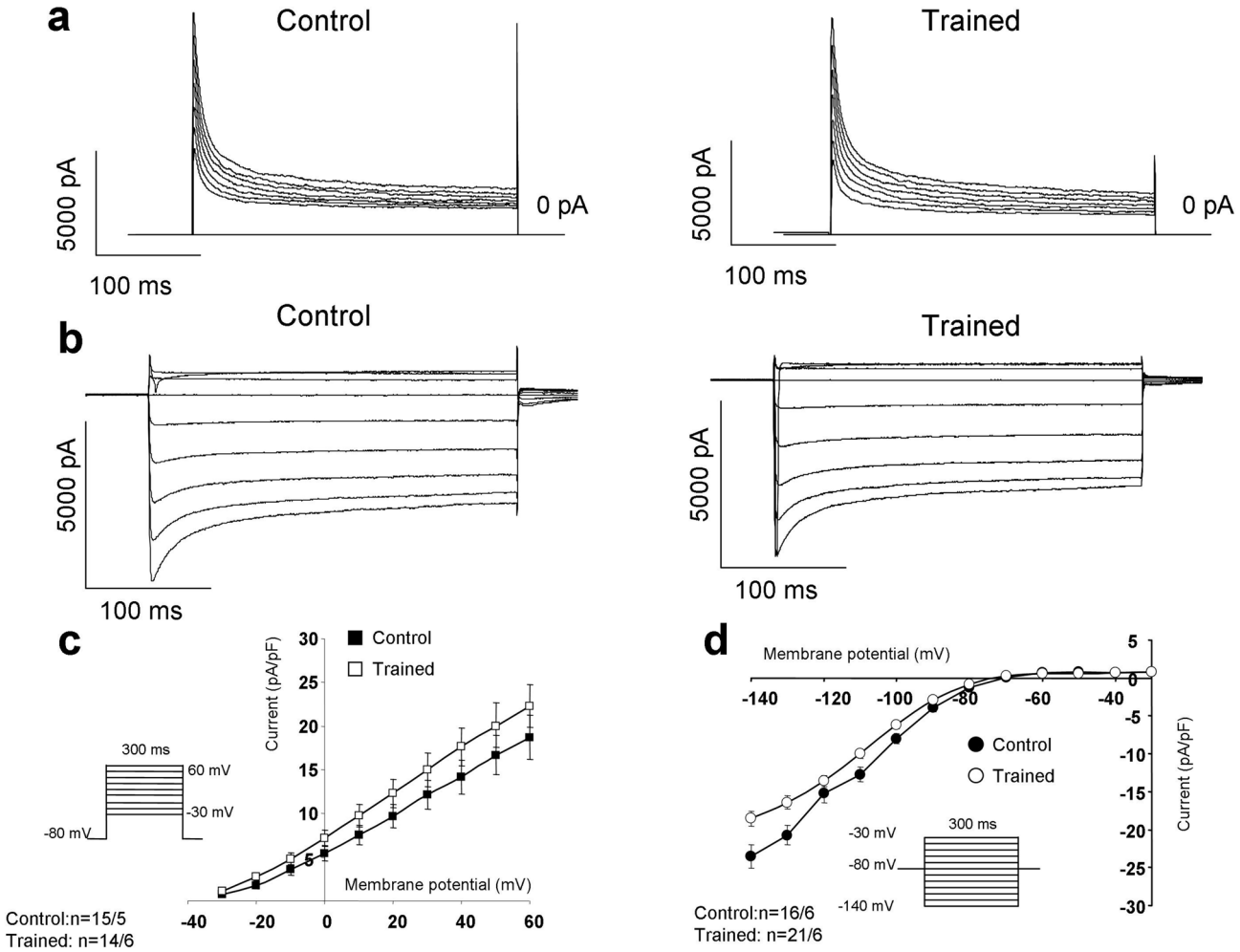

Figure 7. Investigation of the main repolarizing potassium currents on isolated cells. As representative current traces (Panel **a**,**b**) and current–voltage diagrams (panel **c**) illustrate, the currents were found identical between control and trained groups.

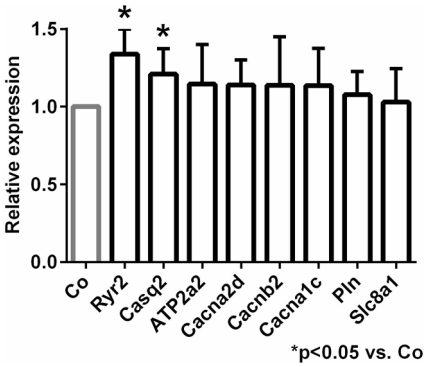

Figure 8. Myocardial gene expression analysis.

our rat model, exercise induced electrophysiological remodeling is confined to Ca^{2+} homeostasis and arrhythmias were promoted by increased triggering activity. It is important to note, however, that potassium channel remodeling might occur in large mammals and may critically alter transmural dispersion of potassium currents, providing an enhanced arrhythmogenic substrate. Considering that several potassium channels show Ca^{2+} dependence to some extent[47], the indirect influence of Ca^{2+} homeostasis alterations on repolarization may also play an important role, and in turn may explain the increased long-term ECG QT variability in the trained group (Table 2).

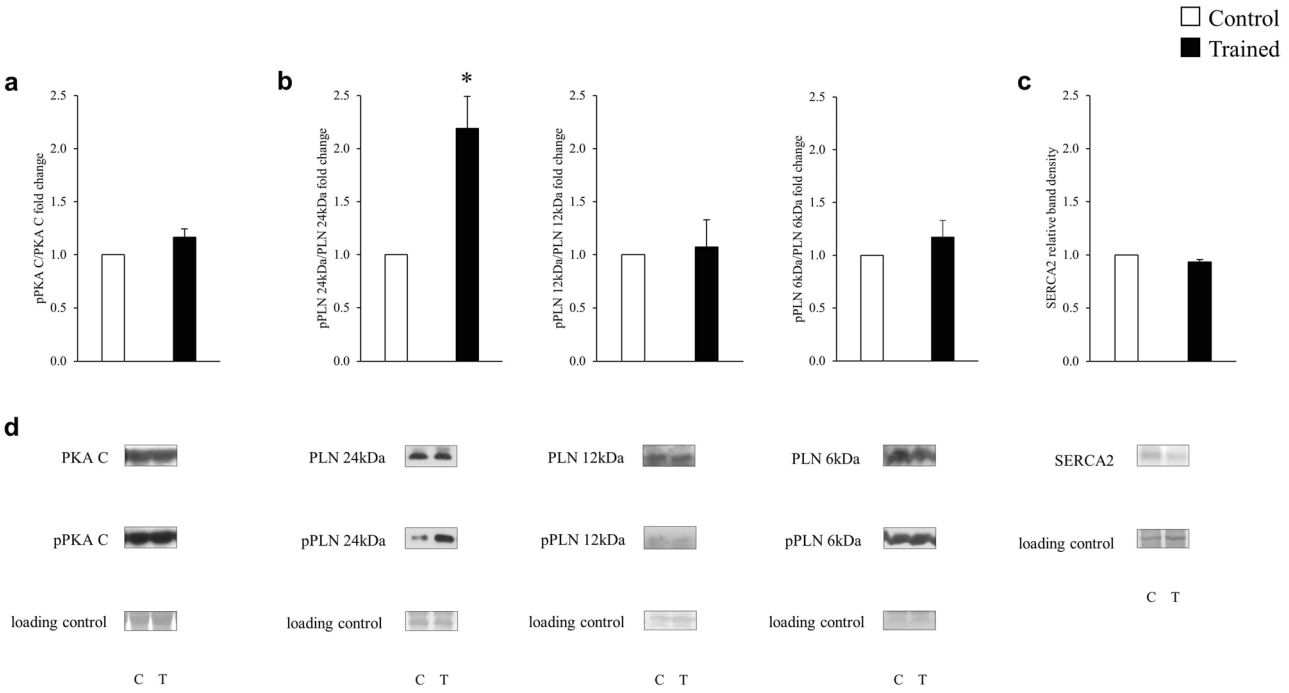

Figure 9. The effect of training on the SERCA phosphorylation pathway. The pan and phosphorylated PKA C (**a**), PLN (**b**) and the SERCA2 (**c**) protein expression.

Conclusion

Our results lead us to conclude that sudden cardiac death associated with training-induced remodeling could possibly arise as the disadvantageous consequence of Ca^{2+} homeostasis adaptation in the athlete's heart. The increased Ca^{2+} content of the SR provides larger available Ca^{2+} upon its release, which is an adaptive response to meet the enhanced cardiac output demand during exercise. However, the enhanced Ca^{2+} load of the SR in trained hearts may also serve as a potential arrhythmia trigger source inducing spontaneous Ca^{2+} release events. The spontaneous Ca^{2+} release could be amplified the presence of increased sympathetic tone or electrolyte disturbances during training, exposing cardiomyocytes to extra Ca^{2+} load. The enhanced source of arrhythmogenic triggers, coupled with possible impaired repolarization reserve in human may lead to the development of life threatening arrhythmias such as '*torsades de pointes*' tachyarrhythmia or ventricular fibrillation in top athletes.

Limitations. (i) Our rat model did not show alterations of the repolarization process, transmural dispersion and therefore changes in the arrhythmia substrate could not be observed. This observation may derive from the species-dependent characteristics of repolarization. Since the rat action potential repolarization relies on I_{to} and I_{K1}, I_{Kur} (Kv1.5), the action potential prolonging effect of a possible I_{Kr} and I_{Ks} downregulation could not be detected, and should be studied experimentally in other species like rabbit, guinea-pig or dog. (ii) In addition, the Ca^{2+} removal from the intracellular space in rats depends more on the SERCA activity compared to larger species, including human.

Received: 6 April 2020; Accepted: 21 October 2020
Published online: 11 November 2020

References

1. Marshall, K. D. *et al.* Heart failure with preserved ejection fraction: chronic low-intensity interval exercise training preserves myocardial O2 balance and diastolic function. *J. Appl. Physiol.* **114**, 131–147. https://doi.org/10.1152/japplphysiol.01059.2012 (2013).
2. O'Keefe, J. H. *et al.* Potential adverse cardiovascular effects from excessive endurance exercise. *Mayo Clin. Proc.* **87**, 587–595. https://doi.org/10.1016/j.mayocp.2012.04.005 (2012).
3. Benito, B. *et al.* Cardiac arrhythmogenic remodeling in a rat model of long-term intensive exercise training. *Circulation* **123**, 13–22. https://doi.org/10.1161/CIRCULATIONAHA.110.938282 (2011).
4. Olah, A. *et al.* Characterization of the dynamic changes in left ventricular morphology and function induced by exercise training and detraining. *Int. J. Cardiol.* **277**, 178–185. https://doi.org/10.1016/j.ijcard.2018.10.092 (2019).
5. Olah, A. *et al.* Sex differences in morphological and functional aspects of exercise-induced cardiac hypertrophy in a rat model. *Front. Physiol.* **10**, 889. https://doi.org/10.3389/fphys.2019.00889 (2019).
6. D'Souza, A. *et al.* Exercise training reduces resting heart rate via downregulation of the funny channel HCN4. *Nat. Commun.* **5**, 3775. https://doi.org/10.1038/ncomms4775 (2014).
7. Maron, B. J. & Pelliccia, A. The heart of trained athletes: cardiac remodeling and the risks of sports, including sudden death. *Circulation* **114**, 1633–1644. https://doi.org/10.1161/CIRCULATIONAHA.106.613562 (2006).
8. Maron, B. J. Hypertrophic cardiomyopathy and other causes of sudden cardiac death in young competitive athletes, with considerations for preparticipation screening and criteria for disqualification. *Cardiol. Clin.* **25**, 399–414, vi. https://doi.org/10.1016/j.ccl.2007.07.006 (2007).

9. Corrado, D., Michieli, P., Basso, C., Schiavon, M. & Thiene, G. How to screen athletes for cardiovascular diseases. *Cardiol. Clin.* **25**(391–397), v–vi. https://doi.org/10.1016/j.ccl.2007.07.008 (2007).
10. Aschar-Sobbi, R. *et al.* Increased atrial arrhythmia susceptibility induced by intense endurance exercise in mice requires TNFalpha. *Nat. Commun.* **6**, 6018. https://doi.org/10.1038/ncomms7018 (2015).
11. Maron, B. J. & Maron, M. S. Hypertrophic cardiomyopathy. *Lancet* **381**, 242–255. https://doi.org/10.1016/S0140-6736(12)60397-3 (2013).
12. Roman-Campos, D. *et al.* Cardiac structural changes and electrical remodeling in a thiamine-deficiency model in rats. *Life Sci.* **84**, 817–824. https://doi.org/10.1016/j.lfs.2009.03.011 (2009).
13. Basso, C., Corrado, D. & Thiene, G. Arrhythmogenic right ventricular cardiomyopathy in athletes: diagnosis, management, and recommendations for sport activity. *Cardiol. Clin.* **25**, 415–422, vi. https://doi.org/10.1016/j.ccl.2007.08.009 (2007).
14. Hart, G. Exercise-induced cardiac hypertrophy: a substrate for sudden death in athletes?. *Exp. Physiol.* **88**, 639–644 (2003).
15. Varro, A. & Baczko, I. Possible mechanisms of sudden cardiac death in top athletes: a basic cardiac electrophysiological point of view. *Pflugers Arch.* **460**, 31–40. https://doi.org/10.1007/s00424-010-0798-0 (2010).
16. Radovits, T. *et al.* Rat model of exercise-induced cardiac hypertrophy: hemodynamic characterization using left ventricular pressure-volume analysis. *Am. J. Physiol. Heart Circ. Physiol.* **305**, H124-134. https://doi.org/10.1152/ajpheart.00108.2013 (2013).
17. Olah, A. *et al.* Complete reversion of cardiac functional adaptation induced by exercise training. *Med. Sci. Sports Exerc.* **49**, 420–429. https://doi.org/10.1249/MSS.0000000000001127 (2017).
18. Szepesi, J. *et al.* Comparison of the efficiency of Na^+/Ca^{2+} exchanger or Na^+/H^+ exchanger inhibition and their combination in reducing coronary reperfusion-induced arrhythmias. *J. Physiol. Pharmacol.* **66**, 215–226 (2015).
19. Nagy, N. *et al.* Does small-conductance calcium-activated potassium channel contribute to cardiac repolarization?. *J. Mol. Cell. Cardiol.* **47**, 656–663. https://doi.org/10.1016/j.yjmcc.2009.07.019 (2009).
20. Kohajda, Z. *et al.* The effect of a novel highly selective inhibitor of the sodium/calcium exchanger (NCX) on cardiac arrhythmias in in vitro and in vivo experiments. *PLoS ONE* **11**, e0166041. https://doi.org/10.1371/journal.pone.0166041 (2016).
21. Oravecz, K. *et al.* Inotropic effect of NCX inhibition depends on the relative activity of the reverse NCX assessed by a novel inhibitor ORM-10962 on canine ventricular myocytes. *Eur. J. Pharmacol.* **818**, 278–286. https://doi.org/10.1016/j.ejphar.2017.10.039 (2018).
22. Olah, A. *et al.* Physiological and pathological left ventricular hypertrophy of comparable degree is associated with characteristic differences of in vivo hemodynamics. *Am. J. Physiol. Heart Circ. Physiol.* **310**, H587-597. https://doi.org/10.1152/ajpheart.00588.2015 (2016).
23. al-Ani, M., Munir, S. M., White, M., Townend, J. & Coote, J. H. Changes in R-R variability before and after endurance training measured by power spectral analysis and by the effect of isometric muscle contraction. *Eur. J. Appl. Physiol. Occup. Physiol.* **74**, 397–403. https://doi.org/10.1007/bf02337719 (1996).
24. Northcote, R. J., Canning, G. P. & Ballantyne, D. Electrocardiographic findings in male veteran endurance athletes. *Br. Heart J.* **61**, 155–160. https://doi.org/10.1136/hrt.61.2.155 (1989).
25. Chapman, J. H. Profound sinus bradycardia in the athletic heart syndrome. *J. Sports Med. Phys. Fitness* **22**, 45–48 (1982).
26. Jensen-Urstad, K., Saltin, B., Ericson, M., Storck, N. & Jensen-Urstad, M. Pronounced resting bradycardia in male elite runners is associated with high heart rate variability. *Scand. J. Med. Sci. Sports* **7**, 274–278 (1997).
27. Chen, Y. *et al.* Exercise intensity-dependent reverse and adverse remodeling of voltage-gated Ca(2+) channels in mesenteric arteries from spontaneously hypertensive rats. *Hypertens. Res.* **38**, 656–665. https://doi.org/10.1038/hr.2015.56 (2015).
28. de Waard, M. C. *et al.* Detrimental effect of combined exercise training and eNOS overexpression on cardiac function after myocardial infarction. *Am. J. Physiol. Heart Circ. Physiol.* **296**, H1513-1523. https://doi.org/10.1152/ajpheart.00485.2008 (2009).
29. da Costa Rebelo, R. M., Schreckenberg, R. & Schluter, K. D. Adverse cardiac remodelling in spontaneously hypertensive rats: acceleration by high aerobic exercise intensity. *J. Physiol.* **590**, 5389–5400. https://doi.org/10.1113/jphysiol.2012.241141 (2012).
30. Diaz, M. E., Graham, H. K., O'Neill, S. C., Trafford, A. W. & Eisner, D. A. The control of sarcoplasmic reticulum Ca content in cardiac muscle. *Cell Calcium* **38**, 391–396. https://doi.org/10.1016/j.ceca.2005.06.017 (2005).
31. Nagy, N. *et al.* Selective Na(+)/Ca(2+) exchanger inhibition prevents Ca(2+) overload-induced triggered arrhythmias. *Br. J. Pharmacol.* **171**, 5665–5681. https://doi.org/10.1111/bph.12867 (2014).
32. Stokes, D. L. Keeping calcium in its place: Ca(2+)-ATPase and phospholamban. *Curr. Opin. Struct. Biol.* **7**, 550–556. https://doi.org/10.1016/s0959-440x(97)80121-2 (1997).
33. Autry, J. M. & Jones, L. R. Functional co-expression of the canine cardiac Ca^{2+} pump and phospholamban in *Spodoptera frugiperda* (Sf21) cells reveals new insights on ATPase regulation. *J. Biol. Chem.* **272**, 15872–15880. https://doi.org/10.1074/jbc.272.25.15872 (1997).
34. Kimura, Y., Kurzydlowski, K., Tada, M. & MacLennan, D. H. Phospholamban inhibitory function is activated by depolymerization. *J. Biol. Chem.* **272**, 15061–15064. https://doi.org/10.1074/jbc.272.24.15061 (1997).
35. Cornea, R. L., Jones, L. R., Autry, J. M. & Thomas, D. D. Mutation and phosphorylation change the oligomeric structure of phospholamban in lipid bilayers. *Biochemistry* **36**, 2960–2967. https://doi.org/10.1021/bi961955q (1997).
36. Colyer, J. Control of the calcium pump of cardiac sarcoplasmic reticulum. A specific role for the pentameric structure of phospholamban?. *Cardiovasc. Res.* **27**, 1766–1771. https://doi.org/10.1093/cvr/27.10.1766 (1993).
37. Fujii, J., Maruyama, K., Tada, M. & MacLennan, D. H. Expression and site-specific mutagenesis of phospholamban. Studies of residues involved in phosphorylation and pentamer formation. *J. Biol. Chem.* **264**, 12950–12955 (1989).
38. Oxenoid, K. & Chou, J. J. The structure of phospholamban pentamer reveals a channel-like architecture in membranes. *Proc. Natl. Acad. Sci. USA* **102**, 10870–10875. https://doi.org/10.1073/pnas.0504920102 (2005).
39. Reddy, L. G., Jones, L. R. & Thomas, D. D. Depolymerization of phospholamban in the presence of calcium pump: a fluorescence energy transfer study. *Biochemistry* **38**, 3954–3962. https://doi.org/10.1021/bi981795d (1999).
40. Stokes, D. L., Pomfret, A. J., Rice, W. J., Glaves, J. P. & Young, H. S. Interactions between Ca^{2+}-ATPase and the pentameric form of phospholamban in two-dimensional co-crystals. *Biophys. J.* **90**, 4213–4223. https://doi.org/10.1529/biophysj.105.079640 (2006).
41. Gyorke, S., Stevens, S. C. & Terentyev, D. Cardiac calsequestrin: quest inside the SR. *J. Physiol.* **587**, 3091–3094. https://doi.org/10.1113/jphysiol.2009.172049 (2009).
42. Gyorke, I., Hester, N., Jones, L. R. & Gyorke, S. The role of calsequestrin, triadin, and junctin in conferring cardiac ryanodine receptor responsiveness to luminal calcium. *Biophys. J .* **86**, 2121–2128. https://doi.org/10.1016/S0006-3495(04)74271-X (2004).
43. Terentyev, D. *et al.* Modulation of SR Ca release by luminal Ca and calsequestrin in cardiac myocytes: effects of CASQ2 mutations linked to sudden cardiac death. *Biophys. J .* **95**, 2037–2048. https://doi.org/10.1529/biophysj.107.128249 (2008).
44. Gyorke, S. & Terentyev, D. Modulation of ryanodine receptor by luminal calcium and accessory proteins in health and cardiac disease. *Cardiovasc. Res.* **77**, 245–255. https://doi.org/10.1093/cvr/cvm038 (2008).
45. Gyorke, S. *et al.* Regulation of sarcoplasmic reticulum calcium release by luminal calcium in cardiac muscle. *Front. Biosci.* **7**, d1454-1463 (2002).
46. Terentyev, D., Viatchenko-Karpinski, S., Valdivia, H. H., Escobar, A. L. & Gyorke, S. Luminal Ca^{2+} controls termination and refractory behavior of Ca^{2+}-induced Ca^{2+} release in cardiac myocytes. *Circ. Res.* **91**, 414–420. https://doi.org/10.1161/01.res.0000032490.04207.bd (2002).
47. Nagy, N. *et al.* Role of Ca(2)+-sensitive K+ currents in controlling ventricular repolarization: possible implications for future antiarrhytmic drug therapy. *Curr. Med. Chem.* **18**, 3622–3639. https://doi.org/10.2174/092986711796642463 (2011).

Acknowledgements
We are grateful for helpful suggestions of Prof. Dr. David Eisner (University of Manchester). This work was supported by grants from the National Research Development and Innovation Office (NKFIH PD-125402 (for NN), FK-129117 (for NN), K-119992 and K-120277, the János Bolyai Research Scholarship of the Hungarian Academy of Sciences (for BO and NN), the UNKP-17-4-I-SE-78 New National Excellence Program of the Ministry for Innovation and Technology (for AO), GINOP-2.3.2-15-2016-00006, the Ministry of Human Capacities Hungary (20391-3/2018/FEKUSTRAT and EFOP-3.6.2-16-2017-0006 (LIVE LONGER)), by the Semmelweis University Innovation Found STIA-KF-17 (to AO). University of Szeged Open Access Fund, No.: 5066.

Author contributions
Study conception and design: A.V., J.P., N.N., K.A. Performing experiments: P.G., K.O., V.D.H., B.Ö., J.S., Z.K., A.P., A.B.B., A.O., J.P. Data analysis and visualization: A.O., T.R., J.P., N.N. Writing initial manuscript: N.N. Critical revisions: All authors. Supervision: T.R., B.M., J.G.Y.P., I.B., A.V., J.P. Funding acquisition: T.R., I.B., A.V., N.N.

Competing interests
The authors declare no competing interests.

Additional information
Correspondence and requests for materials should be addressed to A.V.

Reprints and permissions information is available at www.nature.com/reprints.

Publisher's note Springer Nature remains neutral with regard to jurisdictional claims in published maps and institutional affiliations.

Open Access This article is licensed under a Creative Commons Attribution 4.0 International License, which permits use, sharing, adaptation, distribution and reproduction in any medium or format, as long as you give appropriate credit to the original author(s) and the source, provide a link to the Creative Commons licence, and indicate if changes were made. The images or other third party material in this article are included in the article's Creative Commons licence, unless indicated otherwise in a credit line to the material. If material is not included in the article's Creative Commons licence and your intended use is not permitted by statutory regulation or exceeds the permitted use, you will need to obtain permission directly from the copyright holder. To view a copy of this licence, visit http://creativecommons.org/licenses/by/4.0/.

© The Author(s) 2020

OXFORD

SOT | Society of Toxicology
www.toxsci.oxfordjournals.org

TOXICOLOGICAL SCIENCES, 168(2), 2019, 365–380

doi: 10.1093/toxsci/kfy299
Advance Access Publication Date: December 18, 2018
Research Article

Evaluation of Possible Proarrhythmic Potency: Comparison of the Effect of Dofetilide, Cisapride, Sotalol, Terfenadine, and Verapamil on hERG and Native I_{Kr} Currents and on Cardiac Action Potential

Péter Orvos,[*,†,1] Zsófia Kohajda,[*,‡,1] Jozefina Szlovák,[*] Péter Gazdag,[*] Tamás Árpádffy-Lovas,[*] Dániel Tóth,[*] Amir Geramipour,[*] László Tálosi,[§] Norbert Jost,[*,‡,¶] András Varró,[*,‡,¶,2] and László Virág[*,‡,¶]

[*]Department of Pharmacology and Pharmacotherapy, Faculty of Medicine; [†]Department of Ophthalmology, University of Szeged, Szeged H-6720, Hungary; [‡]MTA-SZTE Research Group for Cardiovascular Pharmacology, Hungarian Academy of Sciences, Szeged H-6720, Hungary; [§]Department of Pharmacognosy, Faculty of Pharmacy; and [¶]Department of Pharmacology and Pharmacotherapy, Interdisciplinary Excellence Centre, University of Szeged, Szeged H-6720, Hungary

[1]These authors contributed equally to this study.
[2]To whom correspondence should be addressed at Department of Pharmacology and Pharmacotherapy, Faculty of Medicine, University of Szeged, Dóm tér 12, Szeged H-6720, Hungary. Fax: +36-62-545-682. E-mail: varro.andras@med.u-szeged.hu.

The authors certify that all research involving human subjects was done under full compliance with all government policies and the Helsinki Declaration.

ABSTRACT

The proarrhythmic potency of drugs is usually attributed to the I_{Kr} current block. During safety pharmacology testing analysis of I_{Kr} in cardiomyocytes was replaced by *human ether-a-go-go-related gene* (hERG) test using automated patch-clamp systems in stable transfected cell lines. Aim of this study was to compare the effect of proarrhythmic compounds on hERG and I_{Kr} currents and on cardiac action potential. The hERG current was measured by using both automated and manual patch-clamp methods on HEK293 cells. The native ion currents (I_{Kr}, I_{NaL}, I_{CaL}) were recorded from rabbit ventricular myocytes by manual patch-clamp technique. Action potentials in rabbit ventricular muscle and undiseased human donor hearts were studied by conventional microelectrode technique. Dofetilide, cisapride, sotalol, terfenadine, and verapamil blocked hERG channels at 37°C with an IC_{50} of 7 nM, 18 nM, 343 μM, 165 nM, and 214 nM, respectively. Using manual patch-clamp, the IC_{50} values of sotalol and terfenadine were 78 μM and 31 nM, respectively. The IC_{50} values calculated from I_{Kr} measurements at 37°C were 13 nM, 26 nM, 52 μM, 54 nM, and 268 nM, respectively. Cisapride, dofetilide, and sotalol excessively lengthened, terfenadine, and verapamil did not influence the action potential duration. Terfenadine significantly inhibited I_{NaL} and moderately I_{CaL}, verapamil blocked only I_{CaL}. Automated hERG assays may over/underestimate proarrhythmic risk. Manual patch-clamp has substantially higher sensitivity to certain drugs. Action potential studies are also required to analyze complex multichannel effects. Therefore, manual patch-clamp and action potential experiments should be a part of preclinical safety tests.

Key words: safety pharmacology; proarrhythmia; hERG; I_{Kr}; cardiac action potential.

© The Author(s) 2018. Published by Oxford University Press on behalf of the Society of Toxicology.
All rights reserved. For permissions, please e-mail: journals.permissions@oup.com

Downloaded from https://academic.oup.com/toxsci/article/168/2/365/5250700 by 81728827 user on 27 April 2021

Life threatening cardiac arrhythmias and sudden cardiac death caused by drugs are one of the major safety issues for pharmaceutical industry and regulatory agencies (Polonchuk, 2012). In the past, several drugs such as cisapride, grepafloxacin, terfenadine, and terodiline have been withdrawn from major markets because of their proarrhythmic effect (Hishigaki and Kuhara, 2011; Varró and Baczkó, 2011). The therapeutic use of these agents, in the worst case, has led to ventricular fibrillation-induced cardiac arrest and consequently sudden cardiac death. Furthermore, drug withdrawn from the market is particularly costly and may harm the prestige of the company as well (Farre *et al.*, 2007).

Many of drugs and potential drug candidate molecules exert their arrhythmogenic effects through the $K_v11.1$ voltage-gated potassium ion channel encoded by the *human ether-a-go-go-related gene* (hERG, KCNH2) (Alexander *et al.*, 2011). This pore-forming protein expressed in ventricular cardiocytes, and represents the α-subunit of the ion channel responsible for rapid delayed rectifier potassium current (I_{Kr}) (Sanguinetti *et al.*, 1995; Trudeau *et al.*, 1995). hERG channel has been found extremely promiscuous in its interactions with a wide range of pharmacological entities (Farre *et al.*, 2007). The I_{Kr} current plays a fundamental role in the phase 3 of repolarization of the action potential; therefore, inhibition of hERG channel delays cardiac action potential repolarization, which lengthens the action potential duration (APD). The drug-induced repolarization delay might associate with catastrophic polymorphic ventricular tachycardia (torsades de pointes, TdP). This mechanism is the basis of fatal ventricular fibrillation and sudden death (Hancox *et al.*, 2008; Lengyel *et al.*, 2007; Yap and Camm, 2003). Based on this concept investigation of I_{Kr} blocking and action potential repolarization duration lengthening capabilities became of required item of safety pharmacology profile of drugs. At present, to avoid severe cardiotoxicity, every new compound is to go through preclinical safety testing determined by the U.S. Food and Drug Administration, the European Medicines Agency and other regulatory entities. Preclinical studies have to be carried out according to the International Conference on Harmonization's S7B guideline. *In vitro* electrophysiological experiments require on cardiac action potential and/or cardiac ionic currents, whereas *in vivo* studies can directly demonstrate the drug-induced QT interval prolongation.

Among the *in vitro* assays, repolarization lengthening effect of the investigational compounds can be adequately analyzed with conventional microelectrode technique in different cardiac structures such as Purkinje fibers and papillary muscles. This method allows the direct observation the alterations of cardiac action potential waveform in cellular level, but gives no specific information about the currents pass through different types of ion channels (Hodgkin and Huxley, 1945). Today, ion channel function and transmembrane ionic currents such as I_{Kr} are most precisely studied using the conventional manual patch-clamp technique (Neher and Sakmann, 1976; Neher *et al.*, 1978). By this method, measurement of the activity of individual channels or the entire ion channel population of the cell is routinely achievable. This technique has become the "gold standard" in studying ion channel behavior, function, kinetics, and pharmacology, mainly in native mammalian cells (Dabrowski *et al.*, 2008; Dunlop *et al.*, 2008; Farre and Fertig, 2012; Farre *et al.*, 2007, 2008; Fertig *et al.*, 2002). The conventional microelectrode technique and the manual patch-clamp method offer direct, information-rich, and real-time *in vitro* technologies to study proarrhythmic effect of drugs and drug candidate compounds. Although providing excellent data quality, these tests are complicated, time consuming and expensive for the large numbers of compounds before the extensive pharmacodynamic experiments can be initiated, because they require the continuous presence of highly skilled and trained personnel. Therefore, these problems excludes the aforementioned techniques as screening tools in early drug development and optimization (Dabrowski *et al.*, 2008; Dunlop *et al.*, 2008; Farre and Fertig, 2012; Farre *et al.*, 2007, 2009). In recent years, numerous companies have developed and introduced automated patch-clamp platforms for high-throughput screening, which are mainly used with stably expressing cell lines and suitable for rapid and high quality optimization of drug candidates. The breakthrough in automated electrophysiology came when planar patch-clamp method without micromanipulation or visual control was launched (Fertig *et al.*, 2002; Lü and An, 2008). This innovative technology facilitates functional data on ion channel active compounds with the throughput capability that is significantly higher compared with conventional techniques (Dunlop *et al.*, 2008; Farre and Fertig, 2012; Farre *et al.*, 2007, 2009). Therefore, analysis of I_{Kr} current in heart muscle cells was typically replaced by the examination of its recombinant equivalent hERG current using automated patch-clamp systems and stable transfected cell lines.

However, more and more evidence indicates that the different proarrhythmic pharmacological assays result in contradictory outcomes raising serious questions regarding their predictability for *in vivo* situations including clinical settings. Assays often give false-positive and -negative results or over/underestimate the cardiac proarrhythmic effect. Therefore, aim of this study was to compare the effect of different known proarrhythmic compounds on hERG and I_{Kr} currents and on cardiac action potential to determine the value of *in vitro* assays in evaluation of cardiac proarrhythmic risk of these compounds and help to understand the nature of proarrhythmic pharmacological safety drug tests.

MATERIALS AND METHODS

Chemicals

All chemicals, which are not specifically indicated, were purchased from Sigma-Aldrich Ltd (Budapest, Hungary). To study the effect of dofetilide, cisapride monohydrate, terfenadine, and verapamil, stock solutions were prepared from these compounds, where the concentrations were 10 mM and the solubilizing agent was dimethyl sulfoxide (DMSO). Aliquots were stored at −20°C for up to 2–4 weeks. (±)-Sotalol hydrochloride was acquired from Sequoia Research Products Ltd (Pangbourne, UK). Sotalol was dissolved directly in external solution at 10 mM concentration before experiments. For electrophysiological measurements, stock solutions were further diluted with external solution, to give appropriate concentrations for the patch-clamp experiments. The final DMSO concentrations in the tested samples were 1% or less.

Ethics Statement and Species

Patients. Hearts were obtained from organ donors whose nondiseased hearts were explanted to obtain pulmonary and aortic valves for transplant surgery. Before cardiac explantation, organ donors did not receive medication apart from dobutamine, furosemide, and plasma expanders. The investigations conformed to the principles of the *Declaration of Helsinki*. Experimental protocols were approved by the National Scientific and Research Ethical Review Boards (4991-0/2010-1018EKU [339/PI/010]).

Downloaded from https://academic.oup.com/toxsci/article/168/2/365/5250700 by 81728827 user on 27 April 2021

Animals. All experiments were carried out in compliance with the *Guide for the Care and Use of Laboratory Animals* (USA NIH publication NO 85-23, revised 1996) and conformed to the Directive 2010/63/EU of the European Parliament. The protocols have been approved by the Ethical Committee for the Protection of Animals in Research of the University of Szeged, Szeged, Hungary (approval number: I-74-5-2012) and by the Department of Animal Health and Food Control of the Ministry of Agriculture and Rural Development (authority approval number XIII/1211/2012).

Conventional Microelectrode Technique

Action potentials were recorded in ventricular trabeculae and papillary muscle preparations obtained from the right ventricles of rabbit or from undiseased human donor hearts using conventional microelectrode techniques. New Zealand rabbits of either sex weighing 2–3 kg were sacrificed by cervical dislocation after an intravenous injection of 400 U/kg heparin. Then the chest was opened, and the heart was rapidly removed. The heart was immediately rinsed in oxygenated modified Locke's solution containing (in mM): NaCl 128.3, KCl 4, $CaCl_2$ 1.8, $MgCl_2$ 0.42, $NaHCO_3$ 21.4, and glucose 10. The pH of this solution was set between 7.35 and 7.4 when gassed with the mixture of 95% O_2 and 5% CO_2 at 37°C. In case of human donor hearts, after explantation, each heart was perfused with cardioplegic solution and kept cold (4–6°C) for 2–4 h before dissection.

Isolated muscle preparations obtained from the right ventricle were individually mounted in a tissue chamber with the volume of 50 ml. Each preparation was initially stimulated through a pair of platinum electrodes in contact with the preparation using rectangular current pulses of 2 ms duration. These stimuli were delivered at a constant cycle length of 1000 ms for at least 60 min allowing the preparation to equilibrate before the measurements were initiated. Transmembrane potentials were recorded using conventional glass microelectrodes, filled with 3 M KCl and having tip resistances of 5–20 MΩ, connected to the input of a high impedance electrometer (Experimetria, type 309, Budapest, Hungary) which was coupled to a dual beam oscilloscope. The resting potential (RP), action potential amplitude (APA), maximum upstroke velocity (V_{max}), and APD measured at 50% and 90% of repolarization (APD_{50} and APD_{90}, respectively) were off-line determined using a home-made software (APES) running on a computer equipped with an ADA 3300 analog-to-digital data acquisition board (Real Time Devices, Inc., State College, Pennsylvania) having a maximum sampling frequency of 40 kHz. Stimulation with a constant cycle length of 1000 ms was applied in the course of all experiments. Attempts were made to maintain the same impalement throughout each experiment. In case an impalement became dislodged, adjustment was attempted, and if the action potential characteristics of the re-established impalement deviated by less than 5% from the previous measurement, the experiment continued (Jost *et al.*, 2005; Kristóf *et al.*, 2012; Lengyel *et al.*, 2001; Orvos *et al.*, 2015). All measurements were carried out at 37°C.

Conventional Manual Patch-clamp Measurements

Left ventricular myocytes were enzymatically dissociated from hearts of New Zealand rabbits of either sex weighing 2–3 kg using the retrograde perfusion technique. The chest is opened and the heart is quickly removed and placed into cold (4–8°C) solution with the following composition (in mM): NaCl 135, KCl 4.7, KH_2PO_4 1.2, $MgSO_4$ 1.2, HEPES 10, $NaHCO_3$ 4.4, Glucose 10, $CaCl_2$ 1 (pH 7.2). The heart is then mounted on a modified, 60 cm high Langendorff column and perfused with oxygenated perfusate of the same composition warmed to 37°C. After 3–5 min of perfusion to flush blood from the coronary vasculature, the perfusate is switched to one having no exogenously added calcium (ie, to one that is nominally Ca^{2+}-free) until the heart cease contracting (~8 to 10 min). Enzymatic digestion is accomplished by perfusion with the same, nominally Ca^{2+}-free solution with 260 U/ml Collagenase (Worthington Type 2) and 33 μM $CaCl_2$. After 10–15 min the heart is removed from the aortic cannula and placed into enzyme free solution containing 1 mM $CaCl_2$ warmed to 37°C for 15 min. Then, the tissue is minced into small chunks, and following gentle agitation myocytes are separated by filtering the resulting slurry through a nylon mesh. Myocytes are finally harvested by gravity sedimentation. Once the majority of individual myocytes has settled to the bottom of the container, the supernatant is decanted and replaced with Tyrode's solution and the myocytes are resuspended by gentle agitation. This procedure is repeated twice more and the resulting myocyte suspension is stored in HEPES buffered Tyrode's solution at room temperature.

One drop of cell suspension was placed in a transparent recording chamber mounted on the stage of an inverted microscope. The myocytes were allowed to settle and adhere to the bottom for at least 5–10 min before superfusion was initiated with Tyrode solution containing (in mM): NaCl 144, NaH_2PO_4 0.4, KCl 4.0, $CaCl_2$ 1.8, $MgSO_4$ 0.53, glucose 5.5, and HEPES 5.0 (pH 7.4, NaOH). Temperature was set to 37°C. Only rod-shaped cells with clear cross-striations were used. Patch-clamp micropipettes were fabricated from borosilicate glass capillaries using a micropipette puller (Flaming/Brown, type P-97, Sutter Co, Novato, California). These electrodes had resistances between 1.5 and 2.5 MΩ. Membrane currents were recorded with Axopatch 200B patch-clamp amplifiers (Molecular Devices, Inc., Sunnyvale, California) using the whole-cell configuration of the patch-clamp technique. After establishing a high resistance (1–10 GΩ) seal by gentle suction, the cell membrane beneath the tip of the electrode was disrupted by suction or application of short electrical pulses. Membrane currents were digitized after low-pass filtering at 1 kHz using analog-to-digital converters (Digidata 1440 A, Molecular Devices, Inc.) under software control (pClamp 10, Molecular Devices, Inc.). The same software was used for off-line analysis (Kristóf *et al.*, 2012).

When measuring rapid delayed rectifier potassium currents (I_{Kr}), pipette solution was contained (in mM): KOH 110, KCl 40, K_2ATP 5, $MgCl_2$ 5, EGTA 5, HEPES 10 (pH was adjusted to 7.2 by aspartic acid). Nisoldipine (1 μM) was added to the external solution to eliminate L-type Ca^{2+} current (I_{CaL}). The slow component of the delayed rectifier potassium current (I_{Ks}) was inhibited by using the selective I_{Ks} blocker HMR 1556 (0.5 μM). I_{Kr} was activated by 1000 ms long depolarizing voltage pulses with the pulse frequency of 0.05 Hz to the test potential of 20 mV and then the cell was repolarized to −40 mV. The deactivating tail current at −40 mV after the test pulse was assessed as I_{Kr}. The amplitudes of the I_{Kr} tail currents were determined as the difference between the peak tail current and the baseline (Lengyel *et al.*, 2001). Before the depolarizing test pulse 500 ms long prepulse to −40 mV was applied to ensure the baseline region. The holding potential was −80 mV. After control period, maximum 2 increasing concentrations of the test compound were applied, each for approximately 6–8 min (in case of dofetilide 10 min). Unlike during I_{Kr} measurements in native myocytes, the solutions and the voltage protocol for manual patch-clamp experiments on HEK-hERG cell line were the same as used during automated patch-clamp experiments (see below).

Downloaded from https://academic.oup.com/toxsci/article/168/2/365/5250700 by 81728827 user on 27 April 2021

The L-type calcium current (I_{CaL}) was recorded in HEPES-buffered Tyrode's solution supplemented with 3 mM 4-aminopyridine. A special solution was used to fill the micropipettes (composition in mM: CsCl 125, TEACl 20, MgATP 5, EGTA 10, HEPES 10, pH was adjusted to 7.2 by CsOH). I_{CaL} was evoked by 400 ms long depolarizing voltage pulses to various test potentials ranging from −35 to 40 mV. The holding potential was −80 mV. A short prepulse of −40 mV served to inactivate Na^+ current. The amplitude of the I_{CaL} was defined as the difference between the peak inward current at the beginning of the pulse and the current at the end of the pulse (Jost *et al.*, 2013).

The late sodium current (I_{NaL}) was activated by depolarizing voltage pulses to −20 mV from the holding potential of −120 mV. After 5–7 min incubation with terfenadine the external solution was replaced by that containing 20 μM tetrodotoxin (TTX). TTX at this concentration completely blocks the late sodium current. The external solution was HEPES-buffered Tyrode's solution supplemented with 1 μM nisoldipine, 0.5 μM HMR-1556, and 0.1 μM dofetilide to block I_{CaL}, I_{Ks}, and I_{Kr} currents. The composition of the pipette solution (in mM) was: KOH 110, KCl 40, K_2ATP 5, $MgCl_2$ 5, EGTA 5, HEPES 10 (pH was adjusted to 7.2 by aspartic acid) (Kohajda *et al.*, 2016).

Automated Planar Patch-clamp Measurements

The hERG channel current was measured by using planar patch-clamp technology in the whole-cell configuration with a 4 channel medium-throughput fully automated patch-clamp platform (Patchliner Quattro, Nanion Technologies GmbH, Munich, Germany) with integrated temperature control. Data acquisition and online analysis were performed with an EPC-10 Quadro patch-clamp amplifier (HEKA Elektronik Dr Schulze GmbH, Lambrecht/Pfalz, Germany), using PatchMaster 2.65 software (HEKA Elektronik Dr. Schulze GmbH). The pipetting protocols were controlled by PatchControlHT 1.09.30 software (Nanion Technologies GmbH).

Experiments were carried out at room or physiological (37°C) temperature, on HEK293 (human embryonic kidney) cells stably expressing the hERG (Kv11.1) potassium channel. The cell line originated from Cell Culture Service GmbH (Hamburg, Germany). Cells were cultured at 37°C, in 5% CO_2 in IMDM medium (PAA Laboratories GmbH, Pasching, Austria) supplemented with 10% FBS (PAA Laboratories GmbH), 2 mM L-glutamine (Life Technologies Corporation, Carlsbad, California), 1 mM Na-piruvate (PAA Laboratories GmbH), and 500 μg/ml G418 (PAA Laboratories GmbH). Suspension of cells was used for measurements from running cell culture. Cells were washed twice with PBS (Life Technologies Corporation) and then detached with trypsin-EDTA (PAA Laboratories GmbH) for 30–60 s before the measurement. Trypsin was blocked with the serum-containing medium. The cell suspension was next centrifuged (2 min, 100 × g), resuspended in IMDM medium at a final density of 1×10^6–5×10^6 cells/ml, and kept in the cell hotel of the Patchliner. Cells were recovered after 15–30 min and remained suitable for automated patch-clamp recordings for up to 4 h.

The following solutions were used during patch-clamp recording (compositions in mM): internal solution: KCl 50, NaCl 10, KF 60, EGTA 20, HEPES 10, pH 7.2 (KOH); external solution: NaCl 140, KCl 4, glucose-monohydrate 5, $MgCl_2$ 1, $CaCl_2$ 3, HEPES 10, pH 7.4 (NaOH). All solutions were sterile filtered. Aliquots were stored at −20°C and warmed up to room temperature before use. The voltage protocol for hERG ion channel started with a short (100 ms) −40 mV step to establish the baseline region. A depolarizing step was applied to the test potential of 20 mV for 3 s, and then the cell was repolarized to −40 mV to evoke outward tail current. Holding potential was −80 mV. The pulse frequency was approximately 0.1 Hz. Currents were low-pass filtered at 2.9 kHz using the internal Bessel filter of the EPC-10 Quadro patch-clamp amplifier (HEKA Elektronik Dr. Schulze GmbH) and digitized at 10 kHz. The peak tail current was corrected the leak current defined during the first period to −40 mV. Recording started in external solution. After this control period, 6 increasing concentrations of the test compound were applied, each for approximately 3 min (in case of dofetilide 6 min) to record a complete concentration-response curve. Amitriptyline (10 μM) was applied as a reference inhibitor then a wash-out step terminated the protocol.

Statistics

All data are expressed as means ± SEM. The "*n*" number refers to the number of experiments (ie, the number of cells in case of patch-clamp and the number of ventricular muscle preparations—papillary or trabecular muscle—in case of action potential measurements) except native I_{Kr} measurements when it refers to the number of experiments regarding 1 data point of the concentration-response curve and the means ± SEM values were calculated accordingly. Statistical analysis was performed with Student's *t* test for paired data or one-way analysis of variance (ANOVA). The results were considered statistically significant when p was $<.05$.

RESULTS

All compounds (dofetilide, cisapride, sotalol, terfenadine, and verapamil) were tested in hERG assay at both room temperature and 37°C with automated patch-clamp system. The elevation of ambient temperature to physiologic significantly altered the characteristic of hERG current. The current density of peak tail current increased from 21.97 ± 0.40 pA/pF to 32.42 ± 0.69 pA/pF ($n = 19$–24, $p < .05$). The rise time of tail current was decreased and the time constant of decay phase was more rapid (tau changed from 761.52 ± 16.77 ms to 394.15 ± 8.69 ms, $n = 19$–23, $p < .05$).

All investigated compounds inhibited the hERG current at both temperatures. The IC_{50} values of the dofetilide elicited inhibition were very similar (8.4 ± 0.2 nM, $n = 6$ at room temperature and 7.3 ± 0.2 nM, $n = 5$ at 37°C). The other compounds displayed different properties at room temperature versus physiological temperature (37°C). Cisapride, sotalol, terfenadine, and verapamil blocked hERG channels at room temperature with an IC_{50} of 47.5 ± 4.8 nM, $n = 5$; 773.7 ± 9.3 μM, $n = 5$; 266.0 ± 26.8 nM, $n = 6$; and 344.9 ± 26.1 nM, $n = 5$, respectively. However, at 37°C these compounds found to be much more potent (IC_{50} values were 17.7 ± 2.9 nM, $n = 5$; 342.8 ± 24.8 μM, $n = 5$; 165.4 ± 24.5 nM, $n = 6$; and 213.6 ± 22.5 nM, $n = 5$, respectively).

To evaluate the prognostic value of hERG assay these agents were subjected for further investigations. The I_{Kr} current blocking capability of the compounds was tested on rabbit ventricular myocytes with manual patch-clamp method at 37°C. The corresponding IC_{50} values of dofetilide, cisapride, and verapamil were 13.0 ± 2.6 nM ($n = 3$–4), 26.4 ± 4.5 nM ($n = 3$–5), and 268.2 ± 11.2 nM ($n = 4$–5), respectively, showing a good correlation with IC_{50} values obtained in hERG assays. On the contrary, IC_{50} values derived from I_{Kr} measurements was approximately 7 and 3 times lower (51.6 ± 8.8 μM, $n = 2$–6 and 54.3 ± 5.2 nM, $n = 3$–4, respectively) in case of sotalol and terfenadine. The results of both automated and manual patch-clamp experiments are shown in Figures 1–5 and Table 1.

Downloaded from https://academic.oup.com/toxsci/article/168/2/365/5250700 by 81728827 user on 27 April 2021

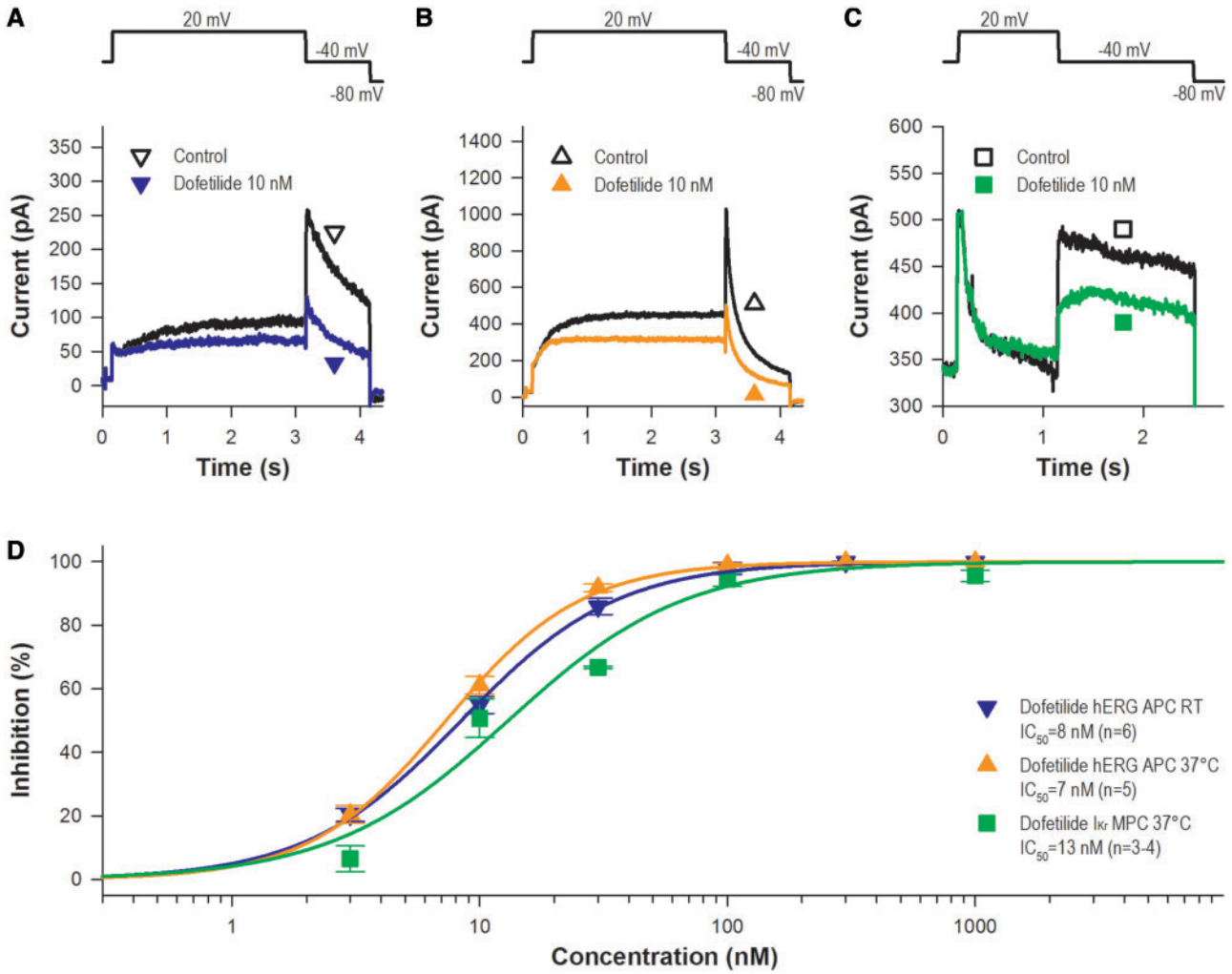

Figure 1. Effect of dofetilide on hERG and I_{Kr} current. A, Example traces for hERG mediated currents obtained from HEK-hERG cell treated with 10 nM dofetilide at room temperature (RT). B, Effect of 10 nM dofetilide on hERG current at 37°C. C, Sample I_{Kr} current sweeps obtained from rabbit left ventricular muscle cell treated with 10 nM dofetilide. The currents were recorded using the voltage protocols shown at the top of panels (A–C). D, Dose-response curves of dofetilide derived from hERG measurements at RT and at 37°C and from I_{Kr} experiments. Abbreviations: APC, automated patch-clamp; MPC, manual patch-clamp.

As sotalol and terfenadine have stronger effect on I_{Kr} measured by manual patch-clamp method compared with hERG automated patch-clamp experiments, the effects of these drugs on hERG current using manual patch-clamp technique at 37°C were also investigated to study how the potency of these drugs are influenced by the experimental techniques themselves. In contrast with the hERG automated patch-clamp assays, the effects of sotalol and terfenadine on hERG current were stronger measured by the manual patch-clamp technique: IC_{50} values calculated from the hERG manual patch-clamp experiments were 77.5 ± 4.8 μM (n = 3–7) and 31.0 ± 3.2 nM (n = 3–5), respectively, showing still somewhat different but far less discrepancy with the native I_{Kr} measurements (Figs. 3 and 4).

To study the safety pharmacology consequences of the hERG and I_{Kr} inhibition of dofetilide, cisapride, sotalol, terfenadine, and verapamil, the effect of these compounds on action potential configuration was studied in rabbit right ventricular papillary muscle preparations. In these investigations, the IC_{50} concentrations obtained from I_{Kr} experiments were applied. Dofetilide, cisapride, and sotalol significantly lengthened the APD at stimulation cycle length of 1000 ms. The prolongation of APD_{90} was 47.8 ± 12.9% (n = 7) in case of 13 nM dofetilide, 68.4 ± 10.0% (n = 6) in case of 26 nM cisapride, whereas 52 μM sotalol extended the APD with 56.0 ± 4.6% (n = 5). Verifying by one-way ANOVA these APD lengthenings were not significantly different. In contrast, terfenadine (1.4 ± 3.0%, n = 8) and verapamil (0.6 ± 1.8%, n = 5) did not significantly affect the APD at 54 and 270 nM concentrations, respectively (Figure 6 and Table 2).

As terfenadine and verapamil did not influence the action potential repolarization, the possible effects of these compounds on the late Na^+ current (I_{NaL}) and on the L-type inward calcium current (I_{CaL}) were also investigated in rabbit ventricular myocytes. These experiments clearly revealed that terfenadine at 54 nM concentration significantly inhibited I_{NaL} (Figure 7, from 82.8 ± 17.9 pA to 45.8 ± 7.9 pA, n = 4, $p < .05$ at −20 mV test potential). A slight but significant block on I_{CaL} by 54 nM terfenadine was also observed (Figure 8). Verapamil at 270 nM did not influenced the I_{NaL} current (control: 56.5 ± 11.2 pA, drug: 49.0 ± 9.2 pA, n = 4, not significant, see Figure 7), whereas a moderate but significant inhibition of I_{CaL} current was observed after application of 270 nM verapamil (Figure 8).

In purpose to confirm our findings in rabbit ventricular myocytes, effect of dofetilide, cisapride, sotalol, terfenadine, and verapamil were also studied on action potential repolarization in

Downloaded from https://academic.oup.com/toxsci/article/168/2/365/5250700 by 81728827 user on 27 April 2021

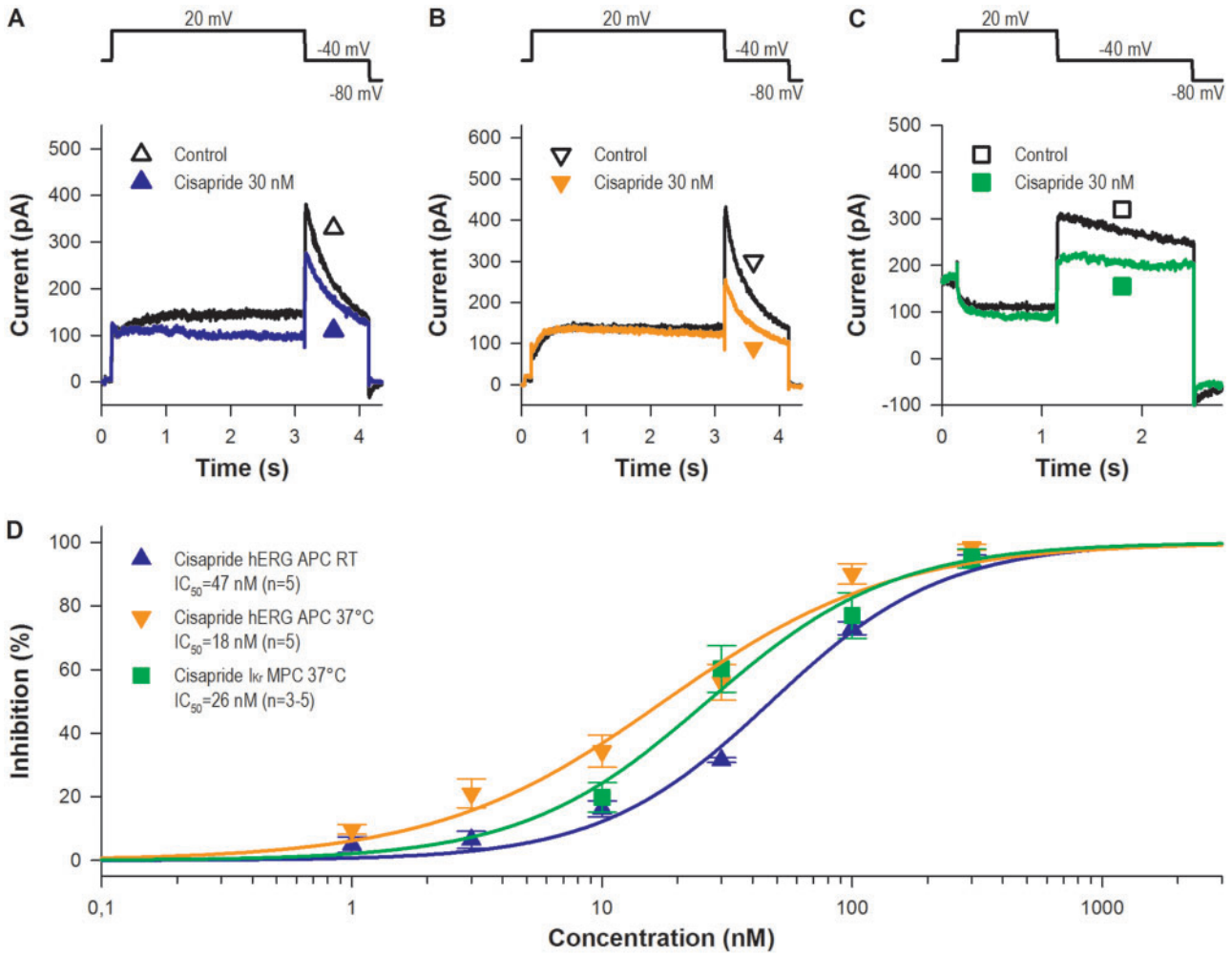

Figure 2. Effect of cisapride on hERG and I_{Kr} current. A, Sample hERG current curves obtained from HEK-hERG cell treated with 30 nM cisapride at room temperature (RT). B, Effect of 30 nM cisapride on hERG current at 37°C. C, Representative I_{Kr} current sweeps obtained from rabbit left ventricular muscle cell treated with 30 nM cisapride. The currents were recorded using the voltage protocols shown at the top of panels (A–C). D, Dose-response curves of cisapride derived from hERG measurements at RT and at 37°C and from I_{Kr} experiments. Abbreviations: APC, automated patch-clamp; MPC, manual patch-clamp.

undiseased human ventricular muscle. As Figure 9 shows, 10 nM dofetilide, 30 nM cisapride, and 30 μM sotalol markedly lengthened the APD at stimulation cycle length of 1000 ms. The prolongation of APD_{90} was 20.4 ± 4.5% ($n = 7$), 27.5 ± 9.8% ($n = 3$), and 28.0 ± 1.8% ($n = 6$), respectively. These values were not significantly different. However, terfenadine even at high 1 μM concentration did not influence the APD at 90% of repolarization (Table 3). Verapamil at 300 nM concentration in 2 experiments did not affect the action potential repolarization in undiseased human right ventricular muscle preparations (Figure 9).

DISCUSSION

Because there are important and not well understood differences between the evaluation of proarrhythmic ability with high-throughput hERG channel, I_{Kr} or action potential experiments, we have studied the effect of 5 drugs with established proarrhythmic potential (dofetilide, cisapride, sotalol, terfenadine, and verapamil) on hERG current (at room temperature and 37°C), on I_{Kr} current (37°C), and on rabbit and human cardiac action potential comparing these assays and helping the rational use of these proarrhythmic pharmacological safety drug tests during preclinical drug development.

Current responses of cells expressing the hERG channel at room temperature and physiological temperature were similar in case of dofetilide. The most noticeable effects of raising the temperature to 37°C were that the peak amplitude was increased, the rise time was decreased and the time constant of decay phase was faster. Despite that, the dose-response curve generated an IC_{50} similar to that obtained at room temperature, and similar to that determined in the I_{Kr} experiments. In addition, these data are in good agreement with our action potential measurements and with previously published data (Mo *et al.*, 2009; Pearlstein *et al.*, 2003; Weerapura *et al.*, 2002).

Conversely, cisapride, sotalol, terfenadine, and verapamil display different potencies at room temperature and 37°C. All these compounds were more potent at physiological temperature and therefore, it is a desirable option to study hERG currents at physiological temperature (Windley *et al.*, 2018). In spite of that, the majority of the commercially available patch-clamp platforms have no integrated temperature control. Apart from the differences in temperature cisapride—like dofetilide—reduced I_{Kr} current and extended the action potential as expected based on hERG measurements, and results are in good agreement with literature (Drolet *et al.*, 1998; Fossa *et al.*, 2004; Martin *et al.*, 2004; Polonchuk, 2012).

Downloaded from https://academic.oup.com/toxsci/article/168/2/365/5250700 by 81728827 user on 27 April 2021

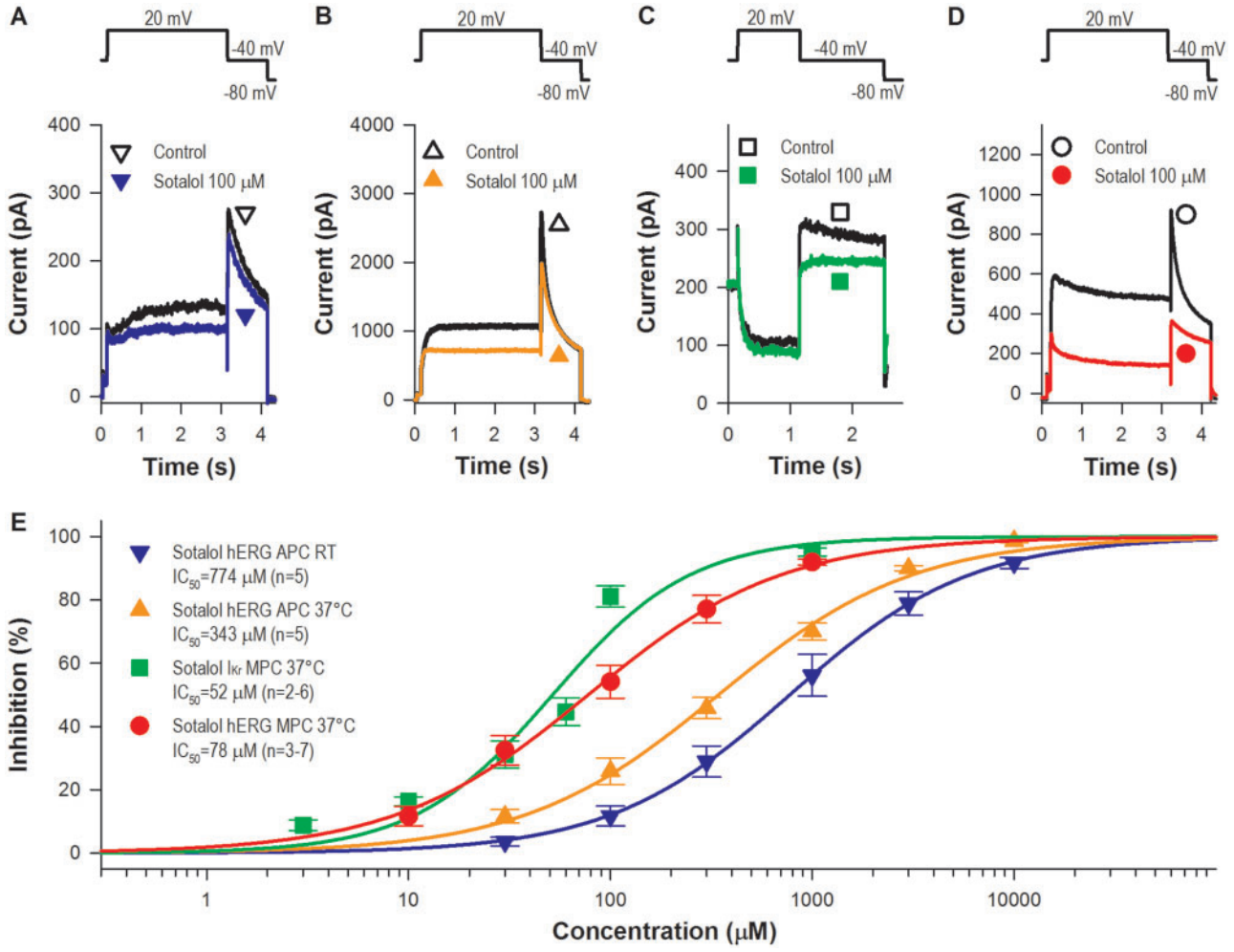

Figure 3. Effect of sotalol on hERG and I_{Kr} current. A, Representative hERG current curves obtained from HEK-hERG cell treated with 100 μM sotalol at room temperature (RT). B, Effect of 100 μM sotalol on hERG current at 37°C. C, Representative I_{Kr} current curves obtained from rabbit left ventricular muscle cell treated with 100 μM sotalol. D, Representative hERG current curves obtained from HEK-hERG cell treated with 100 μM sotalol using manual patch-clamp technique. The currents were recorded using the voltage protocols shown at the top of panels (A–D). E, Concentration-response curves of sotalol obtained from hERG experiments at RT, at 37°C using automated and manual patch-clamp techniques and from I_{Kr} measurements. Abbreviations: APC, automated patch-clamp; MPC, manual patch-clamp.

However, verapamil blocked I_{Kr} current with an IC_{50} value with similar to that calculated from hERG measurements at 37°C but the drug did not lengthen the action potential in rabbit right ventricular preparations. Other studies also reported submicromolar IC_{50} of verapamil for hERG current (Chouabe *et al.*, 1998; Zhang *et al.*, 1999). Zhang *et al.* (1997) described that 1 μM verapamil suppress I_{Kr} tail current by 49% in guinea-pig.

Unlike the other drugs investigated in this study, sotalol and terfenadine showed significantly greater degree of inhibition on I_{Kr} current compared with hERG. In the literature, majority of publications—using mainly manual patch-clamp—reported IC_{50} values for terfenadine between 10 and 60 nM in hERG cell lines, which are much lower than that found in this study. However, higher IC_{50} values have also been reported—for example 950 nM (Abi-Gerges *et al.*, 2011; automated patch-clamp) or 204 nM (Crumb, 2000; manual patch-clamp), and others (Aslanian *et al.*, 2009; Limberis *et al.*, 2006). These later studies used mainly automated patch-clamp method.

In manual patch-clamp, test solutions are usually prepared in relatively large quantities directly before the experiments, and are continuously perfused. In automated platforms, compound plates with minor volume are used, and comparatively small volumes of test solutions are applied to the cells. One may speculate that the adverse surface-to-volume ratio in compound plates and microchannels and the increased incubation time can lead to possible reduction of compound concentrations, especially in case of hydrophobic, "sticky" agents such as terfenadine. Adhesion and precipitation have been identified as the major sources of potential right-shifted less accurate dose-response curves (Mathes, 2006; Mo *et al.*, 2009; Möller and Witchel, 2011), which correspond to the literature data (Carmeliet, 1998; Limberis *et al.*, 2006; Salata *et al.*, 1995). Our experiments showed that the effect of terfenadine on hERG current was stronger measured by the manual patch-clamp technique. The calculated IC_{50} value was similar or even lower (31 vs 54 nM) to that of found in I_{Kr} measurements, which seems to support the assumption explained above. Therefore, the lower efficacy of terfenadine for hERG found in our automated patch-clamp experiments may not reflect the real potency of the drug. In contrast to terfenadine, sotalol is among the least hydrophobic compounds (Mo *et al.*, 2009), and numerous studies also reported extremely high IC_{50} values in hERG cell lines utilized for manual patch-clamp (the half-blocking concentrations of sotalol were 268–1200 μM in these experiments [Abi-Gerges *et al.*, 2011; Guth *et al.*, 2004; Kirsch

Downloaded from https://academic.oup.com/toxsci/article/168/2/365/5250700 by 81728827 user on 27 April 2021

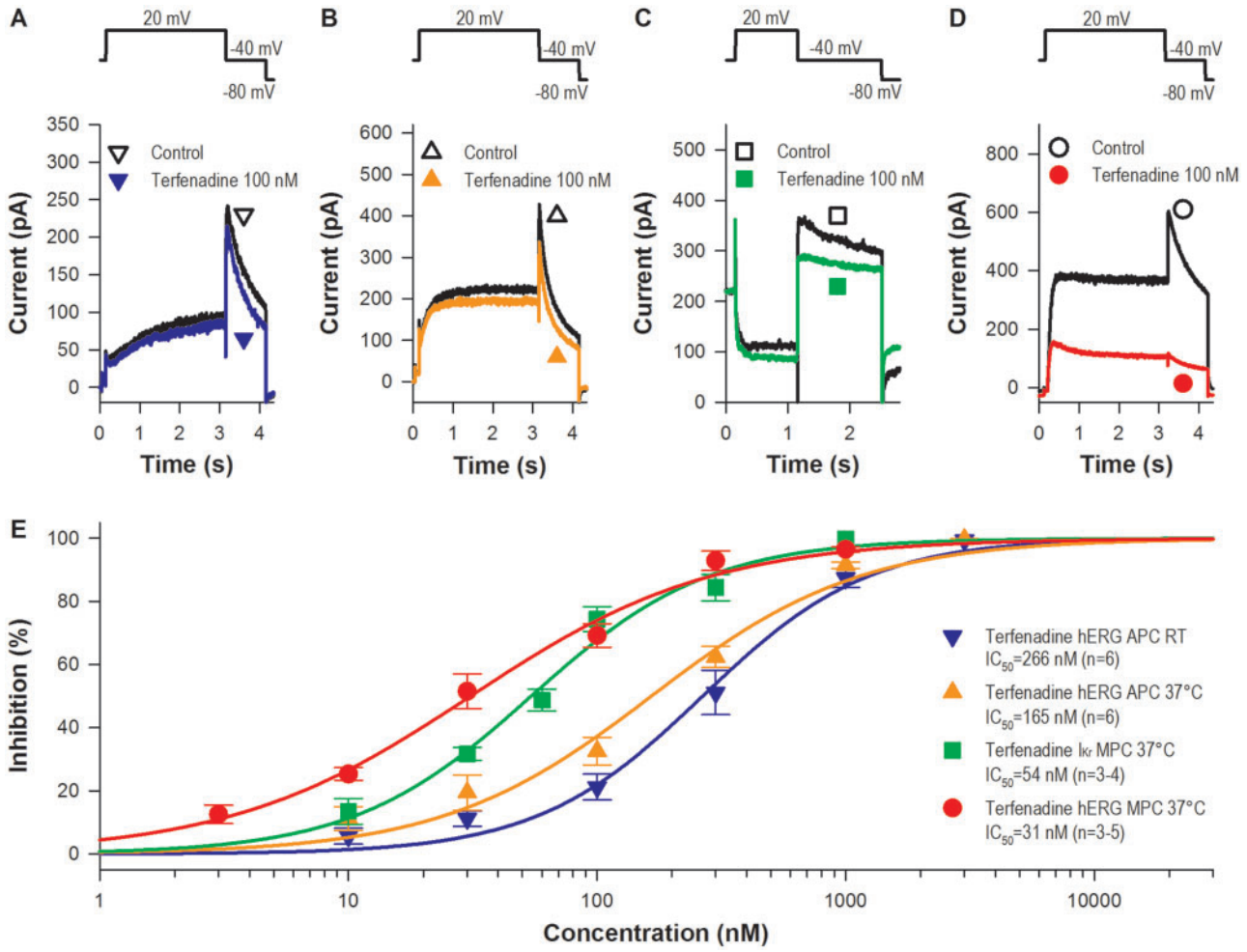

Figure 4. Effect of terfenadine on hERG and I_{Kr} current. A, Representative hERG current sweeps obtained from HEK-hERG cell treated with 100 nM terfenadine at room temperature (RT). B, Effect of 100 nM terfenadine on hERG current at 37°C. C, Representative I_{Kr} current curves obtained from rabbit left ventricular muscle cell treated with 100 nM terfenadine. D, Representative hERG current curves obtained from HEK-hERG cell treated with 100 nM terfenadine using manual patch-clamp technique. The currents were recorded using the voltage protocols shown at the top of panels (A–D). E, Concentration-response curves of terfenadine obtained from hERG experiments at RT, at 37°C using automated and manual patch-clamp techniques and from I_{Kr} measurements. Abbreviations: APC, automated patch-clamp; MPC, manual patch-clamp.

et al., 2004; Perrin *et al.*, 2008; Vormberge *et al.*, 2006]), therefore, this explanation is unlikely. However, IC_{50} value of sotalol calculated from our hERG manual patch-clamp experiments was 77.5 μM showing distinct but moderate difference with the I_{Kr} measurements and it was much less than the corresponding IC_{50} value for automated patch-clamp hERG test. In addition a few study observed similar IC_{50} values for sotalol as such 111 μM (Kramer *et al.*, 2013) and 86 μM (Crumb *et al.*, 2016). Therefore, beyond the high surface-to-volume ratio of recording chips used for automated patch-clamp measurements there should be other important factors, which influence the measurements differently in automated and manual patch-clamp methods.

Also as a possible alternative explanation, the moderate differences between cell line and native myocyte measurements may be due to possible allosteric interaction caused by drugs used in native myocyte but not in cell line measurements for current separation as it was suggested with other organic compound with dofetilide-induced I_{Kr}/hERG inhibition (Yu *et al.*, 2016).

Complex nature of the composition of I_{Kr} channels may also elucidate the difference in potency of sotalol and terfenadine for hERG and native I_{Kr} found in our study. Increasing evidence indicates that the α-subunit composition of the channel can affects its blocking sensitivity. The hERG1 gene encodes at least 2 transcripts: hERG1a, the original isolate, and hERG 1b, an alternate transcript (Lees-Miller *et al.*, 1997; London *et al.*, 1997). The most of hERG screens have been conducted using recombinant cell lines expressing only the hERG 1a subunit, although native ventricular I_{Kr} channels are heteromers containing both hERG 1a and 1b subunits (Jones *et al.*, 2004). Although the potency of most compounds (including sotalol) was similar for the 2 targets, some differences were observed (dofetilide, E-4031 and particularly fluoxetine). Some drugs were more potent at blocking hERG 1a/1b than 1a channels, others exerted greater inhibitory effects on hERG 1a compared with 1a/1b channels. Thus, the existing hERG 1a assays may underestimate the risk of some drugs and overestimate the risk of others (Abi-Gerges *et al.*, 2011; Sale *et al.*, 2008). Also, studies have identified additional interacting proteins affecting hERG drug sensitivity. For example, MinK, MiRPs, and KCR1 coassembles with a pore-forming subunit to create stable complexes whose functional characteristics are similar to the native cardiac potassium

Downloaded from https://academic.oup.com/toxsci/article/168/2/365/5250700 by 81728827 user on 27 April 2021

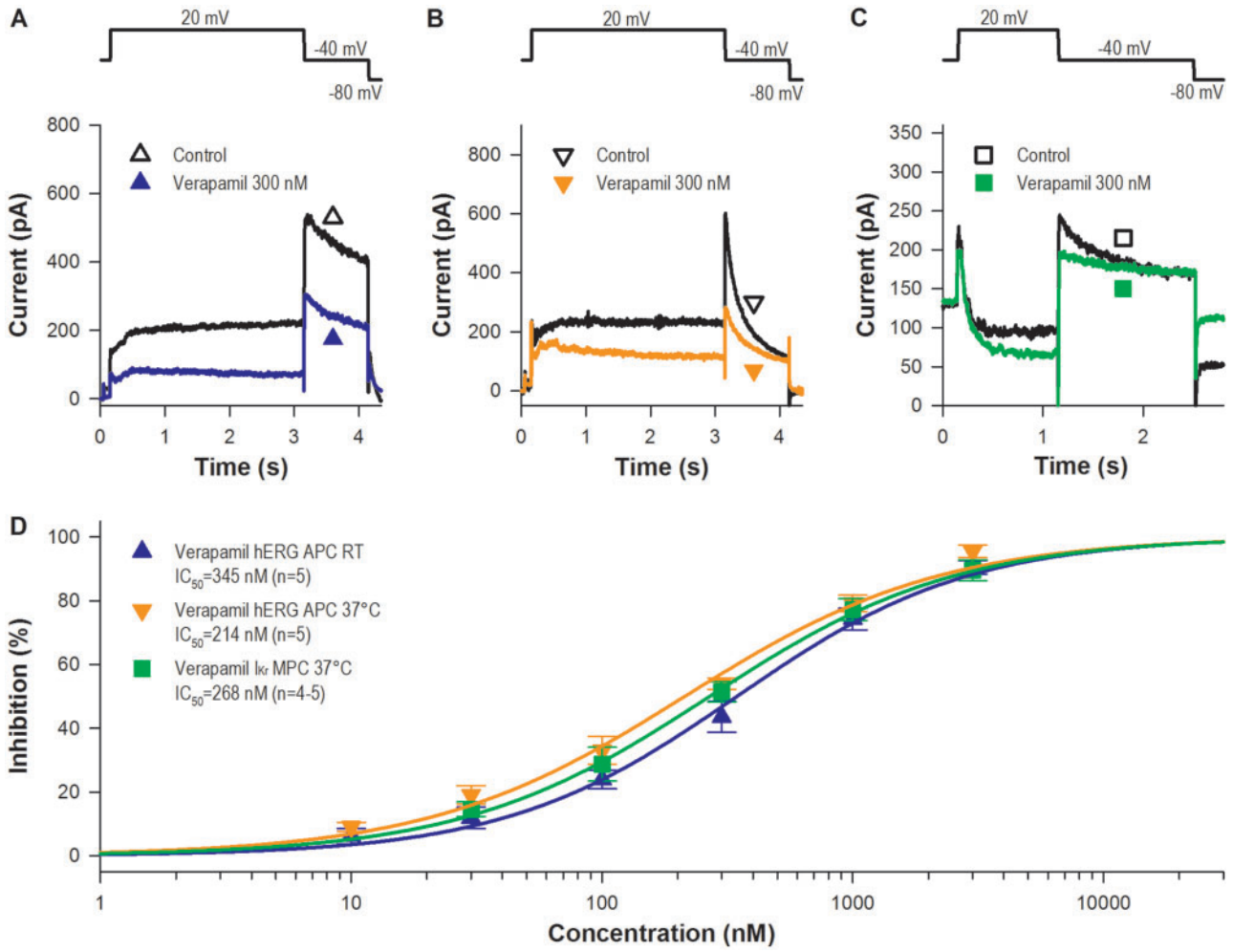

Figure 5. Effect of verapamil on hERG and I_{Kr} current. A, Representative hERG current sweeps obtained from HEK-hERG cell treated with 300 nM verapamil at room temperature (RT). B, Effect of 300 nM verapamil on hERG current at 37°C. C, Representative I_{Kr} current curves obtained from rabbit left ventricular muscle cell treated with 300 nM verapamil. The currents were recorded using the voltage protocols shown at the top of panels (A–C). D, Concentration-response curves of verapamil obtained from hERG experiments at RT and at 37°C using automated patch-clamp technique and from I_{Kr} measurements. Abbreviations: APC, automated patch-clamp; MPC, manual patch-clamp.

Table 1. $IC_{50} \pm$ SEM Values of Inhibitors (Dofetilide, Cisapride, Sotalol, Terfenadine, and Verapamil) Obtained in hERG Assay on Room Temperature (RT), on Physiological (37°C) Temperature and Manual hERG Measurement at 37°C; and in I_{Kr} Assay at 37°C

	Dofetilide (nM)	Cisapride (nM)	Sotalol (μM)	Terfenadine (nM)	Verapamil (nM)
hERG APC RT	8.4 ± 0.2 ($n = 6$)	47.5 ± 4.8 ($n = 5$)	773.7 ± 9.3 ($n = 5$)	266.0 ± 26.8 ($n = 5$)	344.9 ± 26.1 ($n = 5$)
hERG APC 37°C	7.3 ± 0.2 ($n = 5$)	17.7 ± 2.9 ($n = 5$)	342.8 ± 24.8 ($n = 5$)	165.4 ± 24.5 ($n = 5$)	213.6 ± 22.5 ($n = 5$)
hERG MPC 37°C	—	—	77.5 ± 4.8 ($n = 3$–7)	31.0 ± 3.2 ($n = 3$–5)	—
I_{Kr} MPC 37°C	13.0 ± 2.6 ($n = 3$–4)	26.4 ± 4.5 ($n = 3$–5)	51.6 ± 8.8 ($n = 2$–6)	54.3 ± 5.2 ($n = 3$–4)	268.2 ± 11.3 ($n = 4$–5)

Abbreviations: APC, automated patch-clamp; MPC, manual patch-clamp.

channel, adding another level of complexity to mechanisms may affect cardiac safety pharmacology. Their expression and modulation by sotalol could play an important role in determining the amount and character of the I_{Kr} current in individual cardiac myocytes, and may considerably contribute to the action potential prolongation effect of this drug (Abbott *et al.*, 1999; Kupershmidt *et al.*, 2003; McDonald *et al.*, 1997; Weerapura *et al.*, 2002).

Unlike dofetilide, cisapride, and sotalol, terfenadine in spite of inhibiting I_{Kr} had no prolonging effect—even at a high concentration—on APD, which may relate to its blocking effects on other ion channels, such as L-type Ca^{2+} and late Na^{+} currents found in our study, which is the first to report the effect of terfenadine on I_{NaL}. Other studies have also described that terfenadine inhibited not only hERG current but also I_{to}, I_{Ca}, and especially I_{Na} in cardiac myocytes (Ducic *et al.*, 1997; Hondeghem *et al.*, 2011; Lu and Wang, 1999).

Similarly to terfenadine, verapamil did not lengthen the action potential duration. It is known for a long time that verapamil is a Ca-antagonist and as such it blocks L-type Ca^{2+} current (Ehara and Daufmann, 1978; Kohlhardt *et al.*, 1972). Zhang *et al.* (1997) found that application of verapamil at 1 and 5 μM induced

Downloaded from https://academic.oup.com/toxsci/article/168/2/365/5250700 by 81728827 user on 27 April 2021

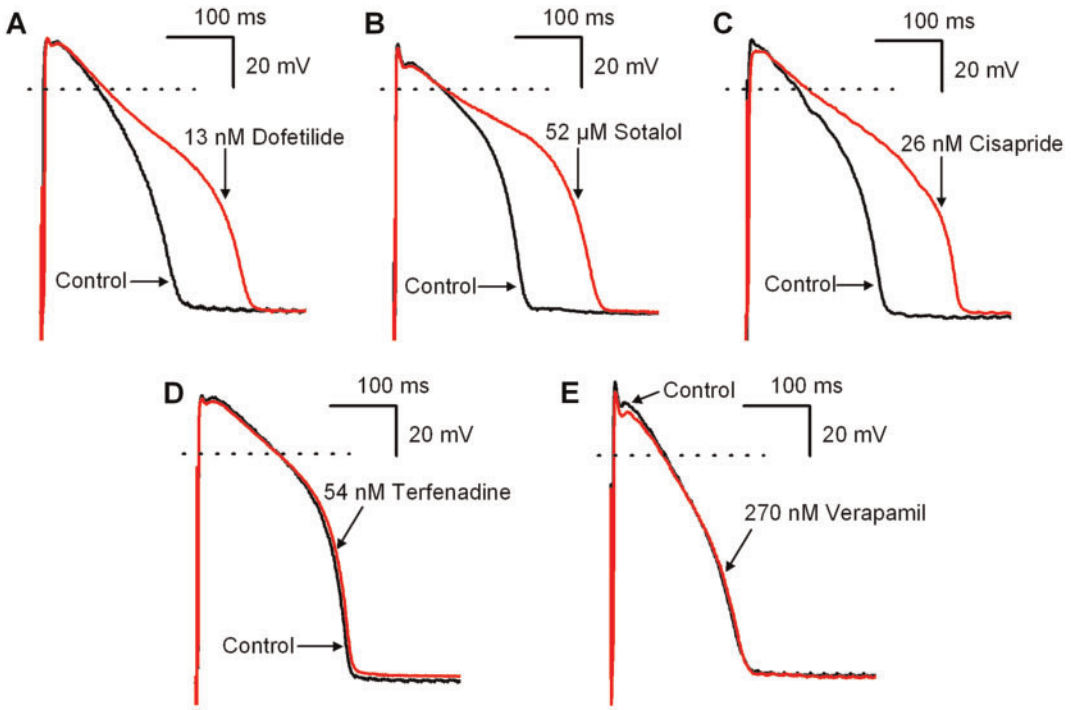

Figure 6. The effects of 13 nM dofetilide (A), 52 μM sotalol (B), 26 nM cisapride (C), 54 nM terfenadine (D), and 270 nM verapamil (E) on action potential waveform of rabbit ventricular muscle at basic cycle length of 1000 ms.

Table 2. The Electrophysiological Effects of 13 nM Dofetilide ($n = 7$), 26 nM Cisapride ($n = 6$), 52 μM Sotalol ($n = 5$), 54 nM Terfenadine ($n = 8$), and 270 nM Verapamil ($n = 5$) in Rabbit Ventricular Muscle Preparations at Basic Cycle Length of 1000 ms

	RP (mV)	APA (mV)	V_{max} (V/s)	APD_{90} (ms)	APD_{90} (%)	APD_{50} (ms)
Control	−88.3 ± 0.3	109.0 ± 2.4	182.1 ± 12.4	190.5 ± 14.1		154.7 ± 15.1
Dofetilide 13 nM	−87.6 ± 0.8	109.3 ± 3.5	187.0 ± 15.9	285.9 ± 40.1*	47.8 ± 12.9	234.4 ± 38.2*
Control	−89.7 ± 0.6	105.1 ± 2.0	139.7 ± 14.0	184.7 ± 6.9		143.0 ± 7.7
Cisapride 26 nM	−88.7 ± 1.3	105.7 ± 1.7	129.3 ± 14.8	310.7 ± 20.7*	68.4 ± 10.0	236.3 ± 18.3*
Control	−90.1 ± 0.7	103.4 ± 1.9	170.5 ± 15.3	156.9 ± 10.7		116.6 ± 13.1
Sotalol 52 μM	−91.8 ± 0.6	105.8 ± 3.1	205.3 ± 21.6	244.3 ± 15.9*	56.0 ± 4.6	181.3 ± 21.5*
Control	−91.5 ± 0.6	111.9 ± 1.9	179.9 ± 10.5	205.4 ± 9.1		170.1 ± 9.0
Terfenadine 54 nM	−91.1 ± 1.2	113.7 ± 2.3	201.5 ± 18.5	209.1 ± 13.7	1.4 ± 3.0	174.5 ± 13.0
Control	−84.1 ± 2.2	104.7 ± 2.9	129.3 ± 13.8	176.6 ± 11.5		139.5 ± 13.1
Verapamil 270 nM	−81.6 ± 2.2	105.8 ± 1.9	121.9 ± 12.1	177.3 ± 12.6	0.6 ± 1.8	137.2 ± 14.0

Results are means ± SEM. *$p < .05$.

Abbreviations: APA, action potential amplitude; APD_{90} and APD_{50}, action potential durations at 50% and 90% of repolarization; RP, resting potential; V_{max}, maximum rate of depolarization.

dual changes in repolarization, prolonging APD_{90} at 1 μM, and shortening at 5 μM in guinea-pig isolated myocytes, however, Chen and Gettes (1979) reported that verapamil did not influence APD in guinea-pig and dog papillary muscles. In our study, the I_{CaL} blocking property of verapamil found to be similar or even weaker than the I_{Kr} blocking potency of the drug. I_{NaL} was not affected by verapamil in our experiments, similarly to earlier studies reporting that verapamil at similar concentration range did not influence fast Na^+ current (Chen and Gettes, 1979; Rosen *et al.*, 1975).

Therefore, the multichannel blocking property of terfenadine and verapamil might explain the lack of action potential prolonging effect of these drugs. It is interesting that dofetilide, cisapride, and sotalol produced a more excessive lengthening of APD in rabbit ventricular tissue preparations compared with that found in human. Thus, there may be species differences in the effects of I_{Kr} blockade, which emphasizes the importance of species model selected for a safety pharmacological study. The expression level and properties of cardiac ion channels are varied in different species that should be taken into account when extrapolating the results from animal models of proarrhythmia to humans. Some studies (Jonsson *et al.*, 2012; Liang *et al.*, 2013; Scheel *et al.*, 2014) using a relatively new approach, the human stem cell-derived cardiomyocytes, and recently 2 other papers (Page *et al.*, 2016; Qu *et al.*, 2018) that applied the conventional microelectrode technique in human ventricular trabeculae investigated possible pro-arrhythmia risk of several drugs including dofetilide, cisapride, terfenadine, sotalol, and verapamil. Our action potential data obtained from human preparations are in good agreement with the results of Qu *et al.* (2018) except

Downloaded from https://academic.oup.com/toxsci/article/168/2/365/5250700 by 81728827 user on 27 April 2021

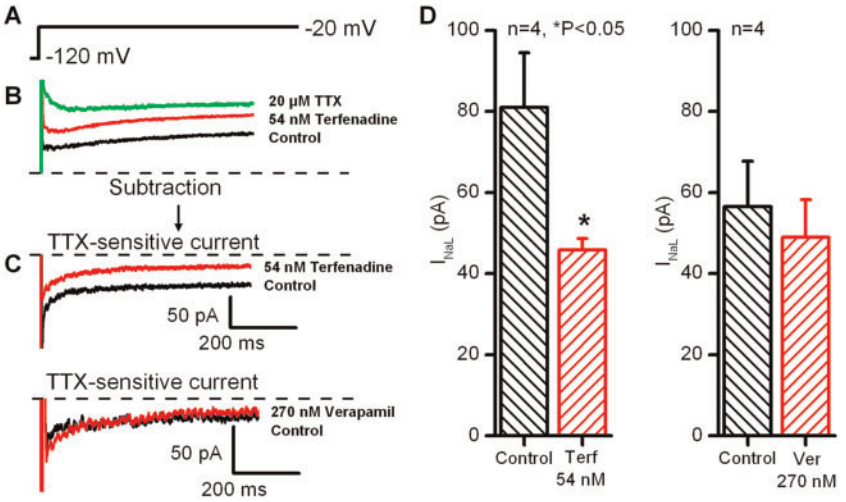

Figure 7. Effect of 54 nM terfenadine and 270 nM verapamil on I_{NaL} current in rabbit ventricular myocytes. A, Applied voltage protocol. B, Original current traces show that 54 nM terfenadine excessively reduced I_{NaL}, whereas 20 μM TTX completely blocks the current. C, TTX sensitive current traces in control conditions and after application of 54 nM terfenadine (*top*) and 270 nM verapamil (*bottom*). D, TTX sensitive current (I_{NaL}) in the absence and presence of 54 nM terfenadine (*left*) and 270 nM verapamil (*right*) at the test potential of −20 mV. Values are means ± SEM, $n = 4$, $^*p < .05$.

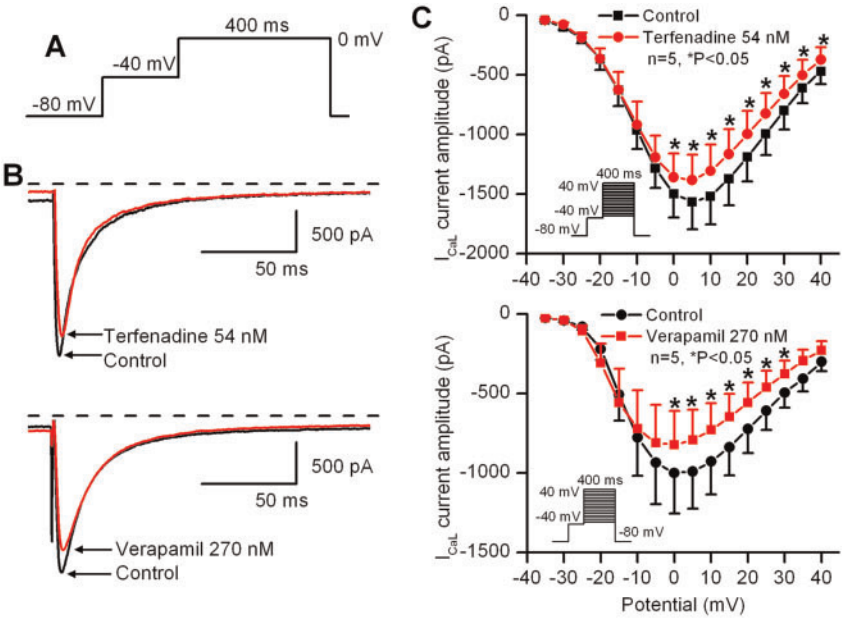

Figure 8. Effect of 54 nM terfenadine and 270 nM verapamil on the L-type I_{Ca} in rabbit ventricular myocytes. A, Voltage protocol. B, Original current traces recorded in control conditions and in the presence of 54 nM terfenadine (*top*) and 270 nM verapamil (*bottom*). C, Current-voltage relationship of I_{CaL} in the absence and presence of 54 nM terfenadine (*top*) and 270 nM verapamil (*bottom*). Values are means ± SEM, $n = 5$, $^*p < .05$.

for cisapride. Qu *et al.* (2018) reported that 30 nM cisapride slightly (by 8%) shortened the action potential. Page *et al.* (2016), however, described similar results with dofetilide, sotalol, and verapamil to that found in this study. Therefore, human *ex vivo* models using native human ventricular preparations would generate more reliable and predictive data on proarrhythmic adverse effects at the preclinical stage of drug development (Page *et al.*, 2016).

As the hERG assay is pulse protocol sensitive, longer pulses and higher frequency would potentiate the drug binding to the channel increasing the potency of the drug depending on the onset and offset kinetics of the compound (Kirsch *et al.*, 2004). Therefore, a shorter impulse, such as an action potential, which is only about 200 ms long in rabbit heart, might decrease the chance of drug binding influencing negatively the potency of a particular drug during action potential measurements.

Another factor might affect the potency of a drug is that during these experiments the drug must penetrate into the tissue preparation to exert its effects. Slow diffusion of drug in the tissue may result in low tissue concentration, which impairs the effect of a particular drug on action potential repolarization.

These additional factors may offset repolarization lengthening of terfenadine and verapamil. I_{Na} blockade of the terfenadine can impair impulse conduction, thus evoke ventricular fibrillation, related to a noticeable widening of the QRS complex, without significant prolongation of QT intervals (Hondeghem *et al.*, 2011; Lu *et al.*, 2012). In this context it has to mention that in this manuscript we did not focus on the accuracy of

Downloaded from https://academic.oup.com/toxsci/article/168/2/365/5250700 by 81728827 user on 27 April 2021

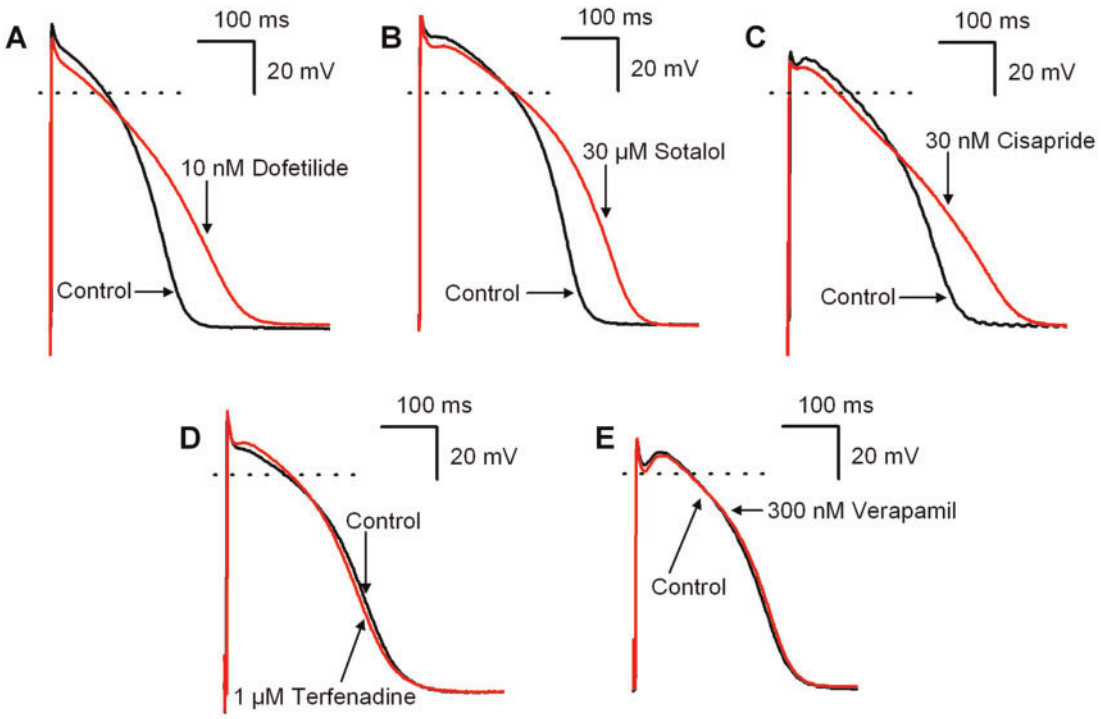

Figure 9. The effects of 10 nM dofetilide (A), 30 μM sotalol (B), 30 nM cisapride (C), 1 μM terfenadine (D), and 300 nM verapamil (E) on action potential waveform in undiseased human ventricular muscle at basic cycle length of 1000 ms.

Table 3. The Electrophysiological Effects of 10 nM Dofetilide ($n = 7$), 30 nM Cisapride ($n = 3$), 30 μM Sotalol ($n = 6$), 1 μM Terfenadine ($n = 3$), and 300 nM Verapamil ($n = 3$) in Human Ventricular Muscle Preparations at Basic Cycle Length of 1000 ms

	RP (mV)	APA (mV)	V_{max} (V/s)	APD_{90} (ms)	APD_{90} (%)	APD_{50} (ms)
Control	−86.9 ± 1.3	110.1 ± 1.4	295.5 ± 35.7	239.4 ± 9.8		180.0 ± 6.7
Dofetilide 10 nM	−87.4 ± 0.8	110.9 ± 2.6	263.4 ± 28.9	287.6 ± 13.6*	20.4 ± 4.5	206.6 ± 7.9*
Control	−83.7 ± 5.0	103.3 ± 2.5	265.9 ± 71.0	260.7 ± 17.8		180.4 ± 19.8
Cisapride 30 nM	−83.9 ± 3.5	102.3 ± 1.8	269.8 ± 61.8	334.6 ± 42.1	27.5 ± 9.8	224.6 ± 22.2
Control	−89.7 ± 1.0	119.2 ± 2.0	230.8 ± 21.3	301.8 ± 19.7		233.0 ± 17.4
Sotalol 30 μM	−88.8 ± 1.5	119.2 ± 2.4	250.0 ± 21.1	387.0 ± 27.6*	28.0 ± 1.8	281.0 ± 20.1*
Control	−84.8 ± 1.9	109.7 ± 3.2	275.9 ± 26.6	269.7 ± 12.7		208.7 ± 10.3
Terfenadine 1 μM	−84.6 ± 1.7	112.4 ± 3.0	325.2 ± 34.6	256.7 ± 16.6	−5.0 ± 1.7	192.0 ± 9.4*
Control	−87.8 ± 2.8	99.1 ± 7.8	203.2 ± 63.3	262.1 ± 17.2		194.4 ± 16.5
Verapamil 300 nM	−90.7 ± 0.8	101.5 ± 6.3	213.3 ± 61.1	270.7 ± 11.2	3.6 ± 2.7	199.9 ± 12.4

Results are means ± SEM. *$p < .05$.

Abbreviations: APA, action potential amplitude; APD_{90} and APD_{50}, action potential durations at 50% and 90% of repolarization; RP, resting potential; V_{max}, maximum rate of depolarization.

predictability of drug-induced TdP or ventricular fibrillation. Other recent well-demonstrated studies strongly suggest that other factors than potassium ion channel inhibition such as Triangulation of action potential waveform, Reverse use dependence, Instability, and Dispersion of repolarization defined as TRIaD and wavelength of excitation (λ) defined as CV (conduction velocity) multiplied by the effective refractory period (ERP) are also important to properly assess drug-induced arrhythmia propensity (Hondeghem, 2008a,b). In our work, we only would like to present further arguments regarding the shortcomings of the widely used hERG screening for arrhythmia predictability.

According to our research, native I_{Kr} assay shows better correlation with APD than hERG measurements and it seems a better tool in evaluation of cardiac proarrhythmic risk. Although it is generally accepted that the most common electrophysiological mechanism for drug-associated cardiac proarrhythmic and sudden death risks result from blocking I_{Kr}, accordingly, inhibition of I_{Kr} current is considered a primary detector for proarrhythmic liability, the possibility of inhibition of other potassium currents such as I_{K1} and I_{Ks} cannot be neglected. It was shown that malfunction of those latter ion channels can cause latent and manifest LQT syndromes (Cubeddu, 2016). Also blocking these K^+ channels may not result in marked repolarization lengthening but by decreasing the repolarization reserve they greatly increase dispersion of repolarization and thereby enhancing proarrhythmic risk (Biliczki *et al.*, 2002; Roden, 2008; Roden and Yang, 2005). Therefore, careful safety pharmacological testing should also include preparation where the repolarization reserve had been previously attenuated to reveal this apparently silent proarrhythmic risk. It

Downloaded from https://academic.oup.com/toxsci/article/168/2/365/5250700 by 81728827 user on 27 April 2021

should be kept in mind that drug-induced proarrhythmic events may have very low incidence (1:10 000–1:100 000) suggesting that multiple channel hits can be 1 possible explanation (Hancox *et al.*, 2008; Lengyel *et al.*, 2007; Varró and Baczkó, 2011; Yap and Camm, 2003). However, drugs, such as amiodarone or ranolazine can induce large action potential lengthening and QT prolongation with a concomitant reduction of the dispersion of repolarization in the ventricle decreasing the risk of arrhythmia. It is most likely due to the multichannel (I_{Kr}, I_{Ks}, I_{Na}, and I_{CaL}) blockade of these drugs especially inhibition of the late I_{Na}, which current is more prominent in the midmyocardial cells and in Purkinje fibers (Antzelevitch *et al.*, 2004). In other words, complex multichannel interactions of drugs with other cardiac ion channels can also contribute to their proarrhythmic effects—but also sometimes tend to mitigate the proarrhythmic effect of I_{Kr} current blockade—thus action potential and *in vivo* cardiac electrophysiological measurements also should be an integral part of proarrhythmic pharmacological safety drug tests, the single ion channel approach is not recommended. Moreover, *in vitro* and *in vivo* studies with reduced repolarization reserve are also essential, adding another level to the cardiac safety pharmacology.

In conclusion, results obtained with automated patch-clamp equipment in HEK-hERG cells usually show a reasonable conformity with outcomes of I_{Kr} current and action potential experiments. However, important and not well understood differences exist between the evaluation of hERG-blocking ability with automated patch-clamp and other techniques such as the I_{Kr}, action potential, and ECG measurements. Therefore, cardiac safety is more accurately evaluated using all these methods simultaneously. The application of high-throughput hERG channel screening as the only or predominant method is not recommended because it may discredit otherwise valuable lead molecules and/or may not detect properly the proarrhythmic potentials of others. This study would like to draw the attention to the limitations of the single ion channel approach especially using high-throughput screening. In recent years, great efforts have been made on improving the assessment of drug-associated TdP risk. The purpose of the comprehensive *in vitro* proarrhythmia assay is to avoid the misidentification of proarrhythmic potential of drugs based only on hERG and QT investigations (Sager *et al.*, 2014). This new paradigm consist of 4 components: an ion channel panel measured in heterologous expression systems, *in silico* action potential models, human-induced pluripotent stem cell-derived cardiomyocyte assay, and human phase 1 ECGs. Based on our studies, characterization of electrophysiological effects of drugs and drug candidate molecules on native ion channels and animal or especially human *ex-vivo* action potential models are also important, and may contribute to the understanding of the complex proarrhythmic mechanisms. However, additional studies with much larger set of compounds are needed to infer the true predictivity of the integrated hERG, I_{Kr}, and AP/ECG assays.

Limitation of the Study

Important transmural and regional differences in current densities and in ion channel subunit protein expression exist within the heart. However, in our study ion currents were measured in single myocytes (mainly midmyocardial) isolated from left ventricular tissue, but action potentials were recorded from right ventricular subendocardial tissue. The reason is mainly technical. Conventional microelectrode recordings from left ventricular tissue were difficult to obtain producing a substantially smaller success rate and left ventricular subendocardial tissue more likely to be contaminated by subendocardial Purkinje cells, which electrotonically influence the recordings and hamper pharmacologic investigations.

Another issue is the problem of species differences. Most of our experiments were performed in rabbit. However, the action potential waveform in rabbit is similar to that of human but the current density, kinetical properties and even the type of channel subunits in rabbit may be different from those in human, which may influence the drug effects on action potential and repolarization.

The third factor is that experimental conditions such as voltage protocol, stimulation frequency, exposure time of the drug, and temperature may affect the action of drugs. If the particular drug rate- or voltage-dependently block the channel its potency in patch-clamp experiments may diverged from that measured in physiological conditions in cardiac muscle.

ACKNOWLEDGMENTS

The authors wish to thank Mrs Zsuzsa Molnár for technical assistance. The authors have declared that no conflicts of interest exist.

FUNDING

This work was supported by grants from the National Research, Development and Innovation Office (K-119992, FK-129117, and a GINOP-2.3.2-15-2016-00012), the Ministry of Human Capacities Hungary (20391-3/2018/FEKUSTRAT and EFOP-3.6.2-16-2017-00006), by the HU-RO Cross-Border Cooperation Programmes (HU-RO/0802/011_AF HURO-CARDIOPOL and HURO/1001/086/2.2.1 HURO-TWIN) and from the Hungarian Academy of Sciences.

REFERENCES

Abbott, G. W., Sesti, F., Splawski, I., Buck, M. E., Lehmann, M. H., Timothy, K. W., Keating, M. T., and Goldstein, S. A. (1999). MiRP1 forms I_{Kr} potassium channels with hERG and is associated with cardiac arrhythmia. *Cell* **97**, 175–187.

Abi-Gerges, N., Holkham, H., Jones, E. M. C., Pollard, C. E., Valentin, J.-P., and Robertson, G. A. (2011). hERG subunit composition determines differential drug sensitivity. *Br. J. Pharmacol.* **164**, 419–432.

Alexander, S. P. H., Mathie, A., and Peters, J. A. (2011). Guide to Receptors and Channels (GRAC), 5th edition. *Br. J. Pharmacol.* **164(Suppl. 1)**, S1–324.

Antzelevitch, C., Belardinelli, L., Zygmunt, A. C., Burashnikov, A., Di Diego, J. M., Fish, J. M., Cordeiro, J. M., and Thomas, G. (2004). Electrophysiological effects of ranolazine, a novel antianginal agent with antiarrhythmic properties. *Circulation* **110**, 904–910.

Aslanian, R., Piwinski, J. J., Zhu, X., Priestley, T., Sorota, S., Du, X. Y., Zhang, X. S., McLeod, R. L., West, R. E., and Williams, S. M. (2009). Structural determinants for histamine H(1) affinity, hERG affinity and QTc prolongation in a series of terfenadine analogs. *Bioorg. Med. Chem. Lett.* **19**, 5043–5047.

Biliczki, P., Virág, L., Iost, N., Papp, J. G., and Varró, A. (2002). Interaction of different potassium channels in cardiac repolarization in dog ventricular preparations: Role of repolarization reserve. *Br. J. Pharmacol.* **137**, 361–368.

Downloaded from https://academic.oup.com/toxsci/article/168/2/365/5250700 by 81728827 user on 27 April 2021

Carmeliet, E. (1998). Effects of cetirizine on the delayed K^+ currents in cardiac cells: Comparison with terfenadine. *Br. J. Pharmacol.* **124**, 663–668.

Chen, C. M., and Gettes, L. S. (1979). Effects of verapamil on rapid Na channel-dependent action potentials of K^+-depolarized ventricular fibers. *J. Pharmacol. Exp. Ther.* **209**, 415–421.

Chouabe, C., Drici, M. D., Romey, G., Barhanin, J., and Lazdunski, M. (1998). hERG and KvLQT1/IsK, the cardiac K^+ channels involved in long QT syndromes, are targets for calcium channel blockers. *Mol. Pharmacol.* **54**, 695–703.

Crumb, W. J., Jr (2000). Loratadine blockade of K(+) channels in human heart: Comparison with terfenadine under physiological conditions. *J. Pharmacol. Exp. Ther.* **292**, 261–264.

Crumb, W. J., Jr, Vicente, J., Johannesen, L., and Strauss, D. G. (2016). An evaluation of 30 clinical drugs against the comprehensive *in vitro* proarrhythmia assay (CiPA) proposed ion channel panel. *J. Pharmacol. Toxicol. Methods* **81**, 251–262.

Cubeddu, L. X. (2016). Drug-induced inhibition and trafficking disruption of ion channels: Pathogenesis of QT abnormalities and drug-induced fatal arrhythmias. *Curr. Cardiol. Rev.* **12**, 141–154.

Dabrowski, M. A., Dekermendjian, K., Lund, P.-E., Krupp, J. J., Sinclair, J., and Larsson, O. (2008). Ion channel screening technology. *CNS Neurol. Disord. Drug Targets* **7**, 122–128.

Drolet, B., Khalifa, M., Daleau, P., Hamelin, B. A., and Turgeon, J. (1998). Block of the rapid component of the delayed rectifier potassium current by the prokinetic agent cisapride underlies drug-related lengthening of the QT interval. *Circulation* **97**, 204–210.

Ducic, I., Ko, C. M., Shuba, Y., and Morad, M. (1997). Comparative effects of loratadine and terfenadine on cardiac K^+ channels. *J. Cardiovasc. Pharmacol.* **30**, 42–54.

Dunlop, J., Bowlby, M., Peri, R., Vasilyev, D., and Arias, R. (2008). High-throughput electrophysiology: An emerging paradigm for ion-channel screening and physiology. *Nat. Rev. Drug Discov.* **7**, 358–368.

Ehara, T., and Daufmann, R. (1978). The voltage- and time-dependent effects of (−)-verapamil on the slow inward current in isolated cat ventricular myocardium. *J. Pharmacol. Exp. Ther.* **207**, 49–55.

Farre, C., and Fertig, N. (2012). HTS techniques for patch clamp-based ion channel screening—advances and economy. *Expert Opin. Drug Discov.* **7**, 515–524.

Farre, C., George, M., Brüggemann, A., and Fertig, N. (2008). Ion channel screening—automated patch clamp on the rise. *Drug Discov. Today Technol.* **5**, e23–28.

Farre, C., Haythornthwaite, A., Haarmann, C., Stoelzle, S., Kreir, M., George, M., Brüggemann, A., and Fertig, N. (2009). Port-a-patch and patchliner: High fidelity electrophysiology for secondary screening and safety pharmacology. *Comb. Chem. High Throughput Screen.* **12**, 24–37.

Farre, C., Stoelzle, S., Haarmann, C., George, M., Brüggemann, A., and Fertig, N. (2007). Automated ion channel screening: Patch clamping made easy. *Expert Opin. Ther. Targets* **11**, 557–565.

Fertig, N., Blick, R. H., and Behrends, J. C. (2002). Whole cell patch clamp recording performed on a planar glass chip. *Biophys. J.* **82**, 3056–3062.

Fossa, A. A., Wisialowski, T., Wolfgang, E., Wang, E., Avery, M., Raunig, D. L., and Fermini, B. (2004). Differential effect of hERG blocking agents on cardiac electrical alternans in the guinea pig. *Eur. J. Pharmacol.* **486**, 209–221.

Guth, B. D., Germeyer, S., Kolb, W., and Markert, M. (2004). Developing a strategy for the nonclinical assessment of proarrhythmic risk of pharmaceuticals due to prolonged ventricular repolarization. *J. Pharmacol. Toxicol. Methods* **49**, 159–169.

Hancox, J. C., McPate, M. J., El Harchi, A., and Zhang, Y. H. (2008). The hERG potassium channel and hERG screening for drug-induced torsades de pointes. *Pharmacol. Ther.* **119**, 118–132.

Hishigaki, H., and Kuhara, S. (2011). hERGAPDbase: A database documenting hERG channel inhibitory potentials and APD-prolongation activities of chemical compounds. *Database J. Biol. Databases Curation* **2011**, bar017.

Hodgkin, A. L., and Huxley, A. F. (1945). Resting and action potentials in single nerve fibres. *J. Physiol.* **104**, 176–195.

Hondeghem, L. M. (2008a). QT prolongation is an unreliable predictor of ventricular arrhythmia. *Heart Rhythm* **5**, 1210–1212.

Hondeghem, L. M. (2008b). Use and abuse of QT and TRIaD in cardiac safety research: Importance of study design and conduct. *Eur. J. Pharmacol.* **584**, 1–9.

Hondeghem, L. M., Dujardin, K., Hoffmann, P., Dumotier, B., and De Clerck, F. (2011). Drug-induced QT_C prolongation dangerously underestimates proarrhythmic potential: Lessons from terfenadine. *J. Cardiovasc. Pharmacol.* **57**, 589–597.

Jones, E. M. C., Roti Roti, E. C., Wang, J., Delfosse, S. A., and Robertson, G. A. (2004). Cardiac I_{Kr} channels minimally comprise hERG 1a and 1b subunits. *J. Biol. Chem.* **279**, 44690–44694.

Jonsson, M. K., Vos, M. A., Mirams, G. R., Duker, G., Sartipy, P., de Boer, T. P., and van Veen, T. A. (2012). Application of human stem cell-derived cardiomyocytes in safety pharmacology requires caution beyond hERG. *J. Mol. Cell. Cardiol.* **52**, 998–1008.

Jost, N., Nagy, N., Corici, C., Kohajda, Z., Horváth, A., Acsai, K., Biliczki, P., Levijoki, J., Pollesello, P., Koskelainen, T., *et al.* (2013). ORM-10103, a novel specific inhibitor of the $Na^+/Ca2^+$ exchanger, decreases early and delayed afterdepolarizations in the canine heart. *Br. J. Pharmacol.* **170**, 768–778.

Jost, N., Virág, L., Bitay, M., Takács, J., Lengyel, C., Biliczki, P., Nagy, Z., Bogáts, G., Lathrop, D. A., Papp, J. G., *et al.* (2005). Restricting excessive cardiac action potential and QT prolongation: A vital role for I_{Ks} in human ventricular muscle. *Circulation* **112**, 1392–1399.

Kirsch, G. E., Trepakova, E. S., Brimecombe, J. C., Sidach, S. S., Erickson, H. D., Kochan, M. C., Shyjka, L. M., Lacerda, A. E., and Brown, A. M. (2004). Variability in the measurement of hERG potassium channel inhibition: Effects of temperature and stimulus pattern. *J. Pharmacol. Toxicol. Methods* **50**, 93–101.

Kohajda, Z., Farkas-Morvay, N., Jost, N., Nagy, N., Geramipour, A., Horváth, A., Varga, R. S., Hornyik, T., Corici, C., Acsai, K., *et al.* (2016). The effect of a novel highly selective inhibitor of the sodium/calcium exchanger (NCX) on cardiac arrhythmias in *in vitro* and *in vivo* experiments. *PLoS One* **11**, e0166041.

Kohlhardt, M., Bauer, B., Krause, H., and Fleckenstein, A. (1972). Na and Ca channels in mammalian cardiac fibres by the use of specific inhibitors. *Pflugers Arch.* **335**, 309–322.

Kramer, J., Obejero-Paz, C. A., Myatt, G., Kuryshev, Y. A., Bruening-Wright, A., Verducci, J. S., and Brown, A. M. (2013). MICE models: Superior to the hERG model in predicting torsade de pointes. *Sci. Rep.* **3**, 2100.

Kristóf, A., Husti, Z., Koncz, I., Kohajda, Z., Szél, T., Juhász, V., Biliczki, P., Jost, N., Baczkó, I., Papp, J. G., *et al.* (2012). Diclofenac prolongs repolarization in ventricular muscle with impaired repolarization reserve. *PLoS One* **7**, e53255.

Downloaded from https://academic.oup.com/toxsci/article/168/2/365/5250700 by 81728827 user on 27 April 2021

Kupershmidt, S., Yang, I. C.-H., Hayashi, K., Wei, J., Chanthaphaychith, S., Petersen, C. I., Johns, D. C., George, A. L., Roden, D. M., and Balser, J. R. (2003). The I_{Kr} drug response is modulated by KCR1 in transfected cardiac and noncardiac cell lines. *FASEB J.* **17**, 2263–2265.

Lees-Miller, J. P., Kondo, C., Wang, L., and Duff, H. J. (1997). Electrophysiological characterization of an alternatively processed ERG K^+ channel in mouse and human hearts. *Circ. Res.* **81**, 719–726.

Lengyel, C., Iost, N., Virág, L., Varró, A., Lathrop, D. A., and Papp, J. G. (2001). Pharmacological block of the slow component of the outward delayed rectifier current (*I*(Ks)) fails to lengthen rabbit ventricular muscle QT(c) and action potential duration. *Br. J. Pharmacol.* **132**, 101–110.

Lengyel, C., Varró, A., Tábori, K., Papp, J. G., and Baczkó, I. (2007). Combined pharmacological block of *I*(Kr) and *I*(Ks) increases short-term QT interval variability and provokes torsades de pointes. *Br. J. Pharmacol.* **151**, 941–951.

Liang, P., Lan, F., Lee, A. S., Gong, T., Sanchez-Freire, V., Wang, Y., Diecke, S., Sallam, K., Knowles, J. W., Wang, P. J., *et al.* (2013). Drug screening using a library of human induced pluripotent stem cell-derived cardiomyocytes reveals disease-specific patterns of cardiotoxicity. *Circulation* **127**, 1677–1691.

Limberis, J. T., Su, Z., Cox, B. F., Gintant, G. A., and Martin, R. L. (2006). Altering extracellular potassium concentration does not modulate drug block of human ether-a-go-go-related gene (hERG) channels. *Clin. Exp. Pharmacol. Physiol.* **33**, 1059–1065.

London, B., Trudeau, M. C., Newton, K. P., Beyer, A. K., Copeland, N. G., Gilbert, D. J., Jenkins, N. A., Satler, C. A., and Robertson, G. A. (1997). Two isoforms of the mouse ether-a-go-go-related gene coassemble to form channels with properties similar to the rapidly activating component of the cardiac delayed rectifier K^+ current. *Circ. Res.* **81**, 870–878.

Lü, Q., and An, W. F. (2008). Impact of novel screening technologies on ion channel drug discovery. *Comb. Chem. High Throughput Screen.* **11**, 185–194.

Lu, H. R., Hermans, A. N., and Gallacher, D. J. (2012). Does terfenadine-induced ventricular tachycardia/fibrillation directly relate to its QT prolongation and torsades de pointes? *Br. J. Pharmacol.* **166**, 1490–1502.

Lu, Y., and Wang, Z. (1999). Terfenadine block of sodium current in canine atrial myocytes. *J. Cardiovasc. Pharmacol.* **33**, 507–513.

Martin, R. L., McDermott, J. S., Salmen, H. J., Palmatier, J., Cox, B. F., and Gintant, G. A. (2004). The utility of hERG and repolarization assays in evaluating delayed cardiac repolarization: Influence of multi-channel block. *J. Cardiovasc. Pharmacol.* **43**, 369–379.

Mathes, C. (2006). QPatch: The past, present and future of automated patch clamp. *Expert Opin. Ther. Targets* **10**, 319–327.

McDonald, T. V., Yu, Z., Ming, Z., Palma, E., Meyers, M. B., Wang, K. W., Goldstein, S. A., and Fishman, G. I. (1997). A minK-hERG complex regulates the cardiac potassium current *I*(Kr). *Nature* **388**, 289–292.

Mo, Z.-L., Faxel, T., Yang, Y.-S., Gallavan, R., Messing, D., and Bahinski, A. (2009). Effect of compound plate composition on measurement of hERG current IC(50) using PatchXpress. *J. Pharmacol. Toxicol. Methods* **60**, 39–44.

Möller, C., and Witchel, H. (2011). Automated electrophysiology makes the pace for cardiac ion channel safety screening. *Front. Pharmacol.* **2**, 73.

Neher, E., and Sakmann, B. (1976). Single-channel currents recorded from membrane of denervated frog muscle fibres. *Nature* **260**, 799–802.

Neher, E., Sakmann, B., and Steinbach, J. H. (1978). The extracellular patch clamp: A method for resolving currents through individual open channels in biological membranes. *Pflüg. Arch. Eur. J. Physiol.* **375**, 219–228.

Orvos, P., Virág, L., Tálosi, L., Hajdú, Z., Csupor, D., Jedlinszki, N., Szél, T., Varró, A., and Hohmann, J. (2015). Effects of *Chelidonium majus* extracts and major alkaloids on hERG potassium channels and on dog cardiac action potential—a safety approach. *Fitoterapia* **100**, 156–165.

Page, G., Ratchada, P., Miron, Y., Steiner, G., Ghetti, A., Miller, P. E., Reynolds, J. A., Wang, K., Greiter-Wilke, A., Polonchuk, L., *et al.* (2016). Human *ex-vivo* action potential model for pro-arrhythmia risk assessment. *J. Pharmacol. Toxicol. Methods* **81**, 183–195.

Pearlstein, R. A., Vaz, R. J., Kang, J., Chen, X.-L., Preobrazhenskaya, M., Shchekotikhin, A. E., Korolev, A. M., Lysenkova, L. N., Miroshnikova, O. V., Hendrix, J., *et al.* (2003). Characterization of hERG potassium channel inhibition using CoMSiA 3D QSAR and homology modeling approaches. *Bioorg. Med. Chem. Lett.* **13**, 1829–1835.

Perrin, M. J., Kuchel, P. W., Campbell, T. J., and Vandenberg, J. I. (2008). Drug binding to the inactivated state is necessary but not sufficient for high-affinity binding to human ether-a-go-go-related gene channels. *Mol. Pharmacol.* **74**, 1443–1452.

Polonchuk, L. (2012). Toward a new gold standard for early safety: Automated temperature-controlled hERG test on the PatchLiner. *Front. Pharmacol.* **3**, 3.

Qu, Y., Page, G., Abi-Gerges, N., Miller, P. E., Ghetti, A., and Vargas, H. M. (2018). Action potential recording and pro-arrhythmia risk analysis in human ventricular trabeculae. *Front. Physiol.* **8**, 1109.

Roden, D. M. (2008). Repolarization reserve: A moving target. *Circulation* **118**, 981–982.

Roden, D. M., and Yang, T. (2005). Protecting the heart against arrhythmias: Potassium current physiology and repolarization reserve. *Circulation* **112**, 1376–1378.

Rosen, M. R., Wit, A. L., and Hoffman, B. F. (1975). Electrophysiology and pharmacology of cardiac arrhythmias. VI. Cardiac effects of verapamil. *Am. Heart J.* **89**, 665–673.

Sager, P. T., Gintant, G., Turner, J. R., Pettit, S., and Stockbridge, N. (2014). Rechanneling the cardiac proarrhythmia safety paradigm: A meeting report from the Cardiac Safety Research Consortium. *Am. Heart J.* **167**, 292–300.

Salata, J. J., Jurkiewicz, N. K., Wallace, A. A., Stupienski, R. F., Guinosso, P. J., and Lynch, J. J. (1995). Cardiac electrophysiological actions of the histamine H1-receptor antagonists astemizole and terfenadine compared with chlorpheniramine and pyrilamine. *Circ. Res.* **76**, 110–119.

Sale, H., Wang, J., O'Hara, T. J., Tester, D. J., Phartiyal, P., He, J.-Q., Rudy, Y., Ackerman, M. J., and Robertson, G. A. (2008). Physiological properties of hERG 1a/1b heteromeric currents and a hERG 1b-specific mutation associated with Long-QT syndrome. *Circ. Res.* **103**, e81–95.

Sanguinetti, M. C., Jiang, C., Curran, M. E., and Keating, M. T. (1995). A mechanistic link between an inherited and an acquired cardiac arrhythmia: hERG encodes the I_{Kr} potassium channel. *Cell* **81**, 299–307.

Scheel, O., Frech, S., Amuzescu, B., Eisfeld, J., Lin, K. H., and Knott, T. (2014). Action potential characterization of human induced pluripotent stem cell-derived cardiomyocytes using automated patch-clamp technology. *Assay Drug Dev. Technol.* **12**, 457–469.

Trudeau, M. C., Warmke, J. W., Ganetzky, B., and Robertson, G. A. (1995). hERG, a human inward rectifier in the voltage-gated potassium channel family. *Science* **269**, 92–95.

Downloaded from https://academic.oup.com/toxsci/article/168/2/365/5250700 by 81728827 user on 27 April 2021

Varró, A., and Baczkó, I. (2011). Cardiac ventricular repolarization reserve: A principle for understanding drug-related proarrhythmic risk. *Br. J. Pharmacol.* **164**, 14–36.

Vormberge, T., Hoffmann, M., and Himmel, H. (2006). Safety pharmacology assessment of drug-induced QT-prolongation in dogs with reduced repolarization reserve. *J. Pharmacol. Toxicol. Methods* **54**, 130–140.

Weerapura, M., Nattel, S., Chartier, D., Caballero, R., and Hébert, T. E. (2002). A comparison of currents carried by hERG, with and without coexpression of MiRP1, and the native rapid delayed rectifier current. Is MiRP1 the missing link? *J. Physiol.* **540**, 15–27.

Windley, M. J., Lee, W., Vandenberg, J. I., and Hill, A. P. (2018). The temperature dependence of kinetics associated with drug block of hERG channels is compound-specific and an important factor for proarrhythmic risk prediction. *Mol. Pharmacol.* **94**, 760–769.

Yap, Y. G., and Camm, A. J. (2003). Drug induced QT prolongation and torsades de pointes. *Heart* **89**, 1363–1372.

Yu, Z., Liu, J., van Veldhoven, J. P., IJzerman, A. P., Schalij, M. J., Pijnappels, D. A., Heitman, L. H., and de Vries, A. A. (2016). Allosteric modulation of Kv11.1 (hERG) channels protects against drug-induced ventricular arrhythmias. *Circ. Arrhythm. Electrophysiol.* **9**, e003439.

Zhang, S., Sawanobori, T., Hirano, Y., and Hiraoka, M. (1997). Multiple modulations of action potential duration by different calcium channel blocking agents in guinea pig ventricular myocytes. *J. Cardiovasc. Pharmacol.* **30**, 489–496.

Zhang, S., Zhou, Z., Gong, Q., Makielski, J. C., and January, C. T. (1999). Mechanism of block and identification of the verapamil binding domain to hERG potassium channels. *Circ. Res.* **84**, 989–998.

Downloaded from https://academic.oup.com/toxsci/article/168/2/365/5250700 by 81728827 user on 27 April 2021

NRC Research Press

ARTICLE

Cardiac electrophysiological effects of ibuprofen in dog and rabbit ventricular preparations: possible implication to enhanced proarrhythmic risk[1]

Bence Pászti, János Prorok, Tibor Magyar, Tamás Árpádffy-Lovas, Balázs Györe, Leila Topál, Péter Gazdag, Jozefina Szlovák, Muhammad Naveed, Norbert Jost, Norbert Nagy, András Varró, László Virág, and István Koncz

Abstract: Ibuprofen is a widely used nonsteroidal anti-inflammatory drug, which has recently been associated with increased cardiovascular risk, but its electrophysiological effects have not yet been properly studied in isolated cardiac preparations. We studied the effects of ibuprofen on action potential characteristics and several transmembrane ionic currents using the conventional microelectrode technique and the whole-cell configuration of the patch-clamp technique on cardiac preparations and enzymatically isolated ventricular myocytes. In dog (200 μM; n = 6) and rabbit (100 μM; n = 7) papillary muscles, ibuprofen moderately but significantly prolonged repolarization at 1 Hz stimulation frequency. In dog Purkinje fibers, repolarization was abbreviated and maximal rate of depolarization was depressed in a frequency-dependent manner. Levofloxacin (40 μM) alone did not alter repolarization, but augmented the ibuprofen-evoked repolarization lengthening in rabbit preparations (n = 7). In dog myocytes, ibuprofen (250 μM) did not significantly influence I_{K1}, but decreased the amplitude of I_{to} and I_{Kr} potassium currents by 28.2% (60 mV) and 15.2% (20 mV), respectively. Ibuprofen also depressed I_{NaL} and I_{Ca} currents by 19.9% and 16.4%, respectively. We conclude that ibuprofen seems to be free from effects on action potential parameters at lower concentrations. However, at higher concentrations it may alter repolarization reserve, contributing to the observed proarrhythmic risk in patients.

Key words: ibuprofen, levofloxacin, repolarization reserve.

Résumé : L'ibuprofène est un anti-inflammatoire non stéroïdien largement utilisé, qui a récemment été associé avec un accroissement du risque cardiovasculaire, mais ses effets électrophysiologiques n'ont pas encore été étudiés adéquatement dans des préparations de cœur isolé. À l'aide de la technique de microélectrode classique et de la technique de « patch-clamp » avec configuration sur cellules entières, nous avons étudié les effets de l'ibuprofène sur les caractéristiques du potentiel d'action ainsi que sur plusieurs courants ioniques transmembranaires dans des préparations de cœur et de myocytes ventriculaires isolés enzymatiquement. Dans le muscle papillaire de chien (200 μM; n = 6) et de lapin (100 μM; n = 7) stimulé à une fréquence de 1 Hz, l'ibuprofène entraînait une prolongation de la repolarisation notable, bien que modérée. Dans les fibres de Purkinje canines, la durée et la vitesse maximale de la repolarisation diminuaient de manière fréquence-dépendante. Chez le lapin (n = 7), la lévofloxacine (40 μM) administrée seule n'entraînait pas de modification de la repolarisation, mais bien une augmentation du prolongement de la repolarisation obtenu avec l'ibuprofène. Dans les myocytes canins, l'ibuprofène (250 μM) n'avait pas d'influence marquée sur I_{K1}, mais entraînait une diminution de l'amplitude des courants potassiques I_{to} et I_{Kr} de 28,2 (60 mV) et de 15,2 % (20 mV), respectivement. L'ibuprofène entraînait aussi une dépression des courants I_{NaL} et I_{Ca} de 19,9 et de 16,4 %, respectivement. Nous en arrivons à la conclusion que l'ibuprofène ne semble pas avoir d'effet sur les paramètres du potentiel d'action à de faibles concentrations. Cependant, à des concentrations plus élevées, il pourrait porter atteinte à la réserve de repolarisation, participant ainsi au risque proarythmique observé chez les patients. [Traduit par la Rédaction]

Mots-clés : ibuprofène, lévofloxacine, réserve de repolarisation.

Received 7 July 2020. Accepted 31 August 2020.

B. Pászti,* T. Magyar, T. Árpádffy-Lovas, L. Topál, P. Gazdag, J. Szlovák, M. Naveed, and I. Koncz.[†] Department of Pharmacology and Pharmacotherapy, Faculty of Medicine, University of Szeged, Szeged, Hungary.

J. Prorok* and N. Nagy. Department of Pharmacology and Pharmacotherapy, Faculty of Medicine, University of Szeged, Szeged, Hungary; MTA-SZTE Research Group of Cardiovascular Pharmacology, Szeged, Hungary.

B. Györe. Department of Oral Surgery, Faculty of Dentistry, University of Szeged, Szeged, Hungary.

N. Jost, A. Varró, and L. Virág.[†] Department of Pharmacology and Pharmacotherapy, Faculty of Medicine, University of Szeged, Szeged, Hungary; Department of Pharmacology and Pharmacotherapy, Interdisciplinary Excellence Centre, University of Szeged, Szeged, Hungary; MTA-SZTE Research Group of Cardiovascular Pharmacology, Szeged, Hungary.

Corresponding author: András Varró (email: varro.andras@med.u-szeged.hu).

*These authors share first authorship.

[†]These authors share senior authorship.

[1]This paper is part of a special issue of selected papers from the Joint North American/European IACS 2019.

Copyright remains with the author(s) or their institution(s). Permission for reuse (free in most cases) can be obtained from copyright.com.

Can. J. Physiol. Pharmacol. Downloaded from cdnsciencepub.com by GEORGE WASHINGTON UNIVERSITY on 04/26/21
For personal use only.

Can. J. Physiol. Pharmacol. Downloaded from cdnsciencepub.com by GEORGE WASHINGTON UNIVERSITY on 04/26/21
For personal use only.

Introduction

Ibuprofen is one of the most widely used nonsteroidal anti-inflammatory drugs (NSAIDs) (Rainsford 2009). However, a recent Danish nationwide case–time–control study (Sondergaard et al. 2017) found that short-term therapy with ibuprofen was associated with an increased risk of cardiac arrest. It is important to mention that this study also concluded that there was an increased risk of out-of-hospital cardiac arrest in diclofenac users. In an observational, historical cohort evaluation (Pratt et al. 1994), it was found that the ibuprofen cohort had a significantly higher arrhythmic event rate. A case report outlined a probable relationship between standard ibuprofen dosing and palpitations (Douglas 2010). Surprisingly, very little is known about the cardiac electrophysiological effect of ibuprofen, and, to our knowledge, the cellular cardiac electrophysiological effects of ibuprofen have been investigated only in one study on guinea pig papillary muscle and sinoatrial node (Yang et al. 2008). In these preparations, ibuprofen dose-dependently shortened action potential duration (APD) and decreased the maximal rate of depolarization (V_{max}) at therapeutically relevant and at high concentrations. The effects of ibuprofen on the action potential parameters and the underlying transmembrane currents have not yet been reported in other cardiac preparations, including those obtained from larger animals (e.g., rabbit or dog), closer to human in heart size, in spontaneous frequency, and in basic electrophysiological properties. Repolarization prolonging properties have also been reported among fluoroquinolone antibiotic agents (Chiba et al. 2000; Garnett and Johannesen 2016; Komatsu et al. 2019), and combination of such antibiotics and NSAIDs is a common practice in the treatment of infections. Therefore, the purpose of our work was to further characterize the cellular electrophysiological effects of ibuprofen and levofloxacin using preparations obtained from the hearts of large animals, namely dogs and rabbits. We found that 50 μM ibuprofen did not influence the action potential parameters including APD in dog and rabbit ventricular muscle preparations but at higher concentrations (100–200 μM), especially when repolarization reserve (Varró et al. 2000; Roden 2006; Varró and Baczkó 2011) had been previously attenuated, some repolarization lengthening occurred. Therefore, although at low therapeutic concentrations the drug could be considered safe regarding its cardiac electrophysiological effects, it is important to further improve our understanding concerning the possible unfavorable association between ibuprofen and increased cardiovascular risk reported in clinical studies.

Methods

Conventional microelectrode technique

All experiments were conducted in compliance with the *Guide for the Care and Use of Laboratory Animals* (USA NIH publication No. 85-23, revised 1996) and conformed to Directive 2010/63/EU of the European Parliament. The protocols were approved by the Review Board of the Department of Animal Health and Food Control of the Ministry of Agriculture and Rural Development, Hungary (XIII/1211/2012). Ventricular (papillary) muscles were obtained from the right ventricle of rabbits and dogs. Free-running (false tendons of) Purkinje fibers were isolated from both ventricles of dog hearts removed through a right lateral thoracotomy. Male New Zealand rabbits (body mass 2–3 kg) were terminated by rapid cervical dislocation, and Beagle dogs (body mass 10–15 kg) of both sexes were anesthetized and sacrificed using high-dose sodium pentobarbital (60 mg/kg i.v.). The preparations were placed in a tissue bath and allowed to equilibrate for at least 2 h while superfused (flow rate 4–5 mL/min) with Locke's solution containing (in mM): NaCl 120, KCl 4, $CaCl_2$ 1.8, $MgCl_2$ 1, $NaHCO_3$ 22, and glucose 11. The pH of this solution was 7.35 to 7.40 when gassed with 95% O_2 and 5% CO_2 at 37 °C. During the equilibration period, the ventricular muscle tissues were stimulated at a basic cycle length of 1000 ms, Purkinje fibers were stimulated at a basic cycle length of 500 ms. Electrical pulses of 0.5–2 ms in duration and twice diastolic threshold in intensity (S_1) were delivered to the preparations through bipolar platinum electrodes. Transmembrane potentials were recorded with the use of glass capillary microelectrodes filled with 3 M KCl (tip resistance 5–15 MΩ). The microelectrodes were coupled through an Ag–AgCl junction to the input of a high-impedance, capacitance-neutralizing amplifier (Experimetria, Type 309, Budapest, Hungary). Intracellular recordings were displayed on a storage oscilloscope (Hitachi V-555) and led to a computer system (APES) designed for online determination of the following parameters: resting membrane potential, action potential amplitude, APD at 50% (APD_{50}) and 90% (APD_{90}) repolarization, and the maximum rate of rise of the action potential upstroke (V_{max}). The following types of stimulation were applied in the course of the experiments: stimulation with a constant cycle length of 1000 ms (ventricular muscles); stimulation with a constant cycle length of 500 ms (Purkinje fibers). In case of Purkinje fibers, stimulation with different constant cycle lengths ranging from 300 to 1000 ms were also applied. Control recordings were obtained after the equilibration period. The effects of ibuprofen and dimethyl sulfoxide (DMSO) not exceeding 18.8% were determined at the given concentrations, after the addition of each compound until 30 min elapsed, in a cumulative manner. Compounds were purchased from Sigma/Merck for all experiments.

Whole-cell configuration of the patch-clamp technique

Untreated adult beagle dogs of either sex (body mass 8–15 kg) were used for the study. All experiments were conducted in compliance with the *Guide for the Care and Use of Laboratory Animals* (USA NIH publication No. 85-23, revised 1996) and conformed to the Directive 2010/63/EU of the European Parliament. The protocols were approved by the review board of Committee on Animal Research of the Albert Szent-Györgyi Medical University (54/1999 OEj).

The isolation and preparation of dog ventricular myocytes were described earlier in detail (Varró et al. 2000). One drop of cell suspension was placed in a transparent recording chamber mounted on the stage of an inverted microscope. The myocytes were allowed to settle and adhere to the bottom for at least 5–10 min before superfusion was initiated with Tyrode solution containing (in mM): NaCl 144, NaH_2PO_4 0.4, KCl 4.0, $CaCl_2$ 1.8, $MgSO_4$ 0.53, glucose 5.5, and HEPES 5.0 (pH 7.4, NaOH). Temperature was set to 37 °C. Only rod-shaped cells with clear cross-striations were used. Patch-clamp micropipettes were fabricated from borosilicate glass capillaries using a micropipette puller (Flaming/Brown, type P-97; Sutter Instrument, Novato, California, USA). These electrodes had resistances between 1.5 and 2.5 MΩ. Membrane currents were recorded with Axopatch 200B patch-clamp amplifiers (Molecular Devices Inc., Sunnyvale, California, USA) using the whole-cell configuration of the patch-clamp technique. After establishing a high resistance (1–10 GΩ) seal by gentle suction, the cell membrane beneath the tip of the electrode was disrupted by suction or application of short electrical pulses. Membrane currents were digitized after low-pass filtering at 1 kHz using analog-to-digital converters (Digidata 1440 A; Molecular Devices Inc., Sunnyvale, California, USA) under software control (pClamp 10; Molecular Devices Inc., Sunnyvale, California, USA). The various ion currents were measured as described earlier in detail (Kohajda et al. 2016). The same software was used for offline analysis.

Statistical analysis

Results are expressed as mean ± SEM. Normality of distributions was verified using the Shapiro–Wilk test, and homogeneity of variances was verified using Bartlett's test in each treatment group. Statistical comparisons were made using Student's *t* test for Tables 1, 2A, and 2B. Variance analysis (ANOVA) for repeated measurements was performed, followed by Bonferroni's post hoc

Can. J. Physiol. Pharmacol. Downloaded from cdnsciencepub.com by GEORGE WASHINGTON UNIVERSITY on 04/26/21
For personal use only.

Table 1. The electrophysiological effects of dimethyl sulfoxide (DMSO, 2.2‰) and ibuprofen (50 μM and 200 μM) in dog right ventricular papillary muscle preparations (VM; A, B, and C), at basic cycle length of 1000 ms; and ibuprofen (200 μM) in dog Purkinje fibers (PF; D) at basic cycle length of 500 ms.

(A)	Sample	RP (mV)	APA (mV)	V_{max} (V/s)	APD_{50} (ms)	APD_{90} (ms)	APD_{90} (%)
Control	Dog VM ($n = 6$)	−83.3 ± 2.3	106.7 ± 1.5	136.7 ± 14.2	157.8 ± 11.6	203.6 ± 7.6	—
DMSO (2.2‰)	Dog VM ($n = 6$)	−85.8 ± 1.7	105.3 ± 1.4	123.3 ± 17.0	153.8 ± 11.5	201.6 ± 8.0	−1.0 ± 1.2
(B)	**Sample**	**RP (mV)**	**APA (mV)**	**V_{max} (V/s)**	**APD_{50} (ms)**	**APD_{90} (ms)**	**APD_{90} (%)**
Control	Dog VM ($n = 8$)	−83.2 ± 1.6	108.1 ± 1.0	175.2 ± 22.3	187.0 ± 9.3	227.5 ± 9.7	—
Ibuprofen (50 μM)	Dog VM ($n = 8$)	−85.3 ± 2.1	106.7 ± 1.9	172.4 ± 29.9	187.7 ± 9.7	225.9 ± 8.9	−0.6 ± 1.0
(C)	**Sample**	**RP (mV)**	**APA (mV)**	**V_{max} (V/s)**	**APD_{50} (ms)**	**APD_{90} (ms)**	**APD_{90} (%)**
Control	Dog VM ($n = 6$)	−89.0 ± 1.8	110.6 ± 2.4	174.6 ± 20.3	173.8 ± 8	214.1 ± 5.9	—
Ibuprofen (200 μM)	Dog VM ($n = 6$)	−89.1 ± 3.2	113.4 ± 3.0	192.9 ± 27.1	181.6 ± 6.3	223.0 ± 4.9*	4.3 ± 1.0
(D)	**Sample**	**RP (mV)**	**APA (mV)**	**V_{max} (V/s)**	**APD_{50} (ms)**	**APD_{90} (ms)**	**APD_{90} (%)**
Control	Dog PF ($n = 7$)	−89.7 ± 0.7	133.5 ± 3.3	580.7 ± 36.0	163.9 ± 10.9	253.4 ± 14.2	—
Ibuprofen (200 μM)	Dog PF ($n = 7$)	−87.3 ± 1.0	135.9 ± 3.4	621.5 ± 93.5	163.7 ± 11.2	242.0 ± 13.7*	−4.5 ± 0.7

Note: Results are expressed as means ± SEM. RP, resting potential; APA, action potential amplitude; V_{max}, maximum rate of depolarization; APD_{50} and APD_{90}, action potential durations at 50% and 90% of repolarization.

*$p < 0.05$, Student's t test for paired data.

Fig. 1. The effects of ibuprofen and dimethyl sulfoxide (DMSO) on action potentials recorded from different cardiac preparations. Original action potential records show that ibuprofen (at 100 μM) slightly but significantly lengthened the action potential duration in rabbit right ventricular papillary muscle (panel C) and in dog right ventricular papillary muscle (at 200 μM, panel A) at a basic cycle length of 1000 ms. However, in dog Purkinje fiber (panel B) the drug significantly shortened the action potential repolarization at a basic cycle length of 500 ms. DMSO at 2.2‰ did not alter action potential duration in any of the preparations at the same cycle lengths (panels D–F). [Color online.]

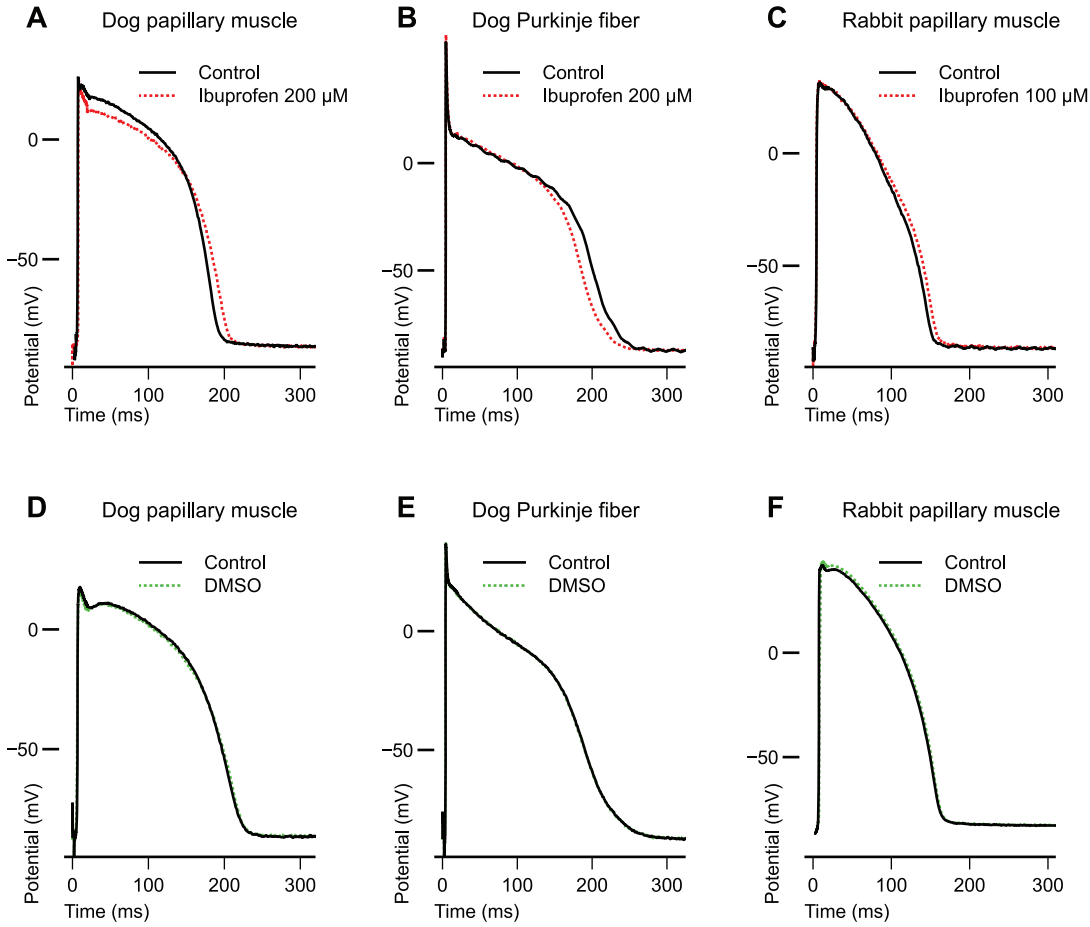

Can. J. Physiol. Pharmacol. Downloaded from cdnsciencepub.com by GEORGE WASHINGTON UNIVERSITY on 04/26/21
For personal use only.

Table 2. The electrophysiological effects of dimethyl sulfoxide (DMSO, 2.2‰), levofloxacin (40 μM), and ibuprofen (100 μM) in rabbit right ventricular papillary muscle (VM) preparations at a basic cycle length of 1000 ms.

(A)	Sample	RP (mV)	APA (mV)	V_{max} (V/s)	APD_{50} (ms)	APD_{90} (ms)	APD_{90} (%)
Control	Rabbit VM ($n = 6$)	−81.7 ± 1.9	119.1 ± 2.3	222.0 ± 21.9	123.8 ± 7.9	158.7 ± 7.7	—
DMSO (2.2‰)	Rabbit VM ($n = 6$)	−81.6 ± 2.6	115.8 ± 4.7	181.9 ± 20.5	123.0 ± 7.2	159.3 ± 7.1	0.7 ± 1.9
(B)	**Sample**	**RP (mV)**	**APA (mV)**	**V_{max} (mV)**	**APD_{50} (ms)**	**APD_{90} (ms)**	**APD_{90} (%)**
Control	Rabbit VM ($n = 7$)	−86.9 ± 1.3	109.0 ± 2.6	127.6 ± 7.5	149.6 ± 9.6	163.8 ± 6.6	—
Levofloxacin (40 μM)	Rabbit VM ($n = 7$)	−85.8 ± 2.0	111.3 ± 4.0	128.0 ± 8.0	156.9 ± 26.0	164.1 ± 7.0	0.1 ± 0.8
(C)	**Sample**	**RP (mV)**	**APA (mV)**	**V_{max} (V/s)**	**APD_{50} (ms)**	**APD_{90} (ms)**	**APD_{90} (%)**
Control	Rabbit VM ($n = 9$)	−86.5 ± 1.6	108.0 ± 3.7	147.7 ± 21.2	121.8 ± 7.1	164.7 ± 8.7	—
Ibuprofen (100 μM)	Rabbit VM ($n = 9$)	−85.6 ± 2.7	107.3 ± 2.3	145.2 ± 19.3	123.3 ± 7.5	169.3 ± 8.7*	2.9 ± 0.9
Levofloxacin (40 μM)	Rabbit VM ($n = 9$)	−87.4 ± 2.2	111.0 ± 3.7	148.5 ± 19.4	138.2 ± 13.1	183.2 ± 12.5*	7.6 ± 1.9

Note: Results are expressed as means ± SEM. APA, action potential amplitude; V_{max}, maximum rate of depolarization; APD_{50} and APD_{90}, action potential durations at 50% and 90% of repolarization.

*$p < 0.05$, Student's t test for paired data (Tables 2A and 2B), ANOVA for repeated measurements followed by Bonferroni's post hoc test (Table 2C).

Fig. 2. Cycle-length-dependent changes in action potential duration at 90% of repolarization (APD_{90}, panels A and C) and in maximal rate of depolarization (V_{max}, panels B and D) measured under control conditions and in the presence of 200 μM ibuprofen and dimethyl sulfoxide (DMSO) at 2.2‰ in dog Purkinje fiber preparations. Values are means ± SEM. Asterisks indicate significant changes ($p < 0.05$). [Color online.]

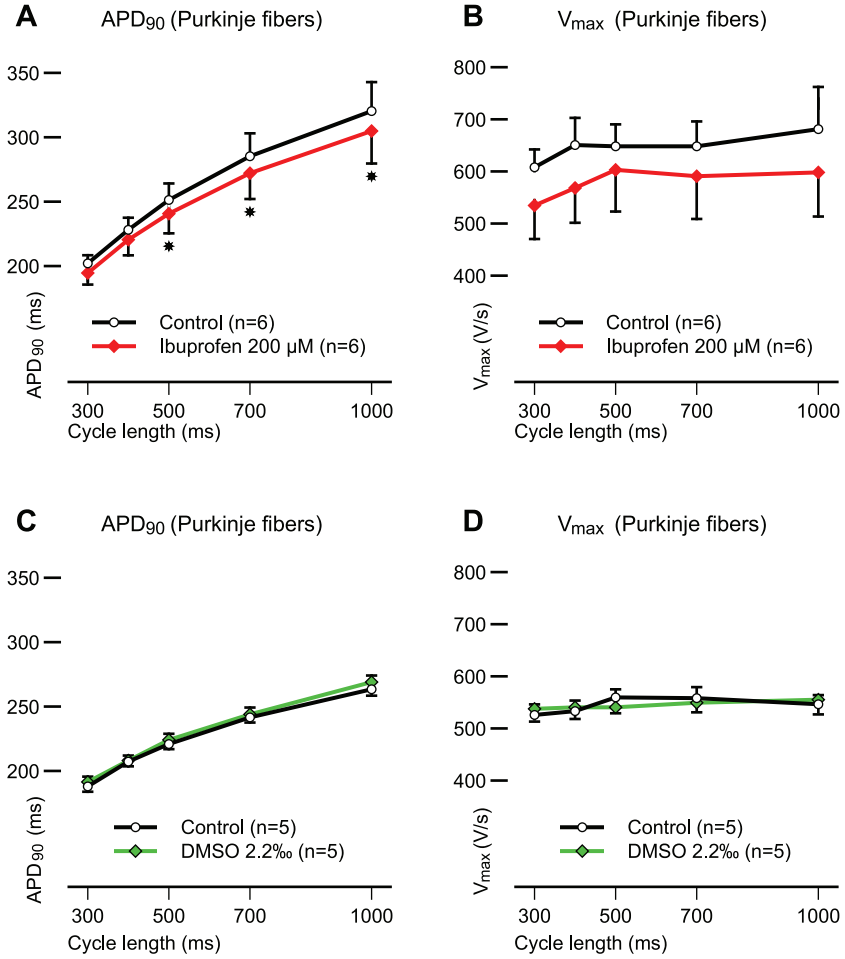

test for Table 2C. Differences were considered significant when $p < 0.05$.

Results

Effects of ibuprofen on transmembrane action potentials

We have investigated the effects of ibuprofen on cardiac action potentials in the concentration range of 50–200 μM (10.3–41.2 μg/mL) in rabbit and dog right ventricular papillary muscle using the conventional microelectrode technique. As Tables 1B and 1C and Figs. 1A and 2C show, ibuprofen in dog right ventricular papillary muscle at 50 and 200 μM and at 1 Hz stimulation frequency did not change the resting membrane potential, the action potential amplitude, or V_{max}, but at 200 μM it moderately lengthened the APD_{50} and APD_{90}. The solvent DMSO at the applied concentration did not

Can. J. Physiol. Pharmacol. Downloaded from cdnsciencepub.com by GEORGE WASHINGTON UNIVERSITY on 04/26/21
For personal use only.

Fig. 3. The effects of levofloxacin alone (panel A) and in combination with 100 μM ibuprofen (panel B) on action potentials recorded from rabbit right ventricular papillary muscle preparation. Original action potential records indicate that 40 μM levofloxacin did not influence the ventricular repolarization in rabbit (panel A); however, in combination with 100 μM ibuprofen, levofloxacin significantly lengthened the action potential duration (panel B). [Color online.]

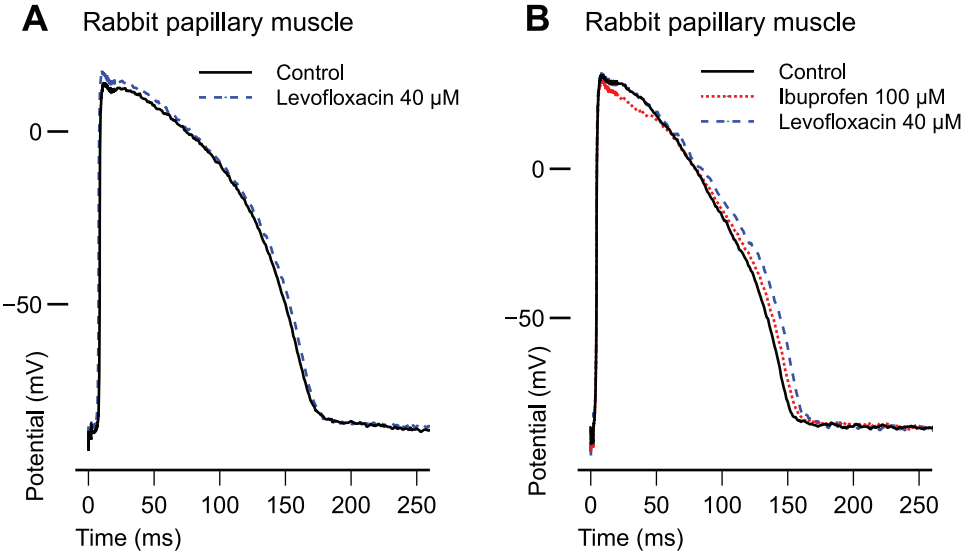

affect any of the measured action potential parameters (Table 1A and Fig. 1E).

In dog Purkinje fibers, action potentials were studied at a 500 ms constant cycle length (Table 1D) and also at various stimulation cycle lengths, ranging from 300–1000 ms (Fig. 2A). At constant cycle length stimulation, ibuprofen at 200 μM concentration elicited significant abbreviation of APD_{90}, while all other characteristics, including the resting potential, action potential amplitude, and V_{max}, remained unchanged. As Fig. 2B indicates, in Purkinje fibers, V_{max} was decreased and APD was shortened in a frequency-dependent manner. The decrease in APD_{90} was more pronounced at slower cycle lengths, being significant from 500 to 1000 ms. V_{max} depression was observed only at high stimulation rate corresponding to 300 ms cycle length. DMSO elicited no changes in the action potential characteristics of the Purkinje fibers at any cycle length (Table 1A; Figs. 1E, 2C, and 2D).

Levofloxacin, a widely known antibiotic, at 40 μM did not change action potential parameters, including APD_{90} in rabbit papillary muscles at 1 Hz stimulation rate (Table 2B and Fig. 3A). However, when levofloxacin was applied in combination with 100 μM ibuprofen, the extent of APD lengthening evoked by levofloxacin was greater than that observed without the application of ibuprofen (Table 2C and Fig. 3B).

To elucidate the mechanism of the changes induced by ibuprofen in the action potential, the effects of ibuprofen on the transmembrane ionic currents were investigated by the whole-cell configuration of the patch-clamp technique in dog ventricular myocytes at 250 μM (51.5 μg/mL). The solvent DMSO at the applied concentration did not influence the amplitude or kinetics of the measured transmembrane ionic currents (Figs. 4–5). In dog ventricular myocytes, 250 μM ibuprofen did not significantly alter the inward rectifier (I_{K1}) potassium (Fig. 4A) and moderately but significantly decreased the transient outward (I_{to}, Figs. 4B and 4D) and rapid delayed rectifier (I_{Kr}, Figs. 4C and 4E) potassium currents.

Because cardiac repolarization is determined not only by outward potassium currents but also by late inward sodium (I_{NaL}) and L-type inward calcium (I_{Ca}) currents, the effect of ibuprofen was also studied on I_{NaL} and I_{Ca} in dog ventricular myocytes. As Fig. 5 indicates, 250 μM ibuprofen moderately, but in a statistically significant manner, decreased the amplitude of both I_{NaL} and I_{Ca}.

Discussion

The most important message of the present study is to show that ibuprofen in normal situations and therapeutically relevant concentrations exerts none or only moderate repolarization lengthening in ventricular muscle preparations, but in a situation where repolarization reserve has been attenuated, the degree of repolarization lengthening was further increased. This raises the possibility that under such conditions it may enhance proarrhythmic risk and consequent sudden cardiac death.

The paucity of reports regarding the cardiac electrophysiological effects of ibuprofen is surprising in spite of its worldwide use and the two decades of concerns regarding increased risk associated with NSAID drugs in general (Bombardier et al. 2000; Huang et al. 2006*a*, 2006*b*). In addition, in a recent meta-analysis, it has been reported that two NSAID drugs, diclofenac and ibuprofen, increase out-of-hospital cardiac arrest and consequent sudden deaths (Sondergaard et al. 2017). Although the mechanism of these observations is not clear and can be linked to causes other than direct ion channel modulation, the possibility of direct effect of ibuprofen on transmembrane ion channels should be also considered. This argument is further strengthened by a previous experimental study (Kristóf et al. 2012), which indicated that diclofenac decreased repolarization reserve by inhibiting I_{Ks} and I_{Kr} in dog heart. In this paper, it has also been shown that diclofenac also facilitated Torsades de pointes ventricular tachycardia (TdP)-like arrhythmia in in vivo rabbit experiments (Kristóf et al. 2012).

The applied concentrations in the present study were similar to those of the work of Yang et al. (2008), and fall into the range of low and high therapeutic plasma levels (10–50 μg/mL) observed in patients (Holubek et al. 2007). It is also worth mentioning that, in certain situations, including high age or altered metabolism caused by disease or drug interactions, plasma levels may rise beyond normal. In addition, much higher (260 and 352 μg/mL)

Can. J. Physiol. Pharmacol. Downloaded from cdnsciencepub.com by GEORGE WASHINGTON UNIVERSITY on 04/26/21
For personal use only.

Fig. 4. Panels A–C show the effects of the solvent dimethyl sulfoxide (DMSO) at 2.2‰ and ibuprofen at 250 μM on the potassium currents I_{K1}, I_{to}, and I_{Kr}, respectively, in ventricular myocytes; the insets show the applied voltage protocols. Values are means ± SEM. Asterisks indicate $p < 0.05$, ANOVA for repeated measurements followed by Bonferroni's post hoc test. Panels D and E show original current traces of the I_{to} and I_{Kr}, currents, respectively, recorded in control conditions and in the presence of DMSO and after the application of 250 μM ibuprofen. In panel E, the dotted arrows indicate the amplitude of I_{Kr} tail currents at –40 mV. I_{K1}, inward rectifier potassium current; I_{Kr}, rapidly activating delayed rectifier potassium current; I_{to}, transient outward potassium current. [Color online.]

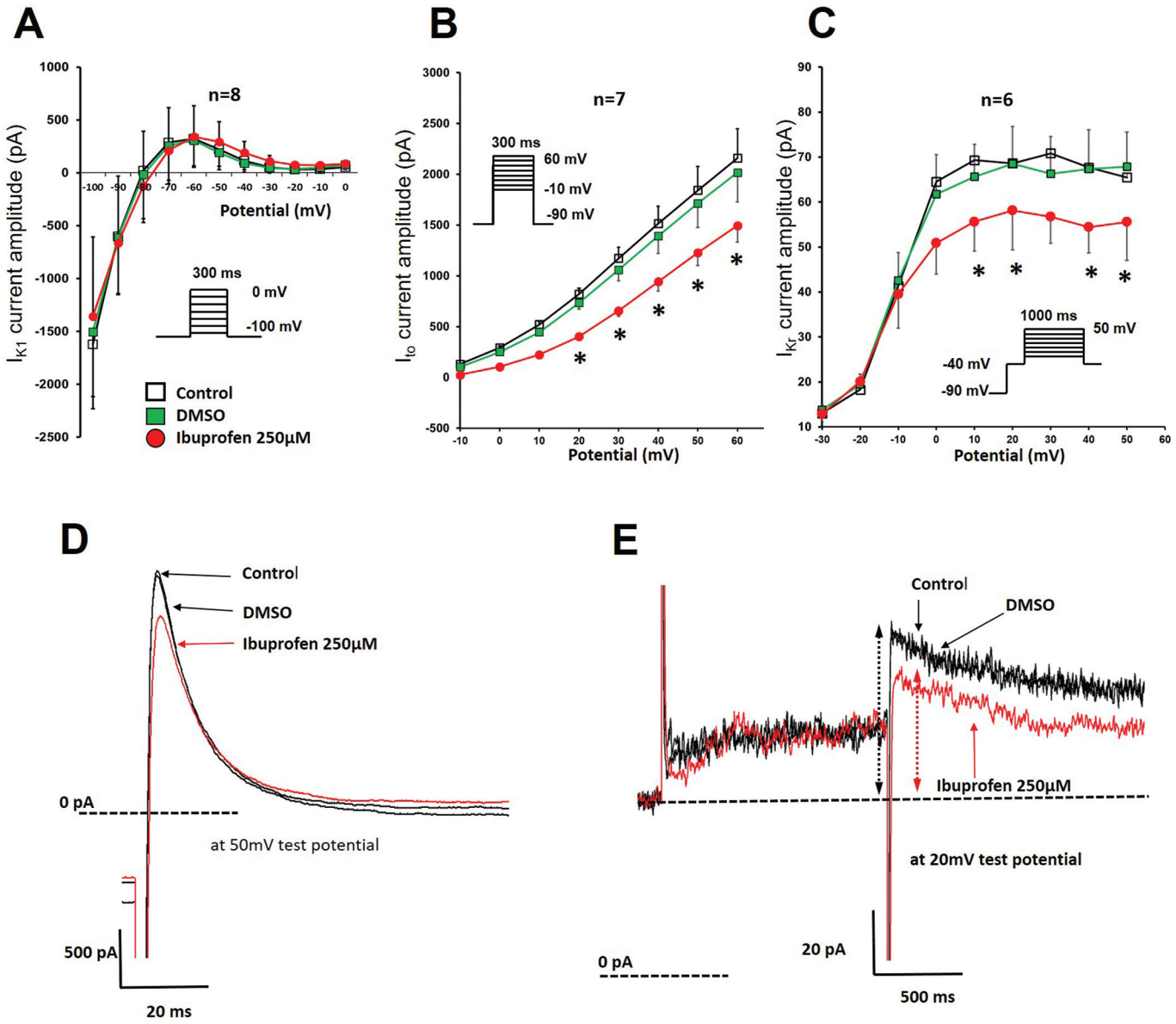

plasma levels have also been reported after drug intoxication (Holubek et al. 2007).

In guinea pig ventricle, it has been previously shown (Yang et al. 2008) that ibuprofen in the concentration range of 10–80 μg/mL shortened APD and depressed V_{max} in a frequency-dependent manner. In addition, ibuprofen also depressed slow response action potentials and sinus nodal frequency both indicative of I_{Ca} inhibition (Yang et al. 2008) with concomitant increase of PP and QRS intervals in the ECG, but with a shorter QTc (Yang et al. 2008). Our present results are in partial agreement with the ones reported by Yang et al. (2008). In the present study, we could confirm the frequency-dependent V_{max} and I_{Ca} inhibition reported by Yang et al. (2008), and we also found inhibition of I_{NaL}. All these effects would lead to shortening in repolarization. However, contrary to the findings reported by Yang et al. (2008), in our experiments moderate but statistically significant repolarization lengthening was observed in ventricular muscle, but not in Purkinje fibers. Also, Yarishkin et al. (2009) reported that diclofenac but not ibuprofen decreased I_{NaL} and I_{Ca} in rat ventricular myocytes. These dissimilarities are most likely due to the difference in the species (neonatal rat vs. rabbit), in the experimental conditions (room temperature vs. 37 °C), and in the preparations (1-day cultured trabecules vs. isolated papillary muscles) used. Unlike rabbit and dog, guinea pig ventricle lacks I_{to} (Zicha et al. 2003), and expresses very strong I_{Ks} (Bartos et al. 2015). Consequently, in guinea pig ventricle, I_{to} and I_{Kr} inhibition have less impact on repolarization when compared with that in rabbit or dog. Therefore, in guinea pig ventricle, the ibuprofen-evoked

Can. J. Physiol. Pharmacol. Downloaded from cdnsciencepub.com by GEORGE WASHINGTON UNIVERSITY on 04/26/21
For personal use only.

Fig. 5. Panels A and B show the effects of the solvent dimethyl sulfoxide (DMSO) at 2.2‰ and ibuprofen at 250 μM on the L-type calcium current (I_{Ca}) and the late sodium current (I_{NaL}), respectively, in ventricular myocytes; the insets show the applied voltage protocols. Values are means ± SEM. Asterisks indicate $p < 0.05$, ANOVA for repeated measurements followed by Bonferroni's post hoc test (A), Student's t test (B). Upper panels show original current traces of the I_{NaL} and I_{Ca} currents, respectively, recorded in control conditions and in the presence of DMSO and after the application of 250 μM ibuprofen. I_{NaL} was defined as tetrodotoxin-sensitive current by subtracting current traces recorded in the presence of 20 μM tetrodotoxin from traces of control, DMSO, and ibuprofen recordings. [Color online.]

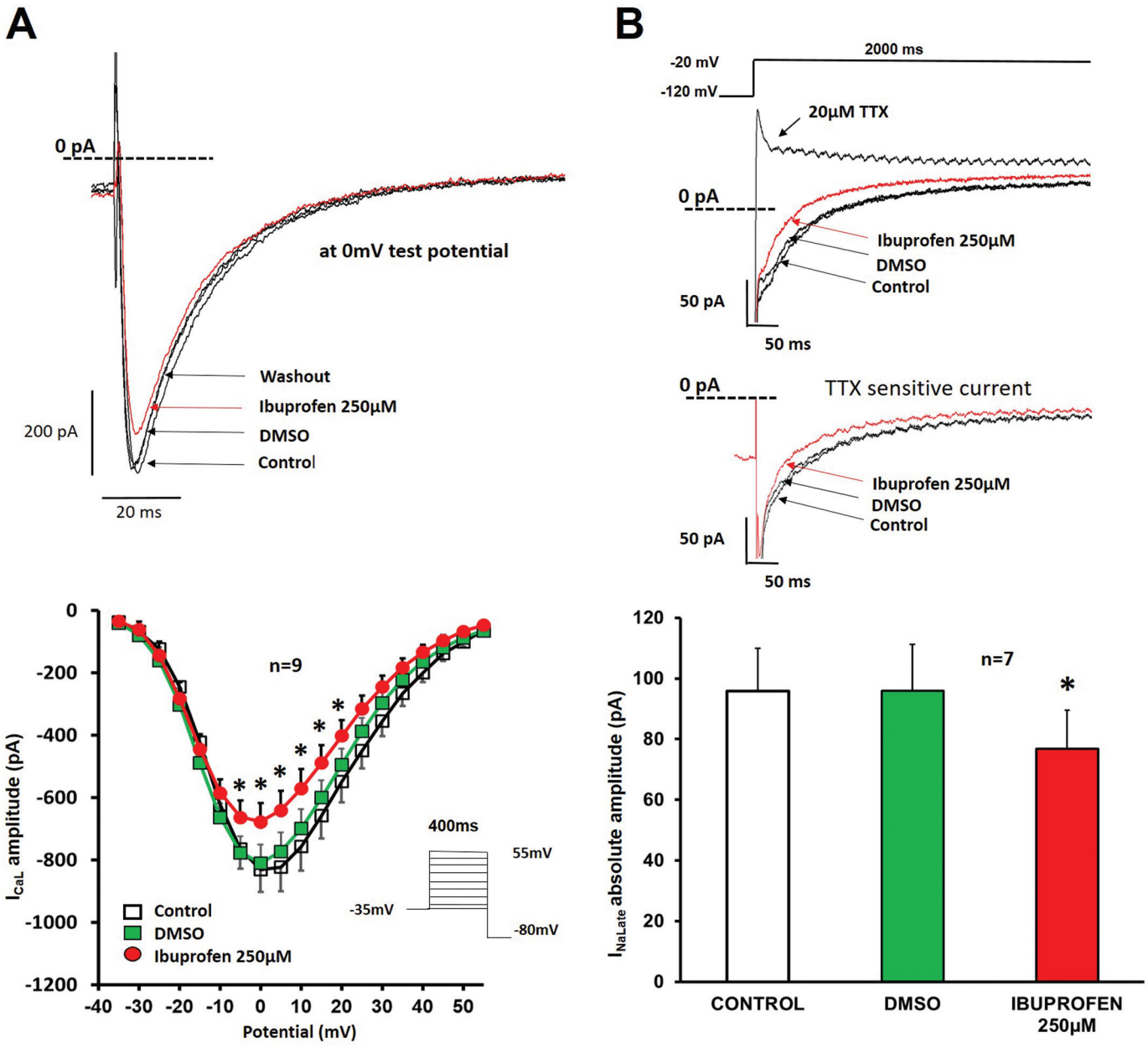

I_{Ca} and I_{NaL} inhibition would change the balance of inward and outward currents, favoring relative augmentation of outward currents, with an overall result of shortened repolarization. Similar effect should be expected in dog Purkinje fibers, in which relatively strong I_{NaL} exists. The opposite effect is expected in rabbit and dog ventricle, where the density of I_{Ks} is weaker than in the guinea pig; therefore, I_{Kr} should have a stronger contribution to repolarization (Jost et al. 2013). In addition, ibuprofen inhibits I_{to}, which also plays an important role in the repolarization reserve (Virág et al. 2011). It should be mentioned that NSAIDs, including ibuprofen, are often used in patients with fever. Therefore, it would be worthwhile to study the effect of ibuprofen and other NSAIDs under hyperthermic conditions as well.

It is well known that fluoroquinolone antibiotics have some repolarization prolonging and proarrhythmic potency (Chiba et al. 2000; Garnett and Johannesen 2016; Komatsu et al. 2019). To test potential interaction between ibuprofen and these antibiotics, we chose to study levofloxacin, which has been reported to possess relatively low proarrhythmic risk (Chiba et al. 2000; Milberg et al. 2007), due to its unpronounced repolarization lengthening (Hagiwara et al. 2001) and human ether-a-go-go-related gene channel inhibiting (Kang et al. 2001) properties compared with others, especially sparfloxacin (Chiba et al. 2000;

Can. J. Physiol. Pharmacol. Downloaded from cdnsciencepub.com by GEORGE WASHINGTON UNIVERSITY on 04/26/21
For personal use only.

Hagiwara et al. 2001). In our experiments, in good agreement with the results of Hagiwara et al., levofloxacin did not evoke significant changes when applied alone. However, when levofloxacin was applied in combination with ibuprofen, noteworthy APD prolongation was observed. Ibuprofen alone elicited a moderate prolongation of APD, and this was increased even further by levofloxacin. It should be emphasized that the observed APD prolongation by ibuprofen, with or without levofloxacin, is not marked, and it is far from being excessive. Nevertheless, this effect should draw attention to the possibility that the combined effect of two drugs with low or even minimal effect on repolarization, and seemingly marginal potassium channel blocking properties may still be additive by collectively decreasing the repolarization reserve. Therefore, in certain situations where repolarization reserve is already attenuated (Varró and Baczkó 2011), e.g., in specific genetic disorders, heart failure, hypertophic cardiomyopathy, low serum potassium concentrations, or ischemic heart disease, this may lead to marked repolarization defects. This may ultimately contribute to enhanced proarrhythmic risk and consequent sudden cardiac death.

In conclusion, it seems that ibuprofen in normal situations, at least regarding its cardiac electrophysiological properties, is a relatively safe drug. However, in certain conditions characterized by attenuated repolarization reserve, ibuprofen may enhance proarrhythmic risk, and may even contribute to the incidence of sudden cardiac death observed in clinical studies. This possibility should be considered and taken into account in clinical practice, because ibuprofen is a very commonly used over-the-counter drug, taken every day by several million people without medical control.

Conflict of interest

The authors declare that there is no conflict of interest associated with this work.

Acknowledgements

This work was funded by the János Bolyai Research Scholarship of the Hungarian Academy of Sciences (for I.K., No. BO/00581/17) and the ÚNKP-18-4 and 19-4 (Bolyai+) New National Excellence Program of the Ministry for Innovation and Technology (for I.K.) and the National Research, Development and Innovation Office – NKFIH PD-116011 (for I.K.), K-119992 (for A.V.), FK-129117 (for N.N.), and the Hungarian Government-Ministry of Human Resources (Grant EFOP-3.6.2-16-2017-00006, LIVE LONGER, and EFOP 3.6.3-VEKOP-16-2017-00009 for T.Á.-L.), GINOP-2.3.2.-15-2016-00048, the Ministry of Human Capacities Hungary (20391-3/2018/FEKUSTRAT), and János Bolyai Research Scholarship of the Hungarian Academy of Sciences (for N.N.). The GINOP and EFOP projects are co-financed by the European Union and the European Regional Development Fund.

References

Bartos, D.C., Grandi, E., and Ripplinger, C.M. 2015. Ion channels in the heart. Compr. Physiol. **5**(3): 1423–1464. doi:10.1002/cphy.c140069. PMID: 26140724.

Bombardier, C., Laine, L., Reicin, A., Shapiro, D., Burgos-Vargas, R., Davis, B., et al. 2000. Comparison of upper gastrointestinal toxicity of rofecoxib and naproxen in patients with rheumatoid arthritis. VIGOR Study Group. N. Engl. J. Med. **343**(21): 1520–1528. doi:10.1056/NEJM200011233432103.

Chiba, K., Sugiyama, A., Satoh, Y., Shiina, H., and Hashimoto, K. 2000. Proarrhythmic effects of fluoroquinolone antibacterial agents: in vivo effects as physiologic substrate for torsades. Toxicol. Appl. Pharmacol. **169**(1): 8–16. doi:10.1006/taap.2000.9041.

Douglas, R.J. 2010. Palpitations following regular ibuprofen dosing in a 13-year-old girl: a case report. J. Med. Case Rep. **4**: 76. doi:10.1186/1752-1947-4-76.

Garnett, C., and Johannesen, L. 2016. Commentary on: "Levofloxacin-Induced QTc prolongation depends on the time of drug administration. CPT: Pharmacometrics Syst. Pharmacol. **5**(9): 452–454. doi:10.1002/psp4.12128. PMID:27647678.

Hagiwara, T., Satoh, S., Kasai, Y., and Takasuna, K. 2001. A comparative study of the fluoroquinolone antibacterial agents on the action potential duration in guinea pig ventricular myocardia. Jpn. J. Pharmacol. **87**(3): 231–234. doi:10.1254/jjp.87.231. PMID:11885973.

Holubek, W., Stolbach, A., Nurok, S., Lopez, O., Wetter, A., and Nelson, L. 2007. A report of two deaths from massive ibuprofen ingestion. J. Med. Toxicol. **3**(2): 52–55. doi:10.1007/BF03160908.

Huang, W.-F., Hsiao, F.-Y., Tsai, Y.-W., Wen, Y.-W., and Shih, Y.-T. 2006*a*. Cardiovascular events associated with long-term use of celecoxib, rofecoxib and meloxicam in Taiwan: an observational study. Drug Safety, **29**(3): 261–272. doi:10.2165/00002018-200629030-00009.

Huang, W.-F., Hsiao, F.-Y., Wen, Y.-W., and Tsai, Y.-W. 2006*b*. Cardiovascular events associated with the use of four nonselective NSAIDs (etodolac, nabumetone, ibuprofen, or naproxen) versus a cyclooxygenase-2 inhibitor (celecoxib): a population-based analysis in Taiwanese adults. Clin. Therap. **28**(11): 1827–1836. doi:10.1016/j.clinthera.2006.11.009.

Jost, N., Virág, L., Comtois, P., Ordög, B., Szuts, V., Seprényi, G., et al. 2013. Ionic mechanisms limiting cardiac repolarization reserve in humans compared to dogs. J. Physiol. **591**(17): 4189–4206. doi:10.1113/jphysiol.2013.261198.

Kang, J., Wang, L., Chen, X.L., Triggle, D.J., and Rampe, D. 2001. Interactions of a series of fluoroquinolone antibacterial drugs with the human cardiac K+ channel HERG. Mol. Pharmacol. **59**(1): 122–126. doi:10.1124/mol.59.1.122.

Kohajda, Z., Farkas-Morvay, N., Jost, N., Nagy, N., Geramipour, A., Horváth, A., et al. 2016. The effect of a novel highly selective inhibitor of the sodium/calcium exchanger (NCX) on cardiac arrhythmias in in vitro and in vivo experiments. PLoS ONE, **11**(11): e0166041. doi:10.1371/journal.pone.0166041.

Komatsu, R., Mizuno, H., Ishizaka, T., Ito, A., Jikuzono, T., Kakoi, T., et al. 2019. Exposure-response analysis of drug-induced QT interval prolongation in telemetered monkeys for translational prediction to human. J. Pharmacol. Toxicol. Methods, **99**: 106606. doi:10.1016/j.vascn.2019.106606.

Kristóf, A., Husti, Z., Koncz, I., Kohajda, Z., Szél, T., Juhász, V., et al. 2012. Diclofenac prolongs repolarization in ventricular muscle with impaired repolarization reserve. PLoS ONE, **7**(12): e53255. doi:10.1371/journal.pone.0053255.

Milberg, P., Hilker, E., Ramtin, S., Cakir, Y., Stypmann, J., Engelen, M.A., et al. 2007. Proarrhythmia as a class effect of quinolones: increased dispersion of repolarization and triangulation of action potential predict torsades de pointes. J. Cardiovasc. Electrophysiol. **18**(6): 647–654. doi:10.1111/j.1540-8167.2007.00793.x.

Pratt, C.M., Hertz, R.P., Ellis, B.E., Crowell, S.P., Louv, W., and Moyé, L. 1994. Risk of developing life-threatening ventricular arrhythmia associated with tefenadine in comparison with over-the-counter antihistamines, ibuprofen and clemastine. Am. J. Cardiol. **73**(5): 346–352. doi:10.1016/0002-9149(94)90006-X.

Rainsford, K.D. 2009. Ibuprofen: pharmacology, efficacy and safety. Inflammopharmacology, **17**(6): 275–342. doi:10.1007/s10787-009-0016-x.

Roden, D.M. 2006. Long QT syndrome: reduced repolarization reserve and the genetic link. J. Intern. Med. **259**(1): 59–69. doi:10.1111/j.1365-2796.2005.01589.x.

Sondergaard, K.B., Weeke, P., Wissenberg, M., Schjerning Olsen, A.-M., Fosbol, E.L., Lippert, F.K., et al. 2017. Non-steroidal anti-inflammatory drug use is associated with increased risk of out-of-hospital cardiac arrest: a nationwide case-time-control study. Eur. Heart J. Cardiovasc. Pharmacother. **3**(2): 100–107. doi:10.1093/ehjcvp/pvw041. PMID:28025218.

Varró, A., and Baczkó, I. 2011. Cardiac ventricular repolarization reserve: a principle for understanding drug-related proarrhythmic risk. Br. J. Pharmacol. **164**(1): 14–36. doi:10.1111/j.1476-5381.2011.01367.x.

Varró, A., Baláti, B., Iost, N., Takács, J., Virág, L., Lathrop, D.A., et al. 2000. The role of the delayed rectifier component IKs in dog ventricular muscle and Purkinje fiber repolarization. J. Physiol. **523**(Pt. 1): 67–81. doi:10.1111/j.1469-7793.2000.00067.x.

Virág, L., Jost, N., Papp, R., Koncz, I., Kristóf, A., Kohajda, Z., et al. 2011. Analysis of the contribution of I(to) to repolarization in canine ventricular myocardium. Br. J. Pharmacol. **164**(1): 93–105. doi:10.1111/j.1476-5381.2011.01331.x.

Yang, Z., Wang, H., Zheng, Y., Zhang, Y., Liu, Y., and Li, C. 2008. Possible arrhythmiogenic mechanism produced by ibuprofen. Acta Pharmacol. Sin. **29**(4): 421–429. doi:10.1111/j.1745-7254.2008.00754.x.

Yarishkin, O.V., Hwang, E.M., Kim, D., Yoo, J.C., Kang, S.S., Kim, D.R., et al. 2009. Diclofenac, a non-steroidal anti-inflammatory drug, inhibits L-type Ca channels in neonatal rat ventricular cardiomyocytes. Korean J. Physiol. Pharmacol. **13**(6): 437–442. doi:10.4196/kjpp.2009.13.6.437.

Zicha, S., Moss, I., Allen, B., Varro, A., Papp, J., Dumaine, R., et al. 2003. Molecular basis of species-specific expression of repolarizing K+ currents in the heart. Am. J. Physiol. Heart Circ. Physiol. **285**(4): H1641–H1649. doi:10.1152/ajpheart.00346.2003.